NUTRIENT DYNAMICS IN A HIGHLY WEATHERED SOIL UNDER NO-TILL AND HEAVY METAL PHYTOAVAILABILITY AS AFFECTED BY BIOCHAR AMENDMENT

By

JOAO ARTHUR ANTONANGELO

Bachelor of Science in Agricultural Engineering
Sao Paulo State University (UNESP)
Botucatu, Sao Paulo, Brazil
2012

Master of Science in Soils and Plant Nutrition
University of Sao Paulo (USP)
Piracicaba, Sao Paulo, Brazil
2015

Submitted to the Faculty of the
Graduate College of the
Oklahoma State University
in partial fulfillment of
the requirements for
the Degree of
DOCTOR OF PHILOSOPHY
July, 2019

NUTRIENT DYNAMICS IN A HIGHLY WEATHERED SOIL UNDER NO-TILL AND HEAVY METAL PHYTOAVAILABILITY AS AFFECTED BY BIOCHAR AMENDMENT

Dissertation Approved:

Dr. Hailin Zhang

Dissertation Adviser

Dr. Brian Arnall

Dr. Jason Warren

Dr. Ajay Kumar

ACKNOWLEDGEMENTS

Foremost, **thank God**, for giving me knowledge, strength and opportunity to undertake this research and complete it satisfactorily. This achievement would not have been possible without its blessings.

Firstly, I would like to express my sincere gratitude to my advisor Dr. Hailin Zhang for the continuous support during my Ph.D., for his patience, motivation, and for sharing his wide knowledge.

Besides my advisor, I would like to thank the rest of my dissertation committee: Dr. Brian Arnall, Dr. Jason Warren, and Dr. Ajay Kumar, for their insightful comments, encouragement and full support.

I thank my labmates at Soil, Water and Forage Analytical Laboratory (SWFAL) for all the help with analyses, among them Barbara McCray, Kendal Henderson, Leslie Maitlen and Christopher Gillespie.

I would like to express my profound gratitude to the Brazilian family for all the fun we have had in the last three years.

Finally but not the least, I would like to thank my family: my parents and sisters for supporting me spiritually throughout my Ph.D., especially my wife Cintia Miyake for fulfilling me with extraordinary support and faith, and my little daughter Sarah Tiemi Antonangelo for providing us with exceptional love.

Name: JOAO ARTHUR ANTONANGELO

Date of Degree: JULY, 2019

Title of Study: NUTRIENT DYNAMICS IN A HIGHLY WEATHERED SOIL UNDER NO-TILL AND HEAVY METAL PHYTOAVAILABILITY AS AFFECTED BY BIOCHAR AMENDMENT

Major Field: SOIL SCIENCE

Abstract: The nutrient dynamics in soils are affected by cropping systems, soil properties and environmental conditions. A field experiment under NT has been conducted in an Oxisol, which assesses rates of inorganic P and K fertilizers for soybean production in conjunction with liming since 1995. The objectives were to evaluate the effect of rates of P and K fertilizers on soybean yields, and to access the P species in solid state by X-ray fluorescence (P-XANES). The optimum amounts of P and K fertilizers were revealed, which will help farmers improve their crop yields while minimize the impact of fertilization on soil and water quality. The long-term mineral phosphate fertilizer application led to P stabilization in soils under more thermodynamically stable forms, such as P-Fe and P-Al, in spite of the effects that soil organic matter (SOM) might have on P reactivity. A second project studied the heavy metal (HM: Zn, Pb and Cd) dynamics in a contaminated soil of NE Oklahoma. High concentrations of HM in soils have negative impacts on plants, human health and the environmental quality. The purpose was to evaluate the effects of biochars on the Zn, Pb and Cd phytoavailability in Tar Creek contaminated soils, as well as on the growth and uptake of these elements by perennial ryegrass (*Lolium perenne*). Biochars produced from switchgrass (SGB) and poultry litter (PLB) feedstocks at 350 and 700 °C (pyrolysis temperatures) were characterized as their potential use as soil amendment. Those pyrolyzed at 700 ^{o}C were used to investigate their effect on ryegrass dry matter yield and the accumulation of HM in shoots and roots. Biochars were applied to the soil at 0, 0.5, 1, 2 and 4% (w/w) and the soils were extracted by DTPA to estimate the available HM contents. Soils amended with low amounts of biochars reduced HM phytoavailability thus reduced plant metal uptake. Biochar also increased plant biomass but reduced metal transfer from roots to shoots. It is effective using readily available bioproducts to remediate HM contaminated soils and to enhance ryegrass forage yield with acceptable amount of HM in the shoots.

TABLE OF CONTENTS

LIST OF TABLES

CHAPTER I

CHAPTER II

CHAPTER III

CHAPTER IV

Table Page

CHAPTER V

Table Page

CHAPTER VI

Table Page

LIST OF FIGURES

CHAPTER II

CHAPTER III

CHAPTER IV

Figure Page

CHAPTER V

Figure Page

CHAPTER VI

Figure Page

CHAPTER I

REVIEW OF LITERATURE

Phosphorus and potassium fertilization on soybean

Soybean yield in any agricultural system is directly affected by P and K fertilization, which also affects protein and oil content. Normal plant growth will be limited when adequate P is not provided by soil or fertilizers (Chaudhary et al., 2008). Deficiency of P can reduce nodulation, nitrogen fixation (N_2), root proliferation and leaf area (Chaudhary et al., 2008; Schulze et al., 2006). On the other hand, positive responses to P fertilization have been reported by soybean in many places around the world (Borges and Mallarino, 2000; Buah et al., 2000; Haq and Mallarino, 2005; Fatima et al., 2006). Such response to P is dependent on soil available P (Raij et al., 1998). Chiezey and Odunze (2009) reported that P application as inorganic fertilizer increased the total dry matter, and grain yield of soybean.

After nitrogen, potassium is the highest containing nutrient in soybean (Oliveira Junior et al., 2013). The K nutritional demand and K potential uptake of this crop are influenced by genetic and climate factors and soil fertility and management. In this sense, soybean has showed response to several rates of K application under various management regimes and agro-climatic situations (Kolar and Grewal, 1994; Premaratne

and Oertli, 1994; Yin and Vyn, 2004; Haq and Mallarino, 2005). Soybean takes up and accumulates K along the growing season. So, any K deficiency during this time may reduce soybean yield (Kolar and Grewal, 1994; Fernández et al., 2009). Initial symptoms of deficiency are characterized as yellow chlorosis in the top and margins of oldest leaves along with the increase of putrescine. However, a suitable K supply to soybean promotes increase in the number of legume per plant, nodulation, size, mass and oil content of grains (Malavolta, 1980), Also, according to Abbasi et al. (2012), positive yield responses to P-K fertilization occurred to all rates of both elements when applied together.

The determination of nutrient contents on plant tissue complements the soil fertility analysis and provides information for a better understanding of the nutritional status of crops. In the case of soybean, the trifolium nutrient contents are used to interpret the efficiency of fertilization (Table 1).

Phosphorus dynamics in very acidic soils

Phosphorus among the primary macronutrients is generally the less required by plants compared with N and K; however, it is the most used fertilizer in Brazil, mainly in the regions where soybean is cultivated, due to the high demand of this element by the crop and low supplying power of the soils. In this sense, P being the 12th most abundant element in the Earth's crust is also the second most limiting nutrient in tropical soils (Novais and Smyth, 1999; Salcedo, 2006). This situation is due to the general lack of P in Brazilian soils and the strong interaction of the element with the soil as well. This behavior is a consequence of its capacity to form high-energy bond compounds with oxides derived from a long-time

weathering process over the parent material, attributed to its high stability in the solid phase (Anjos et al., 1999).

Table 1. Nutrient contents for soybean tissue analysis[1] in clayey soils (basalt) of Parana (PR) state, Brazil

	Trifolium without petiole			Trifolium with petiole		
Nutrient	**Low**	**Sufficient**	**High**	**Low**	**Sufficient**	**High**
	..... g kg^{-1}					
N	< 50.7	50.7 to 61.4	> 61.4	< 41.7	41.7 to 48.9	> 48.9
P	< 2.8	2.8 to 4.2	> 4.2	< 2.5	2.5 to 3.6	> 3.6
K	< 17.6	17.6 to 24.3	> 24.3	< 22.4	22.4 to 26.7	> 26.7
Ca	< 7.3	7.3 to 10.4	> 10.4	< 8.2	8.2 to 10.8	> 10.8
Mg	< 3.6	3.6 to 4.9	> 4.9	< 3.0	3.0 to 4.8	> 4.8
S	< 2.7	2.5 to 3.5	> 4.0	< 2.5	2.3 to 3.4	> 3.5
	..... mg kg^{-1}					
B	< 49	49 to 55	> 55	< 52	52 to 60	> 60
Cu	< 9	9 to 14	> 14	< 8	8 to 11	> 11
Fe	< 137	137 to 229	> 229	< 119	119 to 211	> 211
Mn	< 48	48 to 108	> 108	< 40	40 to 94	> 94
Zn	< 25	25 to 40	> 40	< 22	22 to 38	> 38

[1]Third trifolium totally formed, collected in R2. Source: Harger (2008)

Regardless of the processes that reduces P concentration or phytoavailable P over a given timescale, the starting point (time=0) for the P supply to all soils is the substrate from which it is derived (Cross and Schlesinger, 1995; Johnson et al., 2003; Jenny, 1994; Walker and Syers, 1976). The relationship between soil P availability and soil age has been

intensively studied (Walker and Syers, 1976; Stevens, 1968; Lajtha and Schlesinger, 1988; Crews et al., 1995; Selmants and Hart, 2010). There has been, however, little investigation of how the concentration of available P affected by P concentrations in different size fractions of parent materials (Porder and Ramachandran, 2013). Continental crust contains around 700 ppm of P on average primarily in apatite mineral (Taylor and McClennan, 1985; Okin et al., 2004). In young soils, parent material P should influence total soil P. On the other hand, soils from tropical humid regions, especially those originated from basaltic rocks under several meters' annual rainfall show P deficiency after hundreds of thousands (Porder and Chadwick 2009) to millions of years weathering process. Therefore, parent materials need to be better evaluated linking rock P concentration to soil P availability by newer measurement techniques.

Some of these techniques such as Energy Dispersive X-ray fluorescence (EDXRF) can be applied to the parent material (finely grounded) to quantify the total concentration of a desired element. The incident electromagnetic radiation interacts with the sample and phenomena such as emission, absorption, and scattering may occur (Skoog et al., 2017). Also, the quantitative spatial distribution of elements in the unground parent rocky material can be performed by Micro Energy Dispersive X-ray Fluorescence (Micro-XRF), which presents the same principle of detection as that for EDXRF method. However, the equipment has a high analytical sensitivity working under vacuum (with no influence of O_2 on the absorption of the electromagnetic beam), then allowing the chemical mapping of the sample with an enhanced detection limit.

Furthermore, according to Goulart et al. (1998), although the mineralogical composition of the clay fraction of soils derived from basalt (dusky red magnetic Oxisols) is

known from several studies (Resende, 1976; Curi and Franzmeier, 1987; Fontes and Weed, 1991; Porder and Ramachandran, 2012), a complete description of the nature and origin of their iron oxides, which strongly bind to P, appears to be not available. As the weathering advances, soils gradually change their characteristics from their sources, becoming more electropositive with high capacity to adsorb anions, such as phosphates. This is the typical characteristic of Oxisols. Although initial P adsorption provides a good aspect, the 'aging' of this adsorption in conjunction with the formation of non-labile P fractions becomes a problem. The kaolinite, goethite, hematite and gibbsite mostly found in tropical soils (Fontes and Weed, 1991) are the main minerals responsible for phosphate adsorption ($P\text{-}H_xPO_{4x}$). Moreover, the process of P adsorption by Al oxides and hydroxides is even more evolved in the fixation of the element (Lopes and Cox, 1979).

Thus, while elements with higher mobility prevail as their soluble chemical forms, exchangeable and linked to carbonates, those with lower mobility such as P are found bound to Al, Fe and Mn oxides, organic and other residual soil fractions (Amaral Sobrinho et al., 1994). Therefore, the determination of free and amorphous oxides concentration is necessary in highly weathered soils if Fe hydroxides, such as goethite and hematite are important components of the clay fraction in these soils, which affects P availability to plants.

The P remained in the solution after a known concentration P solution has been equilibrated with a soil for 16 hours is termed P remaining or P_{rem}. The use of P_{rem} has been shown as a good estimator of both phosphate fixation capacity and phosphate buffer capacity of soils and has been used extensively for the recommendation of phosphate fertilization (Sousa and Lobato, 2003). The critical levels of available P in soils vary with the buffer capacity. This is particularly true when using P extractants sensible to soil buffer capacity

such as Mehlich-1 (Alvarez et al., 1999) and less applicable to the use of anionic exchange resin (Raij, 1996; Raij, 1998; Silva, 1999).

Plants absorb P from soil solution. However, the P contents in solution are very low (≤ 0.1 mg L^{-1} P) even when the P supply is increased to adequate levels through fertilization. That is why there is the need to add higher amounts of phosphorus fertilizers than the plants demand to increase P solution concentrations (Nahas, 1991).

The fertilizer P remaining in soils is slowly turned to less available forms by forming precipitated insoluble compounds or by diffusion into the interior of the oxides (Barrow, 1986; Raij, 1991). In the absence of annual addition of phosphate fertilizers, the yield will depend on the amount and availability of the residual P accumulated in soils (Barrow, 1980). It can recover all or nearly all the P applied to the soil through long-term (7 to 10 years) cultivation (Sousa and Lobato, 2003). Thus, the P applied to soils becomes a residual reserve for crop uptake along its productive cycles. So, this portion of P should be considered when deciding P fertilizer addition.

Soil management or chemical amendment responsible for pH changes also influences available P concentration. No-till (NT) is generally known as a promoter of the pH reduction in top layers in short-term, and then justifying the need to apply amendments superficially, without incorporation.

In addition, organic P increases, mainly in soils under NT, and biological processes tend to govern the availability of this nutrient to plants (Cross and Schlesingerand, 1995), especially when the pH values are adequately achieved by liming practice. This means that microbes also immobilize part of the soil solution P. After their death, part of this immobilized P remains in soils as organic compounds and the other part is mineralized

(Moreira and Siqueira, 2002). The content of total soil P varies from 200 to 5,000 mg kg^{-1}, with an average value of 600 mg kg^{-1}, of which 20 to 80% are organic forms (Willard, 1979; Schachtman et al., 1998). Therefore, NT contributes to increase organic P.

Soluble organic compounds and P speciation by XANES-spectroscopy

The mineral adsorption is one of the most important mechanisms of P retention onto soil colloids. Therefore, solid-state speciation has been employed by using X-ray absorption near edge structure spectroscopy (XANES) based on synchrotron light (Ginder-Vogel and Sparks, 2010), a high energy electromagnetic radiation emitted from the shift in the direction of electrons (which moves close to the speed of light) by the action of a magnetic field (Lombi and Susine, 2009). The process of absorption and fluoresce evolves specific energies of X Rays incident on the sample. Such energies are representative of the atomic electric configuration, which confers elements specificity to the X-ray absorption spectroscopy (XAS) technique (Lombi and Susine, 2009). It is essential for the chemical speciation of elements in its solid state from heterogeneous samples, such as soils, with a minimum or absent sample pre-treatment (Abdala et al., 2015). The XANES has been produced some information about anion sorption in metallic oxides and silicate clays: structure, stoichiometry, bond geometry and presence of multinuclear complexes and precipitated phases (Ginder-Vogel and Sparks, 2010); and for this reason, it has been used for soil P speciation, in which the species of this element are distinguished by the comparison of spectral characteristics of an unknown sample with those from a standard spectrum (Hesterberg, 2010).

Organic anions form chelates with Fe and Al and release P into soil solution (Oburger et al., 2011). Such anions are naturally exuded from plant roots especially from dicotyledonous (such as soybean), and are produced by soil microorganisms during organic matter decomposition (Hees et al., 2000; Vyas and Gulati, 2009). Therefore, the concentrations of organic anions are higher under NT and increases even more in the rhizosphere region under stress conditions, such as nutritional deficiency (e.g., lack or fertilizers) and Al toxicity (Fujii et al., 2013; Jones et al., 1996). Active aluminum in soil solution is the primary condition to trigger organic acid exudation by plants (Jones, 1998). Dissolved organic carbons include mostly low molar mass organic anions – LMMOA (Mimmo et al., 2011), such as citric, malic and oxalic acids. By simulating the LMMOA, Santos (2016) observed a reduction of approximately 20% in the exchangeable Al contents in the 0-5 cm soil layer due to the high association constant between Al and DOC. However, the natural abundance of DOC may not be enough to improve the exploitation of phosphorus fertilization, especially in highly weathered soils with high P sorbing capacity (Oburger et al., 2011). Even so, by specialized root structural development, the concentration of some LMMOA in soil solutions can exceed 50 mmol L^{-1} (Oburger et al., 2011).

There was an increase of phosphate linked to Fe(III) oxides in relation to Al(III) oxides by an increasing in the DOC concentration, which suggests a higher dissolution by DOC complexes with Al than Fe and, therefore, higher redistribution of phosphate previously linked to Al oxides to the surface of Fe oxides (Santos, 2016). In this sense, alterations in the XANES speciation (P *K-edge*) showed that phosphate was mobilized from Al oxides towards Fe oxides (Santos, 2016). This can also be explained by the fast mobilization of amorphous Fe-DOC complexes and slow dissolution from crystalline Fe fractions (Jones et al., 1996).

Moreover, the sum of the Fe content extracted from DCB solution and ammonium oxalate acidic solution in an Oxisol was much higher than the Al contents extracted with the same solutions (Santos, 2016). In addition, DOC is also known for its dissolution of Fe-(hydr)oxides, such as hematite and goethite, which may otherwise enhance P sorption through the formation of highly reactive (hydr)oxides minerals (Hersman et al., 1995; Abdala, et al., 2015). Such rates of dissolution depend on the soil pH and tend to reduce when manures are applied due to the consequent raise of soil pH (Abdala et al., 2015). In summary, Al- and Fe-(hydr)oxide dissolution and the abundant amount of P and organic matter presented in these soils will directly affect the formation of Al/Fe-P, and Al/Fe-OC, (Abdala et al., 2015).

From XANES analysis, the pre-edge crest around 2148 *eV* was representative of the crystalline Fe phosphates (Hesterberg et al., 1999; Khare et al., 2005; Ingall et al., 2011) and it is even more prominent in crystalline than non-crystalline minerals (Hesterberg et al., 1999; Kruse and Leinweber, 2008). Similarly, soil samples from native forest showed a small *pre-edge* of non-crystalline minerals indicating that crystalline Fe minerals are originally found in soils under managements that aim to a higher accumulation of organic material (Abdala et al., 2015). Regarding to the *pre-edge,* the same soils from a forest exhibits a crest of 2148 *eV* (Abdala et al., 2015), also representative of the crystalline Fe-phosphates (Ingall et al., 2011). In addition, the Fe(III) reduction by organic matter is favored by a thermodynamic process which can lead to the formation of non-crystalline Fe(II) and Fe(III) minerals (Lovley, 1987), supporting the hypothesis that the amorphous mineral is being formed due to a continuous application of organic material in soils under long-term conventional tillage (Abdala et al., 2015).

Thus, the reduction of the soil P sorption capacity as the result of the application of materials containing high amount of C and its eventual block in the adsorption sites has been shown as non-applicable to soils cultivated under conventional tillage, due to the formation of highly P-reactive Fe and Al amorphous minerals, evidenced in XANES by P *K-edge* spectra (Abdala et al., 2015). On the other hand, the crystallized forms are more commonly found in uncultivated soils, which maintain the organic matter on the surface (Abdala et al., 2015). It cannot be completely excluded the existence of P linked to Al in soils, considering that XANES provides the average of the measurements of the species present around the sample (Abdala et al., 2015).

The pH value from soil samples of an Oxisol, close to 6.0, favored the precipitation of P with Ca and Mg (Pierzynski et al., 2005). On the other hand, lower pH associated with high extractable Fe contents favored the formation of secondary minerals of Fe-P. Notably, the *K-edge* spectra for the orthophosphate (P_{inorg}) reacted with the goethite in pH values between 4.5 and 6.5 in the presence or absence of calcium (Abdala et al., 2015).

Finally, Synchrotron-based techniques have been more available over the years and have great potential to provide detailed information that cannot be obtained with the use of P speciation methods based on wet chemistry. In this sense, a possible resorption of the P released from a phase by an extracting solution can be avoided by the solid-state P speciation through the X-ray absorption near edge structure spectroscopy (XANES), from P K- (~2,1 keV) or L-edges (~140 eV) X-ray absorption spectra (10 eV before the P absorption edge to 50 eV above the absorption edge) followed by the linear combination of X-ray absorption spectra taken for P standards fitted to a X-ray absorption spectrum measured in a solid sample containing P. The L-edge XANES allows a greater discrimination of P phases;

however, this measurement requires P amounts ≥ than 1000 mg kg^{-1} for providing usable spectra. Although being less able to differentiate P forms than the L-edge spectra, the K-edge ones can be well measured in soil samples having less P contents (Hesterberg et al., 1999).

Biochar as a heavy-metal soil amendment

Biochar is a carbon-rich by-product produced from the pyrolysis of biomass feedstock under partial or total absence of oxygen (Lehmann and Joseph, 2015). Amending soil with biochar has received increasing attention as a method for sequestrating carbon in soils, thereby reducing carbon dioxide (CO_2) emissions (Lehmann et al., 2006; Lehmann, 2007). Moreover, increased soil carbon sequestration has improved soil quality due to the vital role of carbon in soil physical, chemical and biological processes (Stevenson, 1994).

Amending soil with biochar is not a new concept and has been practiced over a long period of time. For example, the high fertility of anthropogenic dark earth soils known as a Terra Preta de Indio in the Amazon basin has been related to the high content of charred materials (Glaser et al., 2002). The source of char in these soils is considered to have been a disposal of charcoal from domestic fires and the practice of slash and char agriculture by Pre-Columbian Amazonian Indians (Glaser et al., 2002; Sombroek et al., 2003). However, these soils have remained fertile and rich in biochar derived carbon stock for hundreds to thousands of years after they were abandoned.

In addition to the role of biochar in increasing the sequestration of carbon and influencing CO_2 emissions, biochar has been shown to enhance soil quality as well as to stabilize heavy metals (Ahumada et al., 2014). Biochar has a potential benefit for improving soil fertility (Chan et al., 2008; Novak et al., 2009), improving soil properties such as pH

(Houben et al., 2013), cation exchange capacity (CEC) and water holding capacity (Streubel et al., 2011), enhancing plant growth (Peng et al., 2011), and reducing nutrient leaching (Laird et al., 2010). Moreover, biochar has the ability to immobilize heavy metals such as Cd, Pb and Zn and thereby to reduce bioavailability and toxicity of heavy metals to plants in contaminated soils, notably because it raises the soil pH (Houben et al., 2013) and increases CEC. The biochemical effects of biochars in soils were significantly influenced by biochar addition more than by other practices to elevate soil pH such as liming (Lu et al., 2015). According to the authors, biochar should be prioritized over the lime in order to remediate heavy metal-polluted areas, mainly when acidic conditions can lead to the leaching of metals and threatening of groundwater. Hence, poultry litter-derived biochar (PLB) was very effective in immobilizing Cd, even under conditions of strong acidic deposition, thus preventing Cd leaching to the groundwater (Lu et al., 2015). Besides raising the soil pH, the enhanced organic carbon provided by biochar addition contributes to decrease the available concentration of heavy metals by reducing metal mobility and bonding metals into more stable fractions (Xu et al., 2016; Zhang et al., 2017). The increase of both pH and organic carbon also contribute to a higher CEC, then resulting in a higher heavy metals adsorption (Bolan et al., 2014).

Fellet et al. (2011) reported that the application of orchard prune derived biochar to mine tailings reduced bioavailable (DTPA-extractable) concentrations of Pb, Cd and Zn. Rice straw-derived biochar reduced the Cd concentration in the plant available soil fraction cultivated under greenhouse conditions (Zhang et al., 2017). However, biochars only slightly decreased or even significantly increased extractable heavy metals depending on the feedstock and pyrolytic temperature (Zhang et al., 2016; Karami et al., 2011). The uptake of

heavy metals to ryegrass planted in biochar-treated soils generally decreased with increasing pyrolytic temperature (Zhang et al., 2016). In this sense, biochar has the potential to reduce Cd and Pb accumulation in ryegrass shoot, which may be a viable option for safe cultivation in heavy metal polluted soils (Xu et al., 2016). Moreover, the concentrations of Cu, Pb and Zn had a direct inverse relationship with the concentration of biochars applied, with a significant effect for amendments >1% w/w applied. Particularly, the bioavailability of metals decreases gradually with time when the soil is amended by 5% or 10% of biochar (Houben et al., 2013).

Park et al. (2011) investigated the effects of chicken manure and greenwaste biochar produced at 550 ^{o}C on the immobilization and phytoavailability of Cd, Cu and Pb in metal-spiked and naturally metal contaminated soils, and found the application of biochars significantly decreased Cd and Pb mobility. Their study reported the application of biochar modified Cd and Pb from the easily exchangeable soil fraction to less available organic bond fraction. Additionally, they reported that biochar application increased the root and shoot dry biomass and decreased the accumulation of Cd, Cu and Pb in Indian mustard (*Brassica juncea*), thus illustrating the role of biochar in reducing metal toxicity while supplying plant nutrients. However, the chicken manure biochar was more effective in metal immobilization and plant growth than the greenwaste biochar. Ahmad et al. (2012) showed that mussel shell, cow manure and oak wood biochar application reduced Pb bioavailability and bioaccessibility in a highly contaminated military shooting range soil in Korea. Additionally, their study showed increases in germination percentage and root elongation of lettuce (*Lactuca sativa*) in soil treated with tested amendments, indicating a reduction of Pb toxicity. However, biochar was more effective in decreasing Pb toxicity than the other tested

amendments. The application of poultry litter-derived biochar (PLB) reduced the mobility of copper, cadmium, lead and zinc from 28 to 69%, 77 to 100%, 94 to 99% and 15 to 97%, respectively, in a naturally-contaminated soil.

A study conducted by Karami et al. (2011) observed that the addition of hardwood biochar to a heavy contaminated mine soil reduced pore water (solubility, or mobility) of Pb concentrations and ryegrass Pb levels, while the combination of biochar with greenwaste compost was more effective in reducing Pb in soil pore water and uptake by ryegrass. In that study, the biochar was more effective in reducing pore water Cu than greenwaste compost. Beesley et al. (2010) reported that the addition of hardwood-derived biochar and greenwaste compost to a multi-element contaminated soil significantly reduced concentrations of Cd and Zn in pore water during a 60-d exposure to field conditions and reduced phytotoxicity of these elements resulting in increased shoot emergence of ryegrass (*Lolium perenne* L. var Cadix). In contrast, concentrations of Cu and As in pore water increased with amendment applications. In a laboratory column study, Beesley and Marmiroli (2011) reported that hardwood biochar reduced the concentrations of Cd and Zn in leachate obtained from a multi-metal polluted soil with evidence of surface retention of both metals on biochar. Overall, the influence of biochar on heavy metal extractability varies depending on the feedstock, application rate, and biochars particle size (Yang et al., 2016). Generally, biochar is a promising tool to reduce the mobility of heavy metals in mining areas.

Uchimiya et al. (2010) compared the impacts of broiler litter-derived biochar and pecan shell-derived steam activated carbon amendments on Cu, Ni, and Cd immobilization and the effects of oxidation on mineral retention in synthetic rainwater leaching experiments. Their study found that biochar was most effective in immobilizing Cu, whereas activated

carbon immobilized Ni and Cd to a greater extent than biochar. In an acidic Norfolk sandy loam soil, Uchimiya et al. (2011a) observed that the stabilization of heavy metals (Cu, Pb, Cd and Ni) by biochars were directly related to the quantity of surface oxygen-functional groups of biochars. However, Uchimiya et al. (2011b) reported that the amendment of biochar enhanced copper sorption in a sandy loam soil primarily by cation exchange mechanism, whereas in a clay rich alkaline soil, sorption on mineral component and precipitation assisted in Cu retention. Biochar addition increased sorption capacity of soil matrix for any added contaminants (Uchimiya et al., 2011c).

Biochars are effective in immobilization of heavy metals and this effectiveness varies depending on biochar nature and pyrolysis conditions. Uchimiya et al. (2012a) investigated the impact of pyrolysis temperature on biochars ability to stabilize heavy metals in a Small Arms Range soil using broiler litter biochars produced at 350 ^{o}C and 650 ^{o}C. They found that both biochars were effective for stabilizing Pb and Cu at application rates of $\leq$ 5% without releasing Sb. In other experiments, Uchimiya et al. (2011d) and Uchimiya et al. (2012b) suggested using biochars prepared at high temperature, 650 to 800 ^{o}C and up to 700 ^{o}C, respectively, for remediation purposes.

However, low temperature biochar was more effective in stabilizing Pb than high temperature biochar; this might be due to higher soluble P concentration of low temperature biochar, which resulted in a greater Pb stabilization by the formation of lead phosphate precipitates (Uchimiya et al., 2012a). In similar experiments using oxidized and unoxidized plant-derived biochars, Uchimiya et al. (2012b) observed that oxidized biochars rich in carboxyl functional groups had greater ability for Pb, Cu and Zn stabilization than unoxidized biochars. The effect of biochars on mobility of heavy metals in soil is not only a

function of the pyrolysis temperature, but also the feedstock used, and soil properties. Moreover, the most important factor of biochar to reduce the bioavailability of heavy metals in soil depends on its functional surface groups, specific surface area and porosity.

Finally, phytoremediation combined with biochar addition enhances soil biology (Houben et al., 2013). However, the mechanisms behind the stimulatory effect of biochar on soil biochemical parameters are still unknown, probably more related to the pH effect for microbial activity and soil respiration than to soil enzymes or soluble compounds present in the biochar (Lu et al., 2015).

Tar Creek site

The area now known as Tar Creek is a part of the Tri-state mining district. Tri-state mining district is located in the border region of Oklahoma, Kansas and Missouri. Oklahoma portion of Tri-state mining district includes the communities of Cardin, Commerce, North Miami, Picher, and Quapaw, in Ottawa County, Oklahoma. Due to rich deposit of Zn and Pb ore, this area was mined during the early 1900s to the 1970s. Because of mining and milling operations, large quantities of wastes (coarse material contaminated with Pb, Cd and Zn), locally referred to as chat, were left on ground surface in piles. Chat was used for home gardens, driveways, roadway, parking lots, sandbag and sandblasting sand, and railroad ballast (EPA, 2005), while many of chat piles remain across the region. These uses of chat throughout of those communities resulted in lead contamination outside the areas that were used for mining and milling operations (EPA, 2011). In addition, chat accumulations in Tar Creek site have distorted the land, inhibited productive use, and impacted human health.

References

Abdala, D. B., da Silva, I. R., Vergütz, L., & Sparks, D. L. (2015). Long-term manure application effects on phosphorus speciation, kinetics and distribution in highly weathered agricultural soils. Chemosphere, 119, 504-514.

Abbasi, M. K., Tahir, M. M., Azam, W., Abbas, Z., & Rahim, N. (2012). Soybean yield and chemical composition in response to phosphorus–potassium nutrition in Kashmir. Agron. J., 104, 1476-1484.

Ahmad, M., Lee, S. S., Yang, J. E., Ro, H. M., Lee, Y. H., & Ok, Y. S. (2012). Effects of soil dilution and amendments (mussel shell, cow bone, and biochar) on Pb availability and phytotoxicity in military shooting range soil. Ecotox. Environ. Safe., 79, 225-231.

Ahumada, I., Sepúlveda, K., Fernández, P., Ascar, L., Pedraza, C., Richter, P., & Brown, S. (2014). Effect of biosolid application to Mollisol Chilean soils on the bioavailability of heavy metals (Cu, Cr, Ni, and Zn) as assessed by bioassays with sunflower (Helianthus annuus) and DGT measurements. J. Soils Sediment., 14, 886-896.

Alvarez, V. V. H., Novais, R. D., Barros, N. D., Cantarutti, R. B., & Lopes, A. S. (1999). Interpretação dos resultados das análises de solos. Recomendação para o uso de corretivos e fertilizantes em Minas Gerais, 5, 25-32. (In Portuguese).

Amaral Sobrinho, N. M. B., Velloso, A. C. X., Costa, L. M., & DE OLIVEIRA, C. (1994). Formas químicas de zingo e sua absorção por plantas de milho cultivadas em solo tratado com resíduo siderúrgico. Rev. Bras. Cienc. Solo, 18(2), 313-320. (In Portuguese, Abstract in English).

Anjos, L. D., Pereira, M. G., & Ramos, D. P. (1999). Matéria orgânica e pedogênese. Fundamentos da Matéria Orgânica: ecossistemas tropicais e subtropicais. Porto Alegre, RS. (In Portuguese).

Araújo, D.F.S., da Silva, A. M. R. B., de Andrade Lima, L. L., da Silva Vasconcelos, M. A., Andrade, S. A. C., & Sarubbo, L. A. (2014). The concentration of minerals and physicochemical contaminants in conventional and organic vegetables. Food Control, 44, 242-248.

Barrow, N. J. (1980). Evaluation and utilization of residual phosphorus in soils. In: Khasawneh, F. E.; Sample, E. C.; Kamprath, E. J. (eds.), editor/s. The role of phosphorus in agriculture. Proceedings of a symposium.; June 1-3, 1976; National Fertilizer Development Center, Tennessee Valley Authority, Muscle Shoals, Alabama, USA. Madison, Wisconsin, USA: American Society of Agronomy, Crop Science Society of America, Soil Science Society of America, 333-359.

Barrow, N. J. (1986). Reaction of anions and cations with variable-charge soils. Advances in Agronomy 38: 183-230.

Beesley, L., & Marmiroli, M. (2011). The immobilisation and retention of soluble arsenic, cadmium and zinc by biochar. Environ. Pollut., 159, 474-480.

Beesley, L., Moreno-Jiménez, E., & Gomez-Eyles, J. L. (2010). Effects of biochar and greenwaste compost amendments on mobility, bioavailability and toxicity of inorganic and organic contaminants in a multi-element polluted soil. Environ. Pollut., 158, 2282-2287.

Bolan, N., Kunhikrishnan, A., Thangarajan, R., Kumpiene, J., Park, J., Makino, T., et al. (2014). Remediation of heavy metal (loid) s contaminated soils–to mobilize or to immobilize? J. Hazard Mater., 266, 141-166.

Borges, R., & Mallarino, A. P. (2000). Grain yield, early growth, and nutrient uptake of no-till soybean as affected by phosphorus and potassium placement. Agron. J., 92, 380-388.

Buah, S. S., Polito, T. A., & Killorn, R. (2000). No-tillage soybean response to banded and broadcast and direct and residual fertilizer phosphorus and potassium applications. Agron. J., 92, 657-662.

Chan, K. Y., Van Zwieten, L., Meszaros, I., Downie, A., & Joseph, S. (2008). Using poultry litter biochars as soil amendments. Soil Res., 46, 437-444.

Chaudhary, M. I., Adu-Gyamfi, J. J., Saneoka, H., Nguyen, N. T., Suwa, R., Kanai, S., et al. (2008). The effect of phosphorus deficiency on nutrient uptake, nitrogen fixation and photosynthetic rate in mashbean, mungbean and soybean. Acta Physiol. Plant., 30, 537-544.

Chiezey, U. F., & Odunze, A. C. (2009). Soybean response to application of poultry manure and phosphorus fertilizer in the Sub-humid Savanna of Nigeria. J. Eco. Nat. Environ., 1, 025-031.

Crews, T. E., Kitayama, K., Fownes, J. H., Riley, R. H., Herbert, D. A., Mueller-Dombois, D., & Vitousek, P. M. (1995). Changes in soil phosphorus fractions and ecosystem dynamics across a long chronosequence in Hawaii. Ecology, 76, 1407-1424.

Cross, A. F., & Schlesinger, W. H. (1995). A literature review and evaluation of the. Hedley fractionation: Applications to the biogeochemical cycle of soil phosphorus in natural ecosystems. Geoderma, 64, 197-214.

Curi, N., & Franzmeier, D. P. (1987). Effect of Parent Rocks on Chemical and Mineralogical Properties of Some Oxisols in Brazil 1. Soil Sci. Soc. Am. J., 51, 153-158.

Engelstad, O. P., & Terman, G. L. (1980). In: Khasawneh, F. E.; Sample, E. C.; Kamprath, E. J. (eds.), editor/s. The role of phosphorus in agriculture. Proceedings of a symposium.; June 1-3, 1976; National Fertilizer Development Center, Tennessee Valley Authority, Muscle Shoals, Alabama, USA. Madison, Wisconsin, USA: American Society of Agronomy, Crop Science Society of America, Soil Science Society of America,, 311-332.

Fatima, Z., Zia, M., & Chaudhary, M. F. (2006). Effect of Rhizobium strains and phosphorus on growth of soybean Glycine max and survival of Rhizobium and P solubilizing bacteria. Pak. J. Bot., 38, 459.

Fellet, G., Marchiol, L., Delle Vedove, G., & Peressotti, A. (2011). Application of biochar on mine tailings: effects and perspectives for land reclamation. Chemosphere, 83, 1262-1267.

Fernández, F. G., Brouder, S. M., Volenec, J. J., Beyrouty, C. A., & Hoyum, R. (2009). Root and shoot growth, seed composition, and yield components of no-till rainfed soybean under variable potassium. Plant Soil, 322, 125-138.

Fontes, M. P. F., & Weed, S. B. (1991). Iron oxides in selected Brazilian oxisols: I. Mineralogy. Soil Sci. Soc. Am. J., 55, 1143-1149.

Fujii, K., Aoki, M., & Kitayama, K. (2013). Reprint of "Biodegradation of low molecular weight organic acids in rhizosphere soils from a tropical montane rain forest". Soil Bio Biochem., 56, 3-9.

Glaser, B., Lehmann, J., & Zech, W. (2002). Ameliorating physical and chemical properties of highly weathered soils in the tropics with charcoal–a review. Biol. Fert. Soils, 35, 219-230.

Ginder-Vogel, M., & Sparks, D. L. (2010). The impacts of X-ray absorption spectroscopy on understanding soil processes and reaction mechanisms. In: Developments in soil science, Elsevier, 34, 1-26.

Goulart, A. T., Fabris, J. D., de Jesus Filho, M. F., Coey, J. M. D., Da Costa, G. M., & De Grave, E. (1998). Iron oxides in a soil developed from basalt. Clay. Clay Miner., 46, 369-378.

Haq, M. U., & Mallarino, A. P. (2005). Response of soybean grain oil and protein concentrations to foliar and soil fertilization. Agron. J., 97, 910-918.

Harger, N. (2008). Faixas de suficiência para teores foliares de nutrientes em soja, definidas pelo uso do método DRIS, para solos de origem basáltica (Doctoral dissertation, Tese de Doutorado. Universidade Estadual de Londrina, Londrina. 88p). (In Portuguese, Abstract in English).

Hees, P.A.W. van, Lundström, U. S., & Giesler, R. (2000). Low molecular weight organic acids and their Al-complexes in soil solution—composition, distribution and seasonal variation in three podzolized soils. Geoderma, 94, 173-200.

Hersman, L., Lloyd, T., & Sposito, G. (1995). Siderophore-promoted dissolution of hematite. Geochim. Cosmochim. Ac., 59, 3327-3330.

Hesterberg, D. (2010). Macroscale chemical properties and X-ray absorption spectroscopy of soil phosphorus. In: Developments in soil science, Elsevier, 34, 313-356.

Hesterberg, D., Zhou, W., Hutchison, K. J., Beauchemin, S., & Sayers, D. E. (1999). XAFS study of adsorbed and mineral forms of phosphate. J. Synchrotron Radiat., 6, 636-638.

Houben, D., Evrard, L., & Sonnet, P. (2013). Mobility, bioavailability and pH-dependent leaching of cadmium, zinc and lead in a contaminated soil amended with biochar. Chemosphere, 92, 1450-1457.

Ingall, E. D., Brandes, J. A., Diaz, J. M., de Jonge, M. D., Paterson, D., McNulty, I., et al. (2011). Phosphorus K-edge XANES spectroscopy of mineral standards. J. Synchrotron Radiat., 18, 189-197.

Jenny, H. (1994). Factors of soil formation: a system of quantitative pedology. Courier Corporation.

Johnson, A. H., Frizano, J., & Vann, D. R. (2003). Biogeochemical implications of labile phosphorus in forest soils determined by the Hedley fractionation procedure. Oecologia, 135, 487-499.

Jones, D. L., & Brassington, D. S. (1998). Sorption of organic acids in acid soils and its implications in the rhizosphere. Eur. J. Soil Sci., 49, 447-455.

Jones, D. L., Darah, P. R., & Kochian, L. V. (1996). Critical evaluation of organic acid mediated iron dissolution in the rhizosphere and its potential role in root iron uptake. Plant Soil, 180, 57-66.

Karami, N., R. Clementi, E. Moreno-Jimenez, N.W. Lepp, & L. Beesley. (2011). Efficiency of green waste compost and biochar soil amendments for reducing lead and copper mobility and uptake to ryegrass. J. Hazard. Mater. 191, 41-48.

Khare, N., Hesterberg, D., & Martin, J. D. (2005). XANES investigation of phosphate sorption in single and binary systems of iron and aluminum oxide minerals. Environ. Sci. Tech., 39, 2152-2160.

Kolar, J. S., & Grewal, H. S. (1994). Effect of split application of potassium on growth, yield and potassium accumulation by soybean. Fert. Res., 39, 217-222.

Kruse, J., & Leinweber, P. (2008). Phosphorus in sequentially extracted fen peat soils: AK-edge X-ray absorption near-edge structure (XANES) spectroscopy study. J. Plant Nutr. Soil. Sc., 171, 613-620.

Laird, D., Fleming, P., Wang, B., Horton, R., & Karlen, D. (2010). Biochar impact on nutrient leaching from a Midwestern agricultural soil. Geoderma, 158, 436-442.

Lajtha, K., & Schlesinger, W. H. (1988). The biogeochemistry of phosphorus cycling and phosphorus availability along a desert soil chronosequence. Ecology, 69, 24-39.

Lehmann, J. (2007). Bio-energy in the black. Front. Ecol. Environ., 5, 381-387.

Lehmann, J., Gaunt, J., & Rondon, M. (2006). Bio-char sequestration in terrestrial ecosystems–a review. Mitig. Adapt. Strat. Gl., 11, 403-427.

Lehmann, J., & Joseph, S. (2015). Biochar for environmental management: an introduction. In: Biochar for environmental management, Routledge, 33-46.

Lombi, E., & Susini, J. (2009). Synchrotron-based techniques for plant and soil science: opportunities, challenges and future perspectives. Plant Soil, 320, 1-35.

Lopes, A. S., & Cox, F. R. (1979). Relação de características físicas, químicas e mineralógicas com fixação de fósforo em solos sob cerrados. Rev. Bras. Cienc. Solo, 3, 82-88. (In Portuguese, Abstract in English).

Lovley, D. R. (1987). Organic matter mineralization with the reduction of ferric iron: a review. Geomicrobiol. J., 5, 375-399.

Lu, H., Li, Z., Fu, S., Méndez, A., Gascó, G., & Paz-Ferreiro, J. (2015). Combining phytoextraction and biochar addition improves soil biochemical properties in a soil contaminated with Cd. Chemosphere, 119, 209-216.

Lu, H., Li, Z., Fu, S., Méndez, A., Gascó, G., & Paz-Ferreiro, J. (2015). Effect of biochar in cadmium availability and soil biological activity in an anthrosol following acid rain deposition and aging. Water Air Soil Pollut., 226, 164.

Malavolta, E. (1980). Elementos de nutrição mineral de plantas. São Paulo: Agronômica Ceres. (In Portuguese).

Mimmo, T., Hann, S., Jaitz, L., Cesco, S., Gessa, C. E., & Puschenreiter, M. (2011). Time and substrate dependent exudation of carboxylates by Lupinus albus L. and Brassica napus L. Plant. Physiol. Bioch., 49, 1272-1278.

Moreira, F.M.S., & Siqueira, J. O. (2002). Microbiologia e bioquímica do solo. Editora Ufla. (In Portuguese).

Nahas, E. (1991). Ciclo do fósforo: transformações microbianas. FCAV/UNESP. (In Portuguese).

Novais, R. D., & Smyth, T. J. (1999). Fósforo em solo e planta em condições tropicais (No. 631.422 N934). Universidade Federal de Vicosa, Vicosa, MG (Brasil). Dept. de Solos. (In Portuguese).

Novak, J. M., Busscher, W. J., Laird, D. L., Ahmedna, M., Watts, D. W., & Niandou, M. A. (2009). Impact of biochar amendment on fertility of a southeastern coastal plain soil. Soil Sci., 174, 105-112.

Oburger, E., Jones, D. L., & Wenzel, W. W. (2011). Phosphorus saturation and pH differentially regulate the efficiency of organic acid anion-mediated P solubilization mechanisms in soil. Plant Soil, 341, 363-382.

Okin, G. S., Mahowald, N., Chadwick, O. A., & Artaxo, P. (2004). Impact of desert dust on the biogeochemistry of phosphorus in terrestrial ecosystems. Global Biogeochem. Cy., 18, 1-9.

Oliveira Junior, A., Castro, C., Oliveira, F. A., & Jordão, L. T. (2013). Adubação potássica da soja: cuidados no balanço de nutrientes. International Plant Nutrition institute–Brasil, Piracicaba, 10. (In Portuguese).

Park, J. H., Choppala, G. K., Bolan, N. S., Chung, J. W., & Chuasavathi, T. (2011). Biochar reduces the bioavailability and phytotoxicity of heavy metals. Plant Soil, 348, 439.

Peng, X. Y. L. L., Ye, L. L., Wang, C. H., Zhou, H., & Sun, B. (2011). Temperature-and duration-dependent rice straw-derived biochar: Characteristics and its effects on soil properties of an Ultisol in southern China. Soil Till. Res., 112, 159-166.

Pierzynski, G. M., & McDowell, R. W. (2005). Chemistry, cycling, and potential movement of inorganic phosphorus in soils. In: Mullins, G. L. Phosphorus: agriculture and the environment, 53-86.

Porder, S., & Chadwick, O. A. (2009). Climate and soil-age constraints on nutrient uplift and retention by plants. Ecology, 90, 623-636.

Porder, S., & Ramachandran, S. (2013). The phosphorus concentration of common rocks—a potential driver of ecosystem P status. Plant Soil, 367, 41-55.

Premaratne, K. P., & Oertli, J. J. (1994). The influence of potassium supply on nodulation, nitrogenase activity and nitrogen accumulation of soybean (Glycine max L. Merrill) grown in nutrient solution. Fert. Res., 38, 95-99.

Raij, B. (1998). Bioavailable tests: alternatives to standard soil extractions. Commun. Soil Sci. Plan., 29, 1553-1570.

Raij, B. (1991). Fertilidade do solo e adubação (No. 631.42 R149f). Associaçao Brasileira para Pesquisa da Potassa e do Fosfato, Piracicaba (Brasil). (In Portuguese).

Raij, B. (1996). Recomendações de adubação e calagem para o Estado de São Paulo. Campinas: IAC. (Instituto Agronômico de Campinas. Boletim Técnico, 100), 1996. (In Portuguese).

Resende, M. (1976). Mineralogy, chemistry, morphology and geomorphology of some soils of the central plateau of Brazil. 1976. 237 f (Doctoral dissertation, Tese (Doutorado)-Purdue University, Lafayette).

Salcedo, I. H. (2006). Biogeoquímica do fósforo em solos da região Semi-árida do NE do Brasil. Rev. Geo., 23, 159-184. (In Portuguese).

Santos, R.S. (2016) Phosphorus dynamics in soils amended with low molar mass organic acids. Piracicaba, Universidade de São Paulo, Escola Superior de Agricultura “Luiz de Queiroz”, São Paulo, 67p. (PhD thesis). (In Portuguese, Abstract in English).

Schachtman, D. P., Reid, R. J., & Ayling, S. M. (1998). Phosphorus uptake by plants: from soil to cell. Plant Physiol., 116, 447-453.

Selmants, P. C., & Hart, S. C. (2010). Phosphorus and soil development: does the Walker and Syers model apply to semiarid ecosystems? Ecology, 91, 474-484.

Schulze, J., Temple, G., Temple, S. J., Beschow, H., & Vance, C. P. (2006). Nitrogen fixation by white lupin under phosphorus deficiency. Annals of Botany, 98(4), 731-740.

Silva, N. D. (1999). Nutrição mineral e adubação do algodoeiro no Brasil. Cultura do algodoeiro. Piracicaba, Potafos, 57-92. (In Portuguese).

Skoog, D. A., Holler, F. J., & Crouch, S. R. (2017). Principles of instrumental analysis. Thomson Brooks/Cole, Belmont, CA.

Sombroek, W. I. M., Ruivo, M. D. L., Fearnside, P. M., Glaser, B., & Lehmann, J. (2003). Amazonian dark earths as carbon stores and sinks. In Amazonian dark earths (pp. 125-139). Springer, Dordrecht.

Sousa, D. M. G., & Lobato, E. (2004). Adubação fosfatada em solos da região do Cerrado. Fosforo na Agricultura Brasileira, Yamada, T. and SRS Abdalla (Eds.), 157-196. (In Portuguese).

Stevens, P. R. (1968). A chronosequence of soils near the Franz Josef Glacier. University of Cantebury, Cantebury.

Stevenson, F. J. (1994). Humus chemistry: genesis, composition, reactions. John Wiley & Sons.

Streubel, J. D., Collins, H. P., Garcia-Perez, M., Tarara, J., Granatstein, D., & Kruger, C. E. (2011). Influence of contrasting biochar types on five soils at increasing rates of application. Soil Sci. Soc. of Am. J., 75, 1402-1413.

Taylor, S. R., & McLennan, S. M. (1985). The continental crust: its composition and evolution. Blackwell Scientific, Oxford.

Uchimiya, M., Bannon, D. I., Wartelle, L. H., Lima, I. M., & Klasson, K. T. (2012a). Lead retention by broiler litter biochars in small arms range soil: impact of pyrolysis temperature. J. Agr. Food Chem., 60, 5035-5044.

Uchimiya, M., Bannon, D. I., & Wartelle, L. H. (2012b). Retention of heavy metals by carboxyl functional groups of biochars in small arms range soil. J. Agr. Food Chem., 60, 1798-1809.

Uchimiya, M., Lima, I. M., Klasson, K. T., & Wartelle, L. H. (2010). Contaminant immobilization and nutrient release by biochar soil amendment: roles of natural organic matter. Chemosphere, 80, 935-940.

Uchimiya, M., Chang, S., & Klasson, K. T. (2011a). Screening biochars for heavy metal retention in soil: role of oxygen functional groups. J. Hazardous Mat., 190, 432-441.

Uchimiya, M., Klasson, K. T., Wartelle, L. H., & Lima, I. M. (2011b). Influence of soil properties on heavy metal sequestration by biochar amendment: 1. Copper sorption isotherms and the release of cations. Chemosphere, 82, 1431-1437.

Uchimiya, M., Klasson, K. T., Wartelle, L. H., & Lima, I. M. (2011c). Influence of soil properties on heavy metal sequestration by biochar amendment: 2. Copper desorption isotherms. Chemosphere, 82, 1438-1447.

Uchimiya, M., Wartelle, L. H., Klasson, K. T., Fortier, C. A., & Lima, I. M. (2011d). Influence of pyrolysis temperature on biochar property and function as a heavy metal sorbent in soil. J. Agr. Food Chem., 59, 2501-2510.

Vyas, P., & Gulati, A. (2009). Organic acid production in vitro and plant growth promotion in maize under controlled environment by phosphate-solubilizing fluorescent Pseudomonas. BMC Micro., 9, 174.

Walker, T. W., & Syers, J. K. (1976). The fate of phosphorus during pedogenesis. Geoderma, 15, 1-19.

Willard, L. L. (1979). Chemical equilibria in soils. John Wiley and Sons, New York

Xu, P., Sun, C. X., Ye, X. Z., Xiao, W. D., Zhang, Q., & Wang, Q. (2016). The effect of biochar and crop straws on heavy metal bioavailability and plant accumulation in a Cd and Pb polluted soil. Ecotox. Environ. Safe., 132, 94-100.

Yang, X., Liu, J., McGrouther, K., Huang, H., Lu, K., Guo, X., et al. (2016). Effect of biochar on the extractability of heavy metals (Cd, Cu, Pb, and Zn) and enzyme activity in soil. Environ Sci Pollut R, 23, 974-984.

Yin, X., & Vyn, T. J. (2004). Critical leaf potassium concentrations for yield and seed quality of conservation-till soybean. Soil Sci. Soc. Am. J., 68, 1626-1634.

Zhang, G., Guo, X., Zhao, Z., He, Q., Wang, S., Zhu, Y., et al. (2016). Effects of biochars on the availability of heavy metals to ryegrass in an alkaline contaminated soil. Environ. Pollut., 218, 513-522.

Zhang, R. H., Li, Z. G., Liu, X. D., Wang, B. C., Zhou, G. L., Huang, X. X., et al. (2017). Immobilization and bioavailability of heavy metals in greenhouse soils amended with rice straw-derived biochar. Eco. Eng., 98, 183-188.

CHAPTER II

SOYBEAN YIELD RESPONSE TO PHOSPHORUS FERTILIZATION IN AN OXISOL UNDER LONG-TERM NO-TILL MANAGEMENT

Abstract: Phosphorus (P) fertilizer recommendations for crops must be improved to optimize crop yields and minimize the environmental impact of P. We evaluated the effects of continuous annual fertilization (double crops) on soil-P availability by Mehlich-1 (P_{M-1}) and resin (P_{resin}), plant uptake, P responsive concentrations in the soil and soybean trifolioliate leaflets and the yields of two soybean (*Glycine max* L.) cultivars (BRS1010 and BRS1003) grown in a Brazilian Oxisol under 20 yr of no-till (NT) management. Four treatments representing a combination of annual P rates (0, 20, 40 and 50 kg P ha^{-1}) with a fixed K rate (40 kg ha^{-1}) were evaluated. Resin-extractable P was highly correlated with P_{M-1} (0.86, $p<0.05$) but P_{resin} was nearly 2.5 times as much as P_{M-1}. The soil extractable P was linearly correlated with P contents in trifoliolate leaflets with r of 0.72 and 0.66 (both at $p<0.05$) for P_{M-1} and P_{resin}, respectively. Maximum responsive concentrations of soil P_{M-1} and P_{resin} for the year studied were in the range of 13±2.2 to 20±5.7 and 30±5 to 59±19.2 mg P dm^{-3}, respectively. Soybean yields increased 29% as the rates of annual-P rate increased from 0 to 20 kg ha^{-1} and additional P application did not further improve yields. The trifoliolate leaflet P concentrations of both cultivars were

correlated ($r=0.66$, $p<0.05$) with soybean yields. The maximum responsive concentration of P in the soybean trifoliolate was 2.8±1.9 to 5.4±2.8 g kg^{-1} at R2 stage. Our results confirm that soil test for plant available P and plant tissue test are important to guide P fertilizer recommendations.
Keywords: Phosphorus; Nutrient Dynamics; No-till system; Long-term continuous fertilization; Soybean (*Glycine max* L.)

Introduction

Soybean yield, protein and oil content are directly affected by P fertilization (Adeli et al., 2005). Normal plant growth is limited when adequate P is not provided by soil or fertilizers. Deficiency of P can reduce nodulation, N_2 fixation, root proliferation and leaf area (Schulze et al., 2006; Chaudhary et al., 2008). Positive soybean yield responses to P fertilization have been frequently reported (Dodd and Mallarino, 2005; Fatima et al., 2006; Mabapa et al., 2010; Abbasi et al., 2012; Krueger et al., 2013).

Soil management or chemical amendment resulting in pH changes also influences P availability. No-till is generally known as a promoter of the pH reduction in the top soil layer due to the increase in organic acids and application of fertilizers (Hussain et al., 1999; Redel et al., 2011). The lower pH reduces P availability, which requires other management practices such as lime application. However, the increase in soil organic matter (SOM) under NT management also increases water storage and infiltration, and soil fertility while reducing runoff and the cost of nutrient inputs (Hobbs et al., 2008).

The recommendations of P fertilizers for crop production are generally based on phytoavailable P contents in the soil (van Raij, 1998; Broch and Ranno, 2012). Soil-P

availability is usually assessed by chemical extractants such as Mehlich 1 and 3 (Mehlich, 1984) or resin (van Raij, 1998). Therefore, it is important to understand soil P availability assessed by different extractants, plant uptake rates, and removal of P by harvesting in tropical soils under NT in order to apply P at the best time, and use the right method, rate and source (Cade-Menun, 2005; McLaughlin et al., 2011; Rodrigues et al., 2016; Withers et al., 2018).

The resin method was proposed in 1986 (when NT was initially introduced in Brazil), which was new in comparison to M-1, proposed in 1956. Therefore, it is important to compare the P extraction methods for Oxisols, which represents 40% of Brazilian soils.

Plant tissue analysis is essential to assess nutrient availability and crop response to applied nutrients. In soybean, nutrient contents in the 3rd trifoliolates are commonly used to diagnose nutrient status and guide fertilization decisions (Urano et al., 2007; Harger, 2008). The P content and its critical concentration in diagnostic leaves may vary among cultivars and P uptake may vary under different P availabilities.

Several studies have evaluated P in soil-plant systems under long-term NT. However, most researchers only evaluated the effects of seasonal application of fertilizers (e.g., one crop per year instead of splitting annual P application for both winter and summer crops) and few studies assessed residual P availability from previous P applications in Oxisols. Therefore, there is a need relating the annual application for double crops on the development of a single crop, especially in highly weathered tropical soils under long-term NT. Otherwise, any direct effect of annual P fertilization on soil fertility and soybean response might not be taken into consideration.

Our objectives for this study were to (**i**) assess soil P availability using M-1 and resin methods; (**ii**) study the relationship between P contents of soybean diagnostic leaf with soil test P

as affected by annual P application rates; and (**iii**) evaluate the response of soybean yields to soil test P and trifoliolate P concentrations in an Oxisol under 20 years no-till.

Material and methods

Study area description and soil characterization

A long-term field experiment has been conducted in a Rhodic Hapludox (Soil Survey Staff, 2014) since 1989 in Londrina, Parana State, Brazil (23º 11' S; 51º 10' W, 613 m a.s.l.). Prior to the experiment initiation, the surface soil (0-20 cm) had a clay content of 760 g kg^{-1}, pH (0.01 mol L^{-1} $CaCl_2$, 1:2.5 soil to solution mass ratios) of 4.5; 39 $mmol_c$ dm^{-3} Ca and 12 $mmol_c$ dm^{-3} Mg (extracted by 1 mol L^{-1} KCl, 1:5 soil to solution mass ratio); 9 mg dm^{-3} P and 4 mg dm^{-3} K (extracted by M-1). The regional climate is subtropical humid, with rainfall in all seasons and possible dry period during the winter. The average temperature of the hottest month is 25.5 ºC and 16.4 ºC in the coldest month. The experimental area has been managed under NT since 1995/96.

Experimental design and treatments

The experiment was a randomized block with four replications arranged in a split-plot design with two soybean cultivars (BRS1010 and BRS1003 representing 6.1 and 6.3 relative maturity group, respectively) as subplots. There were 12 treatments: control (no fertilizer application) and 11 combinations of P and K rates broadcast applied for both summer and winter crops; however, only four treatments receiving various amount of P with the same amount of K were selected to evaluate the effect of increasing P rates on soil and plant P concentrations as well as soybean yields (Table 1).

Table 1. Annual application rates of phosphorus (P) and potassium (K) in a Rhodic Hapludox under no-till

Treatments	Fertilization					
	....Summer....		....Winter....		....Whole year....	
	P†	K†	P†	K†	P†	K†
	.....kg ha^{-1}.....					
1	0	0	0	40	0	40
2	0	0	20	40	20	40
3	20	0	20	40	40	40
4	30	0	20	40	50	40

† Triple Superphosphate (~190 g P kg^{-1}) as P source and Potassium Chloride (~500 g K kg^{-1}) as K source

The experiment has been cultivated with soybean in the summer and wheat (*Triticum aestivum* L.) or oat (*Avena strigosa* L.) in the fall/winter season. The main plots were 160 m^2 (8 x 20 m) and subplots were 80 m^2 (4 x 20 m). The field was amended with dolomitic or calcitic lime at rates to raise base saturation to 70%: 1.5 Mg ha^{-1} in 1996/97, 2.0 Mg ha^{-1} in 2001/02, 1 Mg ha^{-1} in 2010/11, and 2 Mg ha^{-1} in 2012/13. In addition, 1 and 2.5 Mg ha^{-1} gypsum were applied in 2012/13 and 2014/15, respectively, to increase Ca and S availability and reduce exchangeable Al in the subsoil. The last P and K treatments were applied in October 2014 for soybean and in February 2015 for oats prior to soil sampling (29 Sept 2015). Rates of P and K fertilizers applied were very similar over the remaining years of the experiment with slight differences due to changes in the application recommendations over the years.

Soil chemical analysis

Soil samples were collected using an auger after oat harvest and prior to soybean sowing. Five subsamples from the 0-20 cm layer were collected to form a composite sample for each

plot. After sampling, soils were dried at 45 ºC for 24 h, ground to pass a 2-mm sieve, and stored in plastic cups for chemical analysis. Soil chemical characteristics pH, organic carbon (OC), extractable Ca, Mg, Al and potential acidity (H+Al) were determined per van Raij (1998) and Bertsch and Bloom (1996). Plant-available K was extracted by M-1 (K_{M-1}) and plant-available P was extracted by both M-1 (P_{M-1}) (Mehlich, 1984) and resin (P_{resin}) (van Raij, 1998). Phosphorus in the extracts was quantified as Murphy and Riley (1962) with a Bel Photonics UV-M51 spectrophotometer and K by atomic emission spectrometer (Helmke and Sparks, 1996). Exchangeable Al was extracted by 1 mol L^{-1} KCl solution with a 1:10 (v/v) soil/solution ratio, and quantified by the titrimetric standard method (Bertsch and Bloom, 1996). The exchangeable acidity ($Al^{3+} + H^{+}_{tit}$) was determined by titration of 25 mL KCl extract with 0.025 mol L^{-1} NaOH, using 1 g L^{-1} phenolphthalein as an indicator (titration from colorless to light pink). Then, the concentration of Al^{3+} was obtained by back-titration of the previously used KCl extract and after the acidification with a drop of concentrated HCl and addition of 40 g L^{-1} NaF + 0.025 mol L^{-1} HCl (titration from light pink to colorless, according to Bertsch and Bloom, 1996). Once the results were obtained, the effective and total cation exchange capacity (CEC*e* = Ca+Mg+Al+K_{M-1}; and CEC*t* = Ca+Mg+[H+Al]+K_{M-1}, respectively), the sum of base (SB = Ca+Mg+K_{M-1}), base saturation [BS% = (SB/CEC*t**100)], and aluminum saturation (Al% = Al/CEC*e**100) were then calculated.

Nutrient contents in soybean tissues and soybean grains

Twenty leaflets (third trifoliolate without the petiole from the apex) and 50 g of soybean seed (subsample of the harvested grains) were collected from subplots at the phenological stage R2 (full flowering) and R8 (full maturity), respectively (Broch and Ranno, 2012; Stammer and

Mallarino, 2018; Zobiole et al., 2012), from both soybean cultivars. Leaf samples were washed and oven-dried for 72 h at 50 ºC, followed by grinding to pass a 1-mm sieve. The ground leaf sample was digested in a microwave oven with HNO_3 and H_2O_2 in closed Teflon tubes under 170 ºC to 180 ºC and 2 MPa (Araújo et al., 2014). The elements in the digests were determined by an inductively coupled plasma atomic emission spectroscopy (ICP-AES, Thermo Scientific iCAP 6200, Waltham, MA). The plant nutrient concentrations were compared to established nutrient sufficiency levels for clayey soils (basalt) of Parana State, Brazil (Harger, 2008). Soybean grain yields (kg ha^{-1}) were calculated based on the sample mass and the area harvested and adjusted to 130 g kg^{-1} moisture content. The 300 grain weight was determined as well.

Data analysis

The soil chemical attributes were subjected to ANOVA by following the experimental design of randomized blocks and the treatment average compared by Tukey test. Nutrient contents of soybean tissue samples and soybean yields of both cultivars were also followed the randomized block design with subdivided plots in order to test the interaction of annual P rate by cultivar by Tukey test. The coefficient of determination was determined for specific variables, and the Pearson correlation was performed for each cultivar separately and both cultivars plotted together. A range of maximum responsive concentrations for soil test P (STP, P_{M-1} and/or P_{resin}) and soybean tissue P (P_{Tissue}) for the studied year were determined by fitting the segmented polynomials linear-plateau (LP) and quadratic-plateau (QP) response models using the NLIN (non-linear) procedure of SAS version 9.4 (SAS Institute, 2011). The models were accepted only when the NLIN convergence criterion method successfully converged and the model was significant ($p<0.05$). As done by Stammer and Mallarino (2018), the data from diagnostic leaves

and yields of both soybean cultivars were firstly plotted together. Cultivars were separated only when NLIN procedure failed to converge. The standard error (SE) of joint points was used to verify if cultivars had different maximum response to STP and P_{Tissue}.

Results and Discussion

Soil chemical properties

The average of pH, OC, extractable Ca, Mg, Al, exchangeable acidity (H+Al), effective cation exchange capacity (CEC*e)*, sum of base (SB) and aluminum saturation (Al%) were not different among P treatments ($p>0.05$), but K, total cation exchange capacity (CEC*t*) and base saturation (BS%) were slightly affected by P treatments ($p<0.05$) (Table 2). The lack of differences for the variables presented in Table 2 was probably due to previous lime applications aimed to raise the base saturation to the same level in all plots and treatments, and then brought all associated chemical attributes to similar levels. Since the last lime application was 3 yr. before soil samples were collected, we then assumed that BS% was probably already declined to 46% (Table 2). The high CEC*t* was probably attributed to the high potential acidity (H+Al), which is reflected by the low BS% values around 50% (Table 2).

Table 2. Chemical attributes in the surface layer (0-20 cm) of an Oxisol under long-term no-till before soybean sowing (September, 2015) with different P fertilization rates

P (kg ha^{-1})	pH $CaCl_2$	OC† g dm^{-3}	K_{M-1}*	Ca	Mg	Al	H+Al	CEC*e*‡	CEC*t*§*	SB¶	BS#*	Al††
						$mmol_c$ dm^{-3}					%	
0	5.2^{ns}	15^{ns}	1.8a	28.5^{ns}	10.6^{ns}	5.1^{ns}	36.4^{ns}	46^{ns}	77b	41.4^{ns}	53.6a	11^{ns}
20	4.9	15	1.0ab	23.3	8.4	6.1	47.5	39	80ab	32.9	41.1b	16
40	5.0	16	1.1ab	27.5	10.6	5.7	44.9	45	84a	39.5	47ab	13
50	4.9	15	0.9b	26	9.8	6.4	47.5	43	84a	36.9	44.1ab	15
p-value	0.05	0.49	0.03	0.11	0.07	0.12	0.05	0.07	0.03	0.08	0.04	0.13
CV (%)‡‡	3	6	34	11	12	12	12	8	4	11	12	19

* Significant at $p<0.05$ (n=4) ns = Non-significant

† OC = Organic carbon

‡ CEC*e* = Effective Cation Exchange Capacity ($Ca+Mg+Al+K_{M-1}$)

§ CEC*t* = Total cation Exchange Capacity ($Ca+Mg+[H+Al]+K_{M-1}$)

¶ SB = Sum of base ($Ca+Mg+ K_{M-1}$) # BS = Base saturation (SB/CEC*t**100)

†† Al% = Aluminum saturation (Al/CEC*e**100)

‡‡ CV = Coefficient of variation

Plant-available P

There was a significant linear correlation between P_{M-1} and P_{resin} (R^2 = 0.86*) when considering all 16 plots (Fig. 1) but resin extracted 2.4 times as much P as that of M-1. However, the interpretations should be similar as long as different P extraction methods are considered and corresponding calibrations are used.

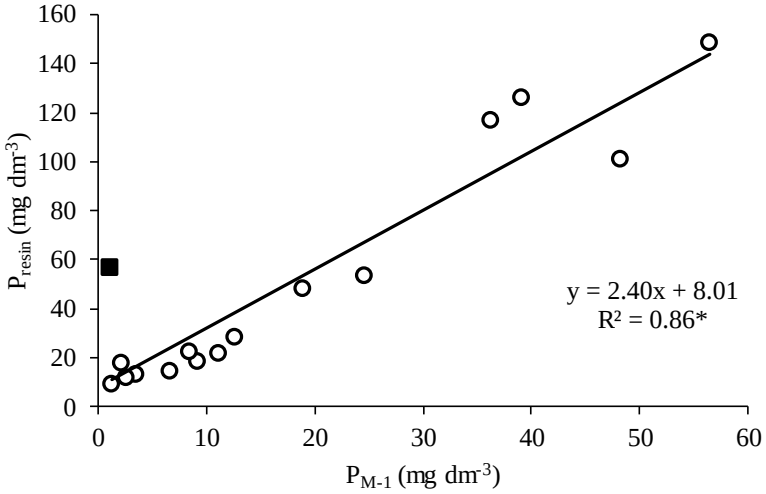

Fig. 1. Relationship between soil available P by M-1 (P_{M-1}) and resin (P_{resin}). * Significant at $p<0.05$. Black filled square point represents an outlier in the dataset (identified according to the Modified Thompson Tau Test: for n=4; τ=1.4250)

Plant-available P increased with the increase of P application rates for both extraction methods (Fig. 2). Similar results were reported by Prado et al. (2004), who conducted a similar experiment in an Oxisol. Plant-available P was the highest for treatment with 50 kg P ha^{-1}, and the control (0 kg P ha^{-1}) showed the lowest P availability. Therefore, we assume that the extent of P saturation on soil mineral fraction with the increased rates of P applied increases overtime. As a consequence, those soil mineral fractions become saturated with phosphate and more P

becomes readily extractable. Fig 2 shows a 5-6 fold increase in extractable P between 20 and 50 kg P ha^{-1} applied annually.

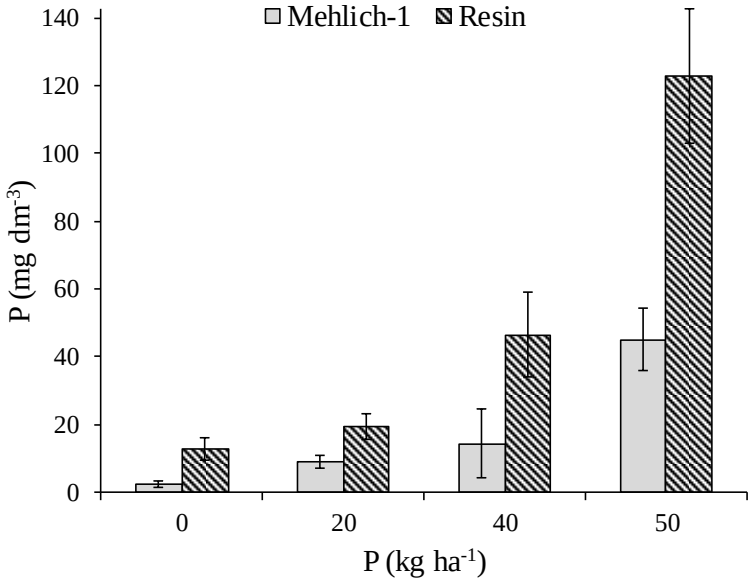

Fig. 2. Soil available phosphorus (P) extracted by M-1 and resin as affected by P fertilizer. Bars represent the standard deviation (significant at $p<0.01$ for n=4)

In general, M-1 extracted less P than resin did. The average P_{M-1} (n=4) was 19, 46, 31, 37% of the amount extracted by resin for the annual P rates of 0, 20, 40, 50 kg P ha^{-1}, respectively. The relationship between the two extractants indicates that with the increase in P availability the difference of P levels between the extraction methods is reduced. Resin is able to access soluble as well as labile fractions of P, which may explain its high extractability at low soil P (the control) (van Raij, 1998). The resin method has the advantage to be used regardless of soil clay content or pH, which is not the case for other extraction methods (van Raij, 1998). For example, while there is a solvent action of acids from M-1 (double-acid solution: 0.0125 mol L^{-1} H_2SO_4 + 0.050 mol L^{-1} HCl, pH 2 to 3), the resin is a synthetic material, as a 3D structure of

organic chains, containing functional groups with Na^+/OH^- charges, which adsorb $H_2PO_4^-$ ions; therefore, it is less affected by soil solution pH. No matter what P extraction method is used, STP is important in order to apply the optimum P rate required for high yields and to minimize P loss.

Naturally, the fertilizer P remaining in soils is slowly turned to less available forms by forming precipitated insoluble compounds or by diffusion into the interior of oxides (Sample et al., 1980; Eriksson et al., 2015). In the absence of annual addition of phosphate fertilizers, the crop yield will depend on the amount and availability of the residual P accumulated in soils. The crops can recover all or nearly all the P applied to the soil during a long-term (7 to 10 yr) cultivation (Sousa et al., 2002). Thus, fertilizer P not taken up by the current crop may be taken up by future crops or becomes a reserve. It should be taken into account when deciding P fertilization to avoid any over application, as what is probably happened in this 26-year experiment under continuous biannual P fertilization.

Organic P increases in soils under NT and biological processes tend to govern the availability of P to plants because microbes also immobilize part of the soluble P (Cross and Schlesinger, 1995), especially when soil pH is adequately adjusted by liming. After the death of microbes, part of the immobilized P remains in soils as organic compounds and the other part may be mineralized (Paul and Clark, 1989; Šantrůčková et al., 2004). Therefore, NT from our experiment may also contribute to increased soluble P in soil solution. In addition, the increase in the contents of available P with the increase in the rates of P (Fig. 2) also suggests that the 40 and 50 kg ha^{-1} y^{-1} P rates of application probably exceeded plant requirements and resulted in P accumulation in the soil. Such practice could be a problem since P loss can occur by runoff, which could negatively affect the environment.

The current adequate STP from M-1 for savannah soils in Brazil with a clay content >60% (Souza and Lobato, 2004) is >8.1 mg dm^{-3}. Only the control (0 kg P ha^{-1}) had a P_{M-1} content <8.1 mg dm^{-3}, which is considered deficient. On the other hand, the adequate STP using resin is 15 mg dm^{-3} (van Raij, 1998). Hence, the control treatments in this study are also considered deficient because the P_{resin} of this treatment was lower than 15 mg dm^{-3}. This suggests external P is needed for optimum crop yields.

Soybean leaf nutrient contents

The N contents in soybean leaf samples were higher ($p<0.05$) for the treatments that received P in comparison to the control (0 kg P ha^{-1}) for both cultivars BRS1010 and BRS1003. However, leaflet N contents were not different between cultivars for any treatment (Table 3). The average N contents were 59.1 and 57.5 g kg^{-1} for BRS1010 and BRS1003, respectively, which are considered sufficient for the diagnostic leaves without petiole according to Harger (2008) and Krueger et al. (2013). The P_{Tissue} followed the same trend as N (Table 3). The increase in soil P phytoavailability promoted increases in P uptake and resulted in 100% P content increase from the control to the highest rate (50 kg ha^{-1}) of P fertilizer applied for both cultivars (Table 3). Such change represents the transition from low (<2.8 g kg^{-1}) to sufficient range (2.8 to 4.2 g kg^{-1}) for trifoliolate leaflets collected without the petiole (Harger, 2008). The increased P rates contributed to the higher uptake of P, which was accompanied by the increased N content. No significant differences were found for the tissue K contents among P treatments except for the highest rate for cultivar BRS1003 in comparison to the control (Table 3). In General, the K values were deficient at R2 stage.

Table 3. Elemental contents of soybean leaves of cultivars BRS1010 and BRS1003 for different P fertilization rates (treatments)

P	BRS1010		BRS1003		Mean		BRS1010		BRS1003		Mean	
kg ha^{-1}	……N (g kg^{-1})……						……P (g kg^{-1})……					
0	50.4	bA	48.8	bA	49.6	b	2.2	bA	2.1	bA	2.1	b
20	59.7	aA	57.9	aA	58.8	a	3.4	aA	3.3	aA	3.3	a
40	62.8	aA	59.9	aA	61.3	a	4.0	aA	3.8	aA	3.9	a
50	63.6	aA	63.4	aA	63.5	a	4.1	aA	3.9	aA	4.0	a
Mean	59.1	A	57.5	A			3.4	A	3.3	A		
	……K (g kg^{-1})……						……Ca (g kg^{-1})……					
0	16.0	aA	18.1	aA	17.0	a	7.1	aA	6.8	aA	6.9	a
20	13.3	aA	15.4	abA	14.3	a	7.3	aA	7.0	aA	7.2	a
40	14.1	aA	15.0	abA	14.6	a	7.3	aA	7.5	aA	7.4	a
50	14.3	aA	13.3	bA	13.8	a	6.9	aA	6.9	aA	6.9	a
Mean	14.4	A	15.5	A			7.1	A	7.1	A		
	……Mg (g kg^{-1})……						……S (g kg^{-1})……					
0	4.1	bA	3.7	bA	3.9	b	1.7	bB	2.0	bA	1.9	b
20	5.0	aA	4.1	abB	4.6	a	2.0	aB	2.2	aA	2.1	a
40	5.1	aA	4.6	aB	4.8	a	2.0	aB	2.1	abA	2.1	a
50	5.1	aA	4.4	aB	4.7	a	2.0	aB	2.2	aA	2.1	a
Mean	4.8	A	4.2	B			1.9	B	2.1	A		
	……Zn (mg kg^{-1})……						……Mn (mg kg^{-1})……					
0	41.6	aA	33.0	aB	37.3	a	105.1	aA	117.0	aA	111.0	a
20	38.0	abA	29.9	abB	33.9	ab	93.8	aA	110.7	aA	102.2	a
40	35.0	bA	28.2	abB	31.6	b	106.1	aB	127.4	aA	116.8	a
50	33.0	bA	26.3	bB	29.7	b	101.0	aA	115.9	aA	108.4	a
Mean	36.9	A	29.3	B			101.5	B	117.8	A		
	……Fe (mg kg^{-1})……						……Cu (mg kg^{-1})……					
0	86.6	aA	102.9	aA	94.8	a	6.6	bA	6.4	bA	6.5	c
20	96.0	aA	102.8	aA	99.4	a	8.0	aA	7.5	aA	7.8	a
40	96.8	aA	98.7	aA	97.8	a	7.9	aA	7.0	abB	7.5	ab
50	97.0	aA	115.8	aA	106.4	a	7.6	aA	6.7	abB	7.1	bc
Mean	94.1	A	105.1	A			7.5	A	6.9	B		

Different lower and capital letters in columns and rows, respectively, are significant at $p<0.01$ (Tukey)

All treatments received P had higher Mg than the control for both cultivars (Table 3). The levels of Mg are considered high (>4.9 g kg^{-1}) for BRS1010 received 20 kg ha^{-1} to 50 kg ha^{-1} of P, and were considered sufficient/adequate (3.6 to 4.9 g kg^{-1}) for the control (Harger, 2008) (Table 3). In addition, BRS1010 had higher Mg in soybean tissue

than that of BRS 1003 for all treatments received P (Table 3). The adequate Mg levels observed can be attributed to a synergistic effect between P and Mg in terms of root uptake since P was adequately supplied for most treatments. For example, the Mg uptake could increase due to the increase in P uptake as a consequence of increased P applied. Indeed, P application rates raised both P and Mg in soybean leaves, as shown in Table 3. Moreover, the Mg acts as a carrier of P, thus increase P uptake resulted in the activation of ATPases in the membranes (Hawkesford et al., 2012; Baker et al., 2015).

Sulfur (S) contents in soybean leaf samples were not significantly different among treatments receiving P for both cultivars, but they were higher than the control (Table 3). The average S contents were 1.9 and 2.1 g kg^{-1} for BRS1010 and BRS1003, respectively. The S is considered low according to Harger (2008), Mallarino (2011) and Krueger et al. (2013). There was inadequate S in the topsoil probably due to the sulfate anion (SO_4^{2-}) leaching to the subsoil.

The micronutrient Zn, Mn, Fe and Cu contents in soybean leaves were not different among treatments with a few exceptions (Table 3). According to Harger (2008), Mallarino, (2011) and Krueger et al. (2013), those values are considered adequate or above the amount required in the case of Zn and Mn. Adequate levels of Zn in the leaves are in the range of 25 to 40 mg kg^{-1} whereas the adequate level of Mn is 108 mg kg^{-1} (Harger, 2008; Mallarino, 2011). However, the contents of Fe and Cu in our tissue samples are considered low according to the same authors (critical levels are 137 and 9 mg kg^{-1} for Fe and Cu, respectively). Moreover, the high contents of Mn inhibit the absorption of Fe and Cu due to competition of such elements for the root absorption sites, since those micronutrients are taken in their bivalent cationic forms through plant roots.

In addition, NT systems accumulate organic matter in the soil surface and then increase dissolved organic C (DOC), which can complex Fe and Cu ions and result in leaching from the root zone. Depending on soil pH, it is possible that free phosphate anions precipitate free Fe ions in the soil solution, which further reduces iron bioavailability (Zambrosi et al., 2008).

M-1 and resin P maximum responsive levels

Both P_{M-1} and P_{resin} were well correlated ($p<0.05$) with P_{Tissue} for both cultivars ($r = 0.73^*$ and $r = 0.65^*$, for BRS1010; $r = 0.72^*$ and $r = 0.69^*$, for BRS1003, respectively). The correlation between P_{M-1} and P_{Tissue} was better than that of P_{resin} and P_{Tissue}. The same trend was observed when both cultivars were combined. The relationship of our data was linear and/or quadratic until a plateau point (Fig. 3). Therefore, according to the distributed points, there is a maximum responsive value (Fig. 3), which was then defined through the linear and quadratic with plateau models applied to the same set of data (Fig. 3).

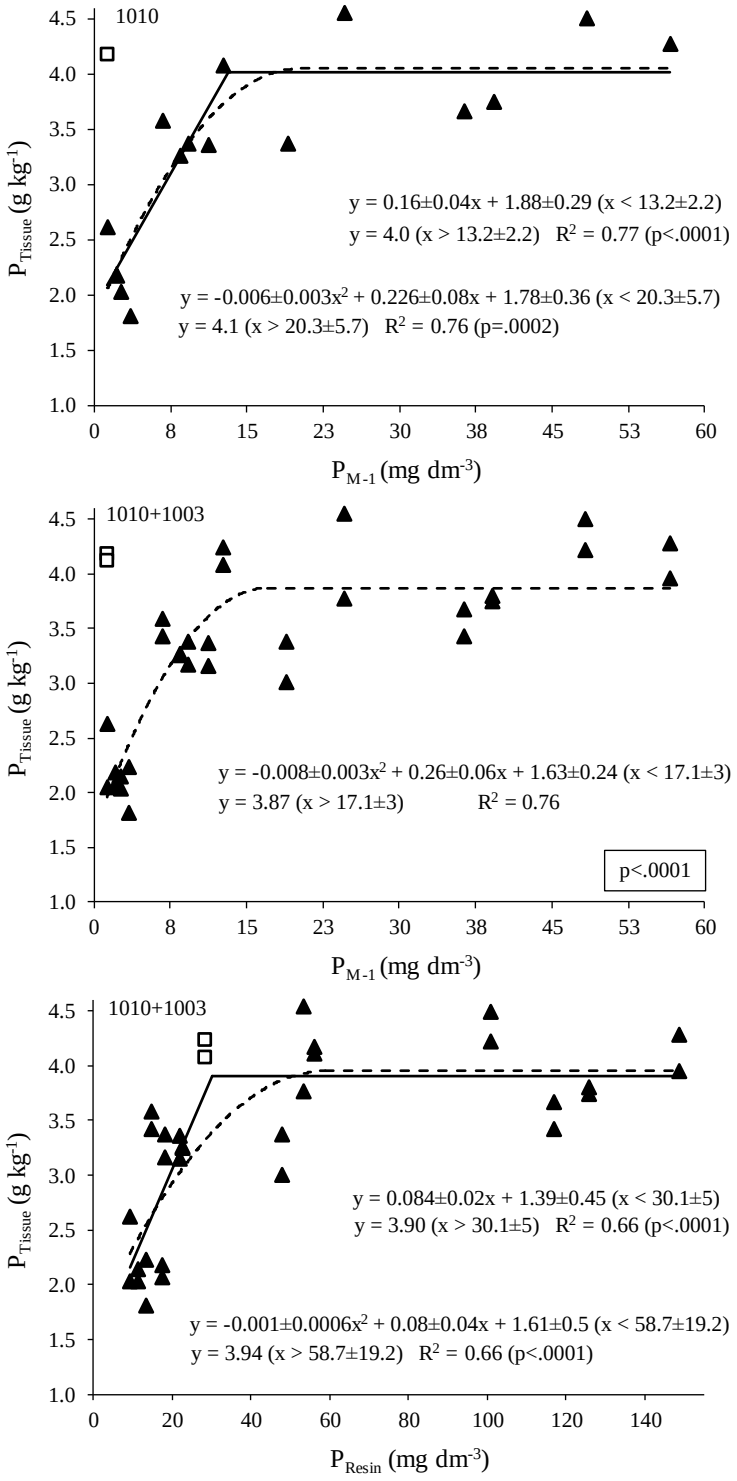

Fig. 3. Linear and quadratic plateau models between Mehlich-1 (P_{M-1}) and resin (P_{resin}) extractable plant available and soybean leaf P (P_{Tissue}) content for cultivars BRS1010 and BRS1003. One outlier of one variable (P_{M-1} and P_{resin}) from replication values was

removed (white square points) according to the Modified Thompson Tau Test (for n=4; τ=1.4250). Values following ± are standard deviations

Both linear plateau (LP) and quadratic plateau (QP) of P_{M-1} converged only for BRS1010 ($p<0.001$), but only QP converged for BRS1003. Therefore, a range of maximum responsive P_{M-1} values was defined only for BRS1010 (13.2±2.5 to 20.3±5.7 mg P dm^{-3}, Fig. 3). On the other hand, the QP converged ($p<0.0001$) when both cultivars were combined (Fig. 3), with a maximum responsive value of 17.1±3 mg dm^{-3} for P_{M-1}. As noticed, such maximum responsive P_{M-1} is in the range (17.1±3 g kg^{-1}) when taking into account both cultivars in comparison to only BRS1010 (13.2±2.5 to 20.3±5.7 mg P dm^{-3}). In the case of resin, a range value was obtained from both LP and QP with a maximum responsive P_{resin} of 30±5 to 59±19 mg dm^{-3} (Fig. 3). Since P_{resin} is extracting 2.4 times as much as P_{M-1} (Fig. 1), then the 41.0 mg dm^{-3} (17.1 mg dm^{-3} of P_{M-1} x 2.4 = 41.0 mg dm^{-3} of P_{resin}) is inside the range obtained from LP and QP of P_{resin}. When both LP and QP converged to the same dataset, the R^2 values from LP were higher than QP (Fig. 3), which probably suggests that LP provides a better fit than QP in this case.

Soybean yield response to P fertilization

Soybean yields were affected by the rates of P applied (Table 4). On average, both cultivars had higher yields for treatments receiving P than the control. The average yield of 2.6 Mg ha^{-1} for the treatment of 20 kg P ha^{-1} is already above the average soybean yield in Brazil at the time (2.5 Mg ha^{-1}) according to Zanon et al. (2016). However, when considering the yield for each cultivar separately, BRS1010 showed a yield higher than

2.5 Mg ha^{-1} for the lower rate of P applied (20 kg ha^{-1}), whereas BRS1003 only showed the same at the rate of 40 kg P ha^{-1}. The results from Table 4 clearly show that BRS1010 yielded higher than BRS1003 on average and for all individual treatments.

Table 4. Yields of soybean cultivars BRS1010 and BRS1003 for different P fertilization rates (treatments)

P	BRS1010		BRS1003		Mean	
kg ha^{-1}	……Yield (kg ha^{-1})……					
0	2110	bA	1951	bA	2030	b
20	2824	aA	2398	abB	2611	a
40	2925	aA	2505	aB	2715	a
50	2902	aA	2442	abB	2672	a
Mean	2690	A	2324	B		

Different lower and capital letters in columns and rows, respectively, are significant at $p<0.01$ (Tukey)

As shown in Table 4, the soybean yields of BRS1010 significantly increased as the application rates of P increased up to 20 kg ha^{-1} and no further increase was observed with more P applied ($p<0.01$). The non-response to the rates higher than 20 kg P ha^{-1} can be explained by the adequate supply of P from previous applications evidenced by the high soil available P discussed earlier. Also, with the 34% increase from the control, the average (n=4) yield for BRS1010 was 2.8 Mg ha^{-1} (Table 4). The P_{M-1} of 8.9 mg dm^{-3} for the 20 kg P ha^{-1} is adequate for soils with >60% of clay content in Brazilian savannah. However, when the P_{resin} values between 16 and 40 mg dm^{-3}, as in the case of 20 kg P ha^{-1} treatment, 15 kg P ha^{-1} is recommended for soils in Sao Paulo state with an expected soybean yield of 2.5 to 3.0 Mg ha^{-1} (Sfredo, 2008). In Parana state, when P_{M-1} is higher than 6.0 mg dm^{-3}, as observed for the 20 kg P ha^{-1} treatment, the P recommendation is 30

kg ha^{-1} for soils containing >40% of clay content (Sfredo, 2008). For P_{resin}, the value around 15 mg dm^{-3} obtained for 20 kg P ha^{-1} treatment also justifies the soybean yield obtained (van Raij, 1998).

As expected, the lowest yields were observed for the control (Table 4). On the other hand, the low rate of 20 kg P ha^{-1} achieved significant higher soybean yield (BRS1010) in comparison to the control. Therefore, no more than 20 kg P ha^{-1} is needed to apply for this cultivar. BRS1003 was slightly different from BRS1010 in yield response to P application. The former had significant yield increase when 40 kg P ha^{-1} was applied, but it was not different from the 20 kg P ha^{-1} applied (Table 4). Therefore, the nutritional requirement for soybean may vary as a function of genetic and environmental factors and management practices, which makes it difficult to standardize the nutritional requirements for soybean. No correlations were observed between rates of P and 300 grain weight for either soybean cultivar studied (data not shown).

The yield improvement in agricultural systems as a consequence of P fertilization strongly depends on plant species in the cropping system, soil available P contents, water availability, and other soil fertility factors. In general, yield increases occur in cultivated species when P contents are below or near 15 mg dm^{-3} with resin (van Raij, 1998). The P_{resin} was above this level for the two highest P rate treatments, which may explain why no significant yield increases were observed. Therefore, the P fertilization has to be cautiously managed through periodical soil testing and interpretation, according to area history, in order to avoid over application.

Maximum responsive P concentrations in soybean diagnostic leaves

As done for STP *Vs* P_{Tissue}, Pearson correlations were performed between soybean yield and leaf P content for both cultivars separately and together. In both cases, the correlation was significant ($p<0.05$) with r-values of 0.77* and 0.56* for BRS1010 and BRS1003, respectively, and 0.66* for both cultivars combined.

With the good relationship, soybean trifoliolate without petiole can be used as a diagnostic tool for estimating P sufficiency for soybean yield. Further, LP and QP were performed for the same variables in order to obtain the maximum responsive values of P_{Tissue} (Fig. 4). The LP and QP were not succeeded to converge from NLIN procedure when both cultivars were plotted together. However, BRS1010 by itself returned LP and QP with succeeded convergence criterion methods and a $p<0.01$ (Fig. 4). In such case, the range is 3.4±0.3 to 5.4±2.8 g P kg^{-1}, which is within the range of 3.5 to 4.7 g kg^{-1} found by Stammer and Mallarino (2018) for trifoliolate collected at the same soybean growth stages (R2), although their leaves were sampled with the petioles. The same authors showed critical P concentrations from LP lower then QP as well. Moreover, similar to their study, we also observed that the estimated P maximum responsive concentration for leaves by the QP model (5.4±2.8 g P kg^{-1}) was higher than the highest observed P concentration (4.5 g P kg^{-1}). On the other hand, only a maximum responsive concentration of 2.8±1.9 g P kg^{-1} was reached from LP ($p<0.05$) for BRS1003, but it was not converged for QP (Fig. 4). Such low P content (2.8 g P kg^{-1}) is close to the critical concentration of 2.5 g P kg^{-1} suggested by Fernandez and Hoeft (2009) in Illinois.

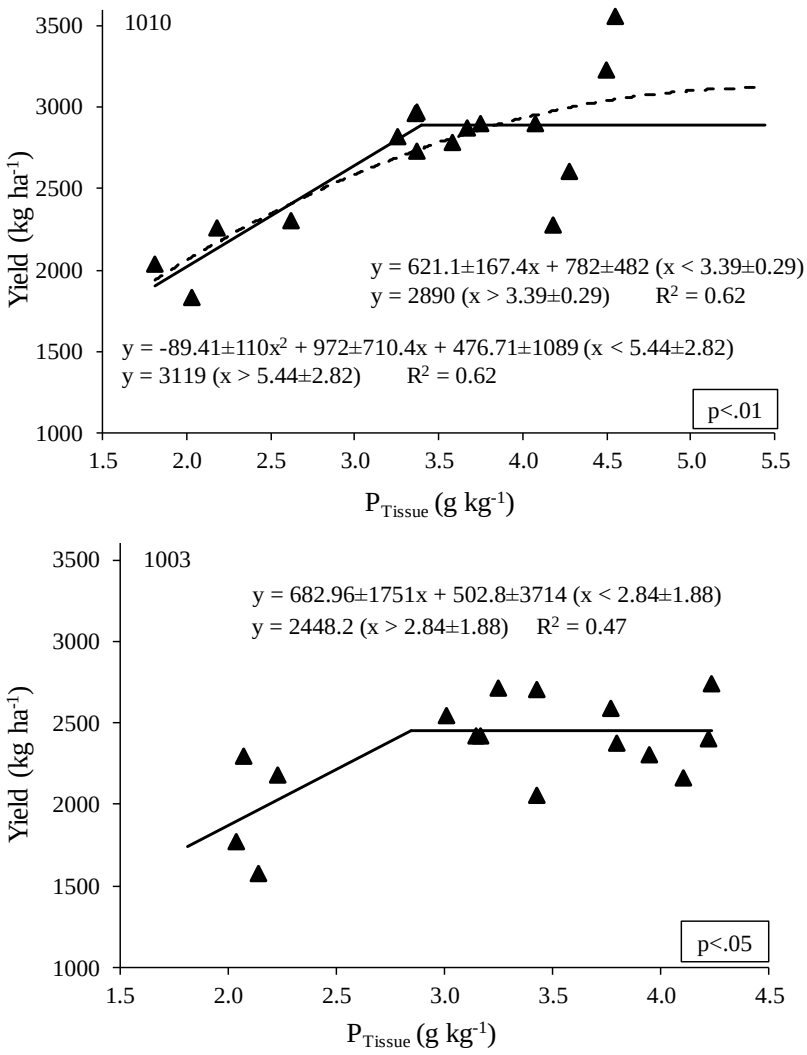

Fig. 4. Linear and quadratic plateau models for P content in trifoliolate with soybean yield for cultivars BRS1010 and BRS1003. Values following ± are standard deviations

As observed for the maximum responsive concentrations of STP, the same variable for the trifoliolate is in the same range of soybean cultivars, given the SE values. For example, in the case of our study, the maximum responsive concentration of BRS1003 is 2.8±1.9 g P kg^{-1} whereas the lower end for BRS1010 is 3.4±0.29 g P kg^{-1}.

The significant and convergence criterion methods of LP and QP responses may vary according to each cultivar.

Conclusions

Plant available P in the soil extracted by M-1 and resin was highly correlated (R^2 of 0.86, $p<0.05$), with resin extracting 2.4 times as much P as M-1. Both extraction methods were correlated with P contents in soybean tissue samples, with higher correlation coefficient for P_{M-1} ($r = 0.72$, $p<0.05$) than for P_{resin} ($r = 0.66$, $p<0.05$) for both cultivars. The maximum responsive concentration for the studied year of P_{M-1} and P_{resin} was 13.2±2.2 to 20.3±5.7 and 30.1±5 to 58.7±19.2 mg P dm^{-3}, respectively. Phosphorus and some other nutrients in soybean tissue samples increased as the application rate of P increased and P_{Tissue} was correlated ($r = 0.66$, $p<0.05$) with yields of both soybean cultivars. Tissue testing from trifoliolate leaflets collected without petiole can be used as an indicator of nutrient status and to guide fertilization. In our case, a general range of 2.8±1.9 to 5.4±2.8 g P kg^{-1} is the maximum responsive concentration for the optimum soybean yields. Soybean yields were increased up to 20 kg P ha^{-1} applied. The additional P applied beyond 20 kg P ha^{-1} during a long-term (26 years) continuous fertilization under NT contributed to soil P pool and may lead to potential P losses. Therefore, P application must be based on either soil test or plant analysis in order to optimize yields and minimize cost and environmental impacts.

References

Abbasi, K., M.M. Tahir, W. Azam, Z. Abbas, and N. Rahim. 2012. Soybean yield and chemical composition in response to phosphorus-potassium nutrition in Kashmir. Agron. J. 104:1476–1484.

Adeli, A., K.R. Sisani, D. Rowe, and H. Tewolde. 2005. Effects of broiler litter on soybean production and soil nitrogen and phosphorus concentrations. Agron. J. 97:314–321.

Araújo, D.F.S., A.M.R.B. Silva, L.L.A. Lima, M.A.S., Vasconcelos, S.A.C. Andrade, and L.A. Sarubbo. 2014. The concentration of minerals and physicochemical contaminants in conventional and organic vegetables. Food Control 44:242-248.

Baker, A., S.A. Ceasar, A.J. Palmer, J.B. Paterson, W. Qi, S.P. Muench, and S.A. Baldwin. 2015. Replace, reuse, recycle: Improving the sustainable use of phosphorus by plants. J. Exp. Bot. 66:3523–3540.

Bertsch, P.M., and P.R. Bloom. 1996. Aluminum. In D.L. Sparks (ed.), Methods of Soil Analysis Part 3—Chemical Methods, p. 517-550.

Broch, D.L., and S.K. Ranno. 2012. Soil fertility, fertilization and soybeans nutrition (In Portuguese). Fundação MS. Tecnologia e Produção: Soja e Milho, 2012.

Cade-Menun, B.J. 2005. Characterizing phosphorus in environmental and agricultural samples by ^{31}P nuclear magnetic resonance spectroscopy. Talanta 66:359–371.

Chaudhary, M.I., J.J. Adu-Gyamfi, H. Saneoka, N.T. Nguyen, R. Suwa, S. Kanai, H.A. El-Shemy, D.A. Lightfoot, and K. Fujita. 2008. The effect of phosphorus deficiency

on nutrient uptake, nitrogen fixation and photosynthetic rate in mashbean, mungbean and soybean. Acta Physiol. Plant 30:537–544.

Cross, A.F., and W.H. Schlesinger. 1995. A literature review and evaluation of the Hedley fractionation: Applications to the biogeochemical cycle of soil phosphorus in natural ecosystems. Geoderma 64:197–214.

Dodd, J.R., and A.P. Mallarino. 2005. Soil-test phosphorus and crop grain yield responses to long-term phosphorus fertilization for corn-soybean rotations. Soil Sci. Soc. Am. J. 69:1118-1128.

Eriksson, A.K., J.P. Gustafsson, and D. Hesterberg. 2015. Phosphorus speciation of clay fractions from long-term fertility experiments in Sweden. Geoderma 241:68–74.

Fatima, Z., M. Zia, and M.F. Chaudhary. 2006. Effect of Rhizobiumstrains and phosphorus on growth of soybean (Glycine Max) and survival of Rhizobium and P solubizing bacteria. Pak. J. Bot. 38:459–464.

Fernandez, F.G., and R.G. Hoeft. 2009. Managing soil pH and crop nutrients. In: Illinois Agronomy Handbook. Univ. of Illinois, Urbana Champaign.

Harger, N. 2008. Sufficiency ranges for foliar contents of nutrients in soybean, defined by the use of the DRIS method, for soils of basaltic origin. Ph.D. diss., Londrina State Univ. Londrina, 88p.

Hawkesford, M., W. Horst, T. Kichey, H. Lambers, J. Schjoerring, I.S. Møller, and P. White. 2012. Functions of macronutrients. In Marschner (ed.), Mineral Nutrition of Higher Plants. 3rd ed. Academic Press, San Diego.

Helmke, P.A., and D.L. Sparks. 1996. Lithium, sodium, potassium, rubidium, and

cesium. In D.L. Sparks (ed.), Methods of Soil Analysis Part 3—Chemical Methods, 5.3:551-574.

Hussain, I., K.R. Olson, and S.A. Ebelhar. 1999. Long-term tillage effects on soil chemical properties and organic matter fractions background of study site. Soil Sci. Soc. Am. J. 63:1335–1341.

Krueger, K., A. Susana Goggi, A.P. Mallarino, and R.E. Mullen. 2013. Phosphorus and potassium fertilization effects on soybean seed quality and composition. Crop Sci. 53:602–610.

Mabapa, P.M., J. B. O. Ogola, J. J. O. Odhiambo, A. Whitbread, and J. Hargreaves. 2010. Effect of phosphorus fertilizer rates on growth and yield of three soybean (Glycine max) cultivars in Limpopo Province. African J. Agric. Res. 5:2653–2660.

Mallarino, A.P. 2011. Interpretation of plant tissue test results for phosphorus and potassium in corn and soybean. In Proceedings of NCERA-13 Workshop.

McLaughlin, M.J., T.M. McBeath, R. Smernik, S.P. Stacey, B. Ajiboye, and C. Guppy. 2011. The chemical nature of P accumulation in agricultural soils-implications for fertiliser management and design: An Australian perspective. Plant Soil 349:69–87.

Mehlich, A. 1984. Mehlich 3 soil test extractant: A modification of Mehlich 2 extractant. Commun. Soil Sci. Pl. Anal. 15:1409-1416.

Murphy, J.A.M.E.S., and J.P. Riley. 1962. A modified single solution method for the determination of phosphate in natural waters. Analytica chimica acta. 27:31-36.

Paul, E.A., and F.E. Clark. 1989. Phosphorus Transformations in Soil. p. 222–232. In Soil Microbiology and Biochemistry. Academic Press, San Diego. 254 p.

Prado, R.M., L.F. Braghirolli, W. Natale, M.C.M. Corrêa, and E. V Almeida. 2004.

Potassium application on the nutritional status and dry matter production of passion fruit cutting. (In Portuguese, with English abstract). Rev. Bras. Frutic. 26:295–299.

Redel, Y.D., M. Escudey, M. Alvear, J. Conrad, and F. Borie. 2011. Effects of tillage and crop rotation on chemical phosphorus forms and some related biological activities in a Chilean Ultisol. Soil Use Manag. 27: 221–228.

Rodrigues, M., P.S. Pavinato, P.J.A. Withers, A.P.B. Teles, and W.F.B. Herrera. 2016. Legacy phosphorus and no tillage agriculture in tropical oxisols of the Brazilian savanna. Sci. Total Environ. 542:1050–1061.

Sample, E.C., R.J. Soper, and G.J. Racz. 1980. Reactions of phosphate fertilizers in soils. p. 263–310. In Khasawneh et al. (eds.), The role of phosphorus in agriculture. Am. Soc. Agron., Madison, WI.

Šantrůčková, H., J. Vrba, T. Picek, and J. Kopáček. 2004. Soil biochemical activity and phosphorus transformations and losses from acidified forest soils. Soil Biol. Biochem. 36:1569–1576.

SAS Institute. 2011. SAS system for Windows. Version 9.3. SAS Institute, Inc., Cary, NC.

Schulze, J., G. Temple, S.J. Temple, H. Beschow, and C.P. Vance. 2006. Nitrogen fixation by white lupin under phosphorus deficiency. Ann. Bot. 98:731–740.

Sfredo, G.J. 2008. Soybean in Brazil: Liming, fertilization and mineral nutrition. (In Portuguese). Londrina, Parana, BR. 147 p.

Soil Survey Staff. 2014. Keys to Soil Taxonomy. 12th ed. USDA-NRCS, Lincoln, NB.

Sousa, D.M.G., and E. Lobato. 2004. Savannah: soil remediation and fertilization (In Portuguese). Embrapa Cerrados.

Sousa, D.M.G., E. Lobato, and T.A., Rein. 2002. Phosphorus fertilization. In Sousa and Lobato (eds.), Savannah: soil correction and fertilization (In Portuguese). Planaltina, Embrapa Cerrados:147-168.

Stammer, A.J., and A.P. Mallarino. 2018. Plant tissue analysis to assess phosphorus and potassium nutritional status of corn and soybean. Soil Sci. Soc. Am. J. 82:260–270.

Urano, E.O.M., C.H. Kurihara, S. Maeda, A.C.T. Vitorino, M.C. Gonçalves, and M.E. Marchetti. 2007. Determination of optimal nutrient contents for soybean by the mathematical chance, diagnosis and recommendation integrated system and compositional nutrient diagnosis methods (In Portuguese, with English abstract). Rev. Bras. Ciência do Solo 31:63–72.

van Raij, B. 1998. Bioavailable tests: alternatives to standard soil extractions. Commun. Soil Sci. Pl. Anal. 29:1553–1570.

Withers, P.J.A., M. Rodrigues, A. Soltangheisi, T.S. De Carvalho, L.R.G. Guilherme, V.D.M. Benites, L.C. Gatiboni, D.M.G. De Sousa, R.D.S. Nunes, C.A. Rosolem, F.D. Andreote, A. De Oliveira, E.L.M. Coutinho, and P.S. Pavinato. 2018. Transitions to sustainable management of phosphorus in Brazilian agriculture. Sci. Rep. 8:1–13.

Zambrosi, F.C.B., L.R.F. Alleoni, and E.F. Caires. 2008. Liming and ionic speciation of an oxisol under no-till system. Sci. Agric. 65:190–203.

Zanon, A.J., N.A. Streck, T. Schmitz, C.M. Alberto, A.C. Bartz, G.M. De Paula, R. Tomiozzo, L. Camargo, C. Augusto, E.L. Tagliapietra, Â.P. Cardoso, P.S. Weber, and K.P. Bexaira. 2016. Growth habit effect on development of modern soybean cultivars after beginning of bloom in Rio Grande do Sul. Bragantia 75:446–458.

Zobiole, L.H.S., R.S. Oliveira Junior., J. Constantin, A. Oliveira JR, C. Castro, F.A. Oliveira, R.J. Kremer, A. Moreira, and L. Romagnoli. 2012. Nutrient accumulation in conventional and glyphosate-resistant soybean under different types of weed control (In Portuguese, with English abstract). Planta Daninha 30:75–85.

CHAPTER III

SOYBEAN PRODUCTION UNDER CONTINUOUS POTASSIUM FERTILIZATION IN A LONG-TERM NO-TILL OXISOL

Abstract: Potassium (K) is essential for soybean production but over use of K fertilizer negatively impact the environment and farming profit. Therefore, the optimum K recommendation needs to be verified, especially in pedo-environmental contrasting regions and long-term cultivated areas. We evaluated the effects of continuous annual K fertilization on plant-available K by Mehlich-1 (K_{M-1}) and ion exchange resin (K_{resin}), plant uptake (K_{Tissue}) and the yields of two soybean cultivars (*Glycine max* L.) grown in an Oxisol under long-term no-till (NT). The treatments included four K rates (0, 40, 75 and 110 kg ha^{-1}) with four replications. K_{resin} was highly correlated with K_{M-1} ($R^2 = 0.94$, $p<0.0001$). Plant-available K was linearly correlated with K_{Tissue} (trifoliate leaflets) with r of 0.76 and 0.82 ($p<0.0001$) for K_{M-1} and K_{resin}, respectively. Maximum K_{M-1} and K_{resin} that expressed the highest K_{Tissue} concentrations were in the ranges of 1.72±0.26 to 2.36±0.35 and 2.58±0.22 to 3.11±0.33 $mmol_c$ K dm^{-3}, respectively. The Ca+Mg/K ratios in tissues decreased by increasing K application. Soybean yields increased from 1823 to 2611 kg ha^{-1} as the rates of annual-K application increased from 0 to 40 kg ha^{-1}. Additional K application did not further improve yields. For yields, the maximum

responsive soil test K was 2.16±0.58 $mmol_c$ K dm^{-3} for K_{M-1} and 3.42±0.91 $mmol_c$ K dm^{-3} for K_{resin}; while the maximum responsive K_{Tissue} at R2 stage was 14.5±0.98 to 18.1±2.2 g K kg^{-1}. Our results confirm that soil test for plant-available K and plant tissue test are important to guide K fertilizer recommendations.
Keywords: Potassium availability; No-till system; Long-term continuous fertilization; Soybean

Introduction

Historically, Brazil has stood out and remains in the forefront as one of the largest fertilizer consumers in the world. With the no-till (NT) advent in 1973, soybean production increased markedly. In this context, a series of experiments were set up to study the impact of nutrient management practices on soybean in rotation with other crops under NT (Borkert et al., 1993; Silva et al., 1995; Antonangelo et al., 2019). About 32 million ha are cultivated soybean under NT in Brazil (Deuschle et al., 2019; Fuentes-Llanillo et al., 2018). Under NT, crop residues on soil surface protect the soil against erosion, and provide considerable nutrient reserves that are slowly mineralized and released to future crops (Rosolem and Calonego, 2013).

The recommendations of potassium (K) fertilizers for crop production are generally based on the exchangeable K in the soil (van Raij, 1998). Potassium availability is usually assessed by different extractants such as Mehlich-1 (Mehlich, 1984) or ion exchange resin (van Raij et al., 1986). Therefore, it is important to consider the chemical extraction mechanism of the extractants, plant uptake rates, K accumulation and K

exportation during growth and harvesting, and nutrient dynamics in the soil in order to apply K at the best time and use the best method, rate and source.

Potassium fertilization may affect soybean yield, grain protein and oil contents (Adeli et al., 2005). Factors related to soil, weather and plant species are extremely important for K availability prediction. Diffusion, a thermal movement, is the main mechanism of K transport in the soil. However, mass flow becomes more important in soils with high contents of K^+ (Ruiz et al., 1999). The rate of K diffusion varies with the K concentration in soil solution and its adsorption, organic matter (OM) content, and the amount and type of clay in the soil. Plant-availability of K is also linked to soil physical aspects, such as water content, pore size and texture (Holthusen et al., 2010) in addition to soil chemical aspects such as pH, cation exchange capacity (CEC) and the concentration and ionic strength of soil solution (Edmeades et al., 1985).

Plants generally contain 20 to 50 g K kg^{-1} in their dried mass for optimum growth (Marschner and Rengel, 2011). The soybeans take up around 17 to 32 kg K ton^{-1} of grain (Oliveira Junior et al., 2013). The K nutrition of soybean is influenced by environmental conditions and soil management during the growing season, genetic and climate factors, soil fertility and soil management. Soybean has shown responses to several rates of K application under various management regimes and agro-climatic conditions (Kolar and Grewal, 1994; Yin and Vyn, 2004). The surface application, broadcast and incorporated, and banding of K fertilizers generally do not affect soybean K uptake, since K is mostly retained by exchangeable sites or in soil solution (Scherer, 1998). Soybean takes up K as the plant develops, so any K deficiency during the growing season may reduce soybean yield (Kolar and Grewal, 1994; Parvej et al., 2016). However, a suitable K supply to

soybean promotes the increase in the number of nodules per plant, nodule size, and even the oil content of grains (Maathuis, 2009). However, most past studies only evaluated the effects of seasonal application of fertilizers (one crop per year). Therefore, there is a need to study the effects of annual K inputs on systems with two crops per year, especially in highly weathered tropical soils under long-term NT.

The determination of nutrient content in plant tissues is a tool that complements soil analysis and provides information related to the nutritional condition of cultivated crops. In the case of soybean, the 3rd trifoliate leaflets are used to indicate nutrient status and can be used as a guide for fertilization (Urano et al., 2007; Parvej et al., 2016). For this, it is essential to relate the K contents in diagnostic leaves and the yields obtained with different cultivars. In addition, it is important to determine which soil test K extractant best correlates with K concentrations in diagnostic leaves.

The objectives of this study were to (i) investigate how soil test K (STK) was affected by 26 years of annual K application rates; (ii) determine which soil test K (extracted by Mehlich-1 or resin) gave the best prediction of K in soybean diagnostic leaves; (iii) evaluate the relationships between soybean yields, soil test K and soybean tissue K in an Oxisol under 20 years of no-till operation.

Material and methods

Study area description and soil characterization

A long-term experiment has been conducted since 1989 at the Experimental Farm EMBRAPA-Soybean, Londrina, Parana State, Brazil (23º 11’ S; 51º 10’ W, 613 m a.s.l.). The soil is a Rhodic Hapludox, and its chemical and physical attributes prior to the

experiment initiation (1989) can be found in Antonangelo et al. (2019). According to *Köeppen*, the weather is Cfa, subtropical humid, with rainfall in all seasons and possible dry period during the winter and the average temperatures of the hottest and coldest month are 25.5 ºC and 16.4 ºC, respectively (Antonangelo et al., 2019). The experiment has been under NT since the 1995/96 season.

Experimental designs and treatments

The experimental design was a randomized block with four replications in a split-plot arrangement with two soybean cultivars (BRS1010 and BRS1003, representing 6.1 and 6.3 relative maturity group). There were 12 treatments: control (no fertilizer) and 11 combinations of K and P rates broadcast applied for both summer and winter crops; however, only four treatments receiving varying amounts of K and same amount of P (190 g kg^{-1} as Triple Superphosphate) were selected to evaluate the effect of increasing K rates on soil, plant K concentrations and soybean yields (Table 1). Rates of K fertilizers applied were very similar over the remaining years of the experiment with slight differences due to changes in the application recommendations over the years.

Table 1. Annual application rates of potassium (K) in a Rhodic Hapludox under no-till

Treatment	Fertilization			K
	....Summer....	....Winter....	....Whole year....	(kg ha^{-1})§
	.....K† kg ha^{-1}.....			
0	0	0	0	0
40	0	40	40	717
75	35	40	75	1550
110	70	40	110	2383

†Potassium Chloride (~500 g K kg^{-1}) was the K source

§Sum of applications for all crops since 1989.

In the experiment, crops like wheat (*Triticum aestivum* L.) or oat (*Avena strigosa* L.) were cultivated in the fall/winter seasons, whereas only soybean was cultivated in the summer. The subplot area was 80 m^2 (4 x 20 m). The last K treatments were applied in October 2014 for soybean (35 or 70 kg K ha^{-1}) and in February 2015 for oats (40 kg K ha^{-1}) prior to soil sampling (29 Sept 2015) for this evaluation. Aiming to raise soil base saturation to 70%, dolomitic or calcitic lime were applied at rates of 1.5 Mg ha^{-1} in 1996/97, 2.0 Mg ha^{-1} in 2001/02, 1 Mg ha^{-1} in 2010/11, and 2 Mg ha^{-1} in 2012/13. In addition, 1.0 Mg ha^{-1} (2012/13) and 2.5 Mg ha^{-1} (2014/15) of gypsum were applied to increase Ca and S availability and reduce exchangeable Al in the subsoil.

Soil chemical analysis

Soil samples were collected using an auger after oat harvest and prior to soybean sowing. Five subsamples from the 0-20 cm layer were collected to form a composite sample for each plot. Soil samples were dried at 45 ºC for 24 h, ground to pass a 2-mm sieve, and stored in plastic cups for chemical analysis. Soil pH, organic carbon (OC), extractable Ca, Mg, Al and potential acidity (H+Al) were determined per van Raij et al. (1986) and Bertsch and Bloom (1996). Plant-available P was extracted by Mehlich 1 (P_{M-1}) and plant-available K was extracted by both M-1 (K_{M-1}) (Mehlich, 1984) and resin (K_{resin}) (van Raij et al., 1986). Potassium in the extracts was quantified by an atomic emission spectrometer (Helmke and Sparks, 1996) and P colorimetrically (Murphy and Riley, 1962) with a Bel 108 Photonics UV-M51 spectrophotometer). Chemical analyses were also described by Antonangelo et al. (2019). Once the results were obtained, the total cation exchange capacity (CEC*t* = Ca+Mg+[H+Al]+K_{M-1}), base saturation (BS% =

(SB/CECt*100), where SB = Ca+Mg+ K_{M-1}), and aluminum saturation (Al% = Al/CEC*e**100, where CEC*e* (effective CEC) = CEC*t*-[H+Al]) were calculated.

Nutrient contents in soybean tissues and grains

Twenty leaflets (third trifoliate without the petiole from the apex) and 50 g of soybean seed (subsample of the harvested grains) were collected from subplots at the phenological stage R2 (full flowering) and R8 (full maturity), respectively (Stammer and Mallarino, 2018), from both soybean cultivars. Leaf samples were washed and oven-dried for 72 h at 50 ^{o}C, followed by grinding to pass through a 1-mm sieve. The ground leaf sample was digested in a microwave oven with HNO_3 and H_2O_2 in closed Teflon tubes at 170 ^{o}C to 180 ^{o}C and 2 MPa (Araujo et al., 2014). The elements in the digests were determined by inductively coupled plasma atomic emission spectrometer (ICP-AES, Thermo Scientific iCAP 6200, Waltham, MA). The plant nutrient concentrations were compared to established nutrient sufficiency levels for clayey soils (basalt) of Parana State, Brazil (Harger, 2008). Soybean grain yields (kg ha^{-1}) were calculated based on the sample mass and the area harvested and adjusted to 130 g kg^{-1} moisture content.

Statistical analysis

The soil chemical attributes were subjected to ANOVA by following the experimental design of randomized blocks and the treatment means were compared using a Tukey test. Nutrient contents of soybean tissue samples and yields of both cultivars were also followed the randomized block design with subdivided plots in order to test the interaction of annual K rate by cultivar with a 2-way ANOVA and using a Tukey test.

The coefficient of determination was determined for specific variables (K_{M-1}, K_{Resin}, K_{Tissue}, Ca, B and soybeans yield), and the Pearson correlation was performed for each cultivar separately and both cultivars plotted together. All data was analyzed considering the values of replicates. A range of maximum responsive concentrations for STK (K_{M-1} and/or K_{resin}) and soybean tissue K (K_{Tissue}) were determined by fitting the segmented polynomials linear-plateau (LP) and quadratic-plateau (QP) response models using the NLIN (non-linear) procedure of SAS version 9.4 (SAS Institute, 2011) with all replicate data. The models were accepted only when the NLIN convergence criterion method successfully converged and the model was significant (at least at $p<0.05$). As per Stammer and Mallarino (2018), the data from diagnostic leaves and yields of both soybean cultivars were plotted together. The standard error (SE) of joint points was used to verify if cultivars had different maximum response to STK and K_{Tissue}.

Results and discussion

Soil chemical properties

The soil pH, OC, P_{M-1}, extractable Ca, Mg and Al were not different among treatments ($p>0.05$) but exchangeable acidity (H+Al) and base saturation (BS%) were to some extent affected by K application rates ($p<0.05$) (Table 2). Moreira et al. (2015) working with a Typic Quartzipsamment reported the same behavior in a greenhouse experiment receiving 50 and 200 mg K g^{-1} soil with 11 soybean cultivars. Similar findings were also observed by Araújo et al. (2013), also in an Oxisol, where most of the soil chemical attributes listed above were not affected by the application of 0, 50, 100, 200 and 400 kg K ha^{-1}. The lack of differences for the other variables presented in Table

2 was probably due to previous lime applications aimed to raise the base saturation to the same level for all treatments. Since the last lime application was 3 yr. before soil samples were collected, we assumed that the average BS% across all rates probably already declined to 47% (Table 2). The high CEC*t* (78.4 mmolc dm^{-3} – average across all rates) was probably due to the high potential acidity (H+Al), which is reflected by BS% values below 60%. Antonangelo et al. (2019) observed very similar results when studying increased P rates applications with a fixed K rate in the same experimental area.

Table 2. Chemical attributes in the surface layer (0-20 cm) of an Oxisol under long-term no-till before soybean sowing (September, 2015) in response to K fertilization rates

K ($kg\ ha^{-1}$)	pH	OC† $g\ dm^{-3}$	P_{M-1} $mg\ dm^{-3}$	Ca	Mg	Al	H+Al*	CEC*t*§	BS#*	Al††
				……mmol$_c$ dm^{-3}……					.....%.....	
0	5.1	15	9.0	26.6	9.9	5.3	39.8b	77.2	49ab	13
40	4.9	15	8.9	23.3	8.4	6.1	47.5a	80.1	41b	16
75	5.1	17	6.7	26.0	9.1	5.3	38.6b	75.9	50a	12
110	4.9	16	8.2	23.8	8.3	6.0	42.7ab	80.2	49ab	14
p-value	0.22	0.08	0.588	0.377	0.122	0.05	0.02	0.306	0.04	0.149
CV (%)	3	7	31	7	11	8	8	5	8	15

* Significant at $p<0.05$ (n=4)
† OC = Organic carbon
§ CEC*t* = Total cation exchange capacity (Ca+Mg+[H+Al]+K_{M-1})
# BS = Base saturation (SB/CEC*t**100, where SB = Ca+Mg+ K_{M-1})
†† Al% = Aluminum saturation (Al/CEC*e**100, where CEC*e* = CECt-[H+Al])
‡‡ CV = Coefficient of variation

Plant-available K in the soil

Mehlich-1 (K_{M-1}) and exchange resin extractable K (K_{Resin}) had a significant linear correlation ($R^2 = 0.94$, $p<0.0001$) (Fig. 1), but K_{Resin} was 0.94 mmol dm^{-3} higher than K_{M-1}. This difference is a significant amount when soil test K is low. Therefore, K_{M-1} and K_{Resin} are not the same when K recommendations are concerned.

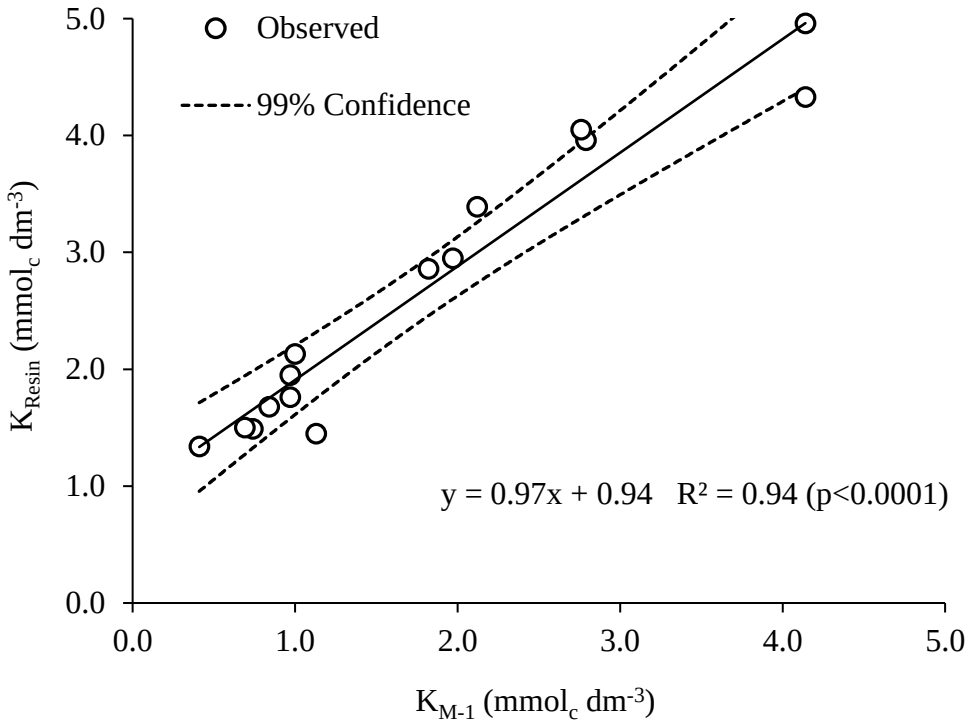

Fig. 1. Relationship between plant available K in the soil measured by Mehlich-1 (K_{M-1}) and ion exchange resin (K_{Resin}). One outlier in the dataset (identified according to the Modified Thompson Tau Test: for n=4; τ=1.4250) was removed

The extractable K measured by both methods increased with increasing K application rates (Fig. 2). The same trend was observed by Prado et al. (2004) and Araújo et al. (2013) in an Oxisol when conducting a similar experiment.

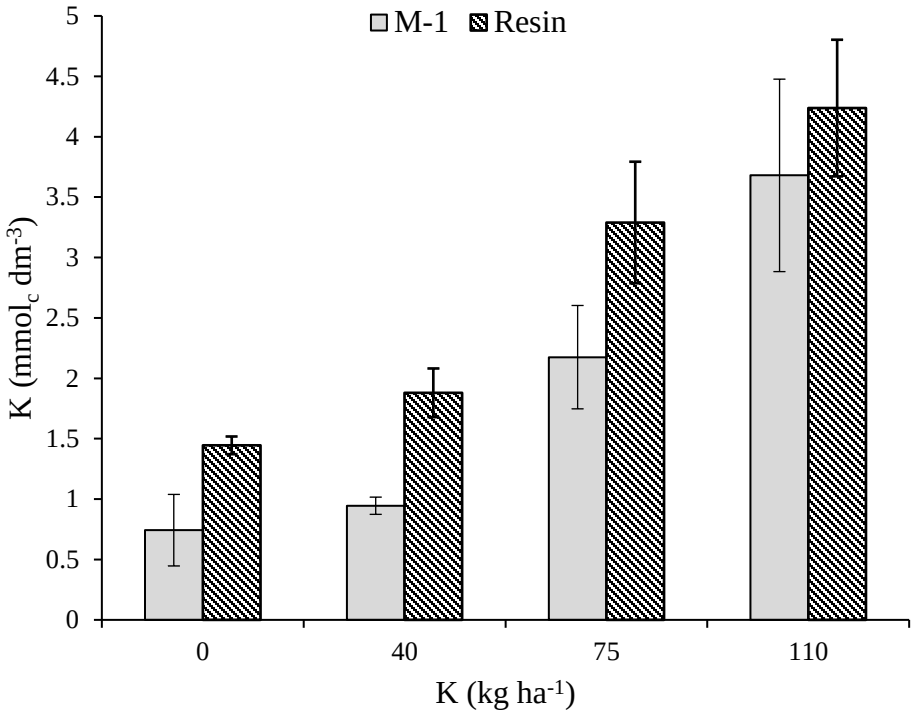

Fig. 2. Soil available potassium extracted by Mehlich-1 (K_{M-1}) and ion exchange resin (K_{Resin}) as affected by K application rates. Error bars represent the standard deviation (significant at $p<0.01$ for n=4)

The ion exchange resin method can be used for soils with distinct chemical and mineralogical characteristics from very acid to alkaline, which is not the case for other extraction methods (van Raij, 1998). However, Mehlich-1 extracted less K than exchange resin for some treatments (Fig. 2). The average amount (n=4) of exchangeable K extracted by Mehlich-1 were 48.4, 50.2, 66.1, 79.1% of the amount extracted by exchange resin for the rates of 0, 40, 75, 110 kg K ha^{-1}, respectively. Therefore, as the availability of K in the soil increases as a function of K rates, K extracted by both extractants become more similar. An opposite result was observed by Medeiros et al. (2010), who reported that exchange resin extracted less exchangeable K in less-developed

soils than Mehlich-1. The same authors attributed those results to the high contents of 2:1 minerals in their soils, which probably had a higher reserve and non-exchangeable K content.

The ion exchange resin was able to extract up to twice as much K as Mehlich-1 did for soils receiving no or low K (0 and 40 kg K ha^{-1}) - (Fig. 2). For the STK in the 110 kg K ha^{-1} treatment, the amounts extracted by Mehlich-1 were only 21% lower than those extracted by exchange resin. The extraction mechanism of K from Mehlich-1 (double-acid solution) is based on the dissolution of H^+ and its respective exchange by K^+ previously adsorbed to the electronegative surface of colloidal and/or organic particles. On the other hand, the exchange resin extracts cations from the complex due to its high CEC in comparison to that of the soil. Therefore, under low available nutrient contents, the exchange resin is able to access forms of K that are not accessible by Mehlich-1 due to the continuous gradient of K desorption associated with the exchange capacity of the resin. Moreover, the cations that occupy the exchangeable sites and the potential release of H^+ from the double-acids to the soil solution are factors that reduce the extractability of Mehlich-1.

When exchangeable K_{M-1} are between 0.6 - 1.3 $mmol_c$ dm^{-3} for soils with 20-40% of clay content, or 0.8 - 1.5 $mmol_c$ dm^{-3} for soils with clay content >40%, the K status is considered deficient, and 40 kg K ha^{-1} is recommended (Sousa and Lobato, 1996; Sfredo, 2008). Our 40 kg K ha^{-1} treatment is, therefore, justified since the average K_{M-1} was below 1.0 $mmol_c$ dm^{-3}. On the other hand, over applying K could be a problem in conventional tillage systems since K can be easily lost by leaching and runoff. However, conservation systems such as NT are able to alleviate losses due to the increased soil

cover and OM, which in turn increases the retention of cations, such as K^+. Therefore, organic acids can serve as adsorbents to reduce K losses (Rosolem and Calonego, 2013). In addition, organic anions, which generally bind polyvalent cations, move to the subsurface and increase K saturation in surface layers (Franchini et al., 1999).

An inconsistency remains regarding the optimum soil test K level. Yield increases usually occur when STK is below 40 mg kg^{-1} in response to K fertilization (Oliveira Junior et al., 2013), whereas no response to K fertilization is observed when STK is higher than 0.19 $cmol_c$ dm^{-3} mg kg^{-1} (Borkert et al., 1993). For this experiment, the rate of 40 kg K ha^{-1} was able to attain those STK levels with either K_{M-1} or K_{resin}, (Fig. 2). Higher rates were not justified and should be avoided. Therefore, K fertilization has to be cautiously managed through the periodical soil testing in order to avoid any over or under application.

Soybean leaf nutrient contents and the effects of K on Ca+Mg/K relationship

The nitrogen contents in soybean leaf samples were not different across treatments or between cultivars (Table 3) although different amounts of K were applied. The average N contents were 58.7 for BRS1010 and 56.1 g kg^{-1} for BRS1003, which are considered sufficient for the trifoliate leaflets without petiole (Clover and Mallarino, 2013; Parvej et al., 2016; Stammer and Mallarino, 2018). The tissue K, however, increased as the application rates of K increased for both cultivars (Table 3). Therefore, the increased K rates contributed to the higher uptake of K but did not affect the levels of N present in the soybean trifoliate leaflets (Table 3). Potassium nutrition strongly affects the N status of non-legume plants (Pettigrew, 2008), but soybean can fix N biologically and is not affected by K as much as non-legume crops.

The highest values of Ca and Mg in diagnostic leaves were found in the control for both cultivars (Table 3). In contrast to K, the contents of Ca and Mg decreased as the rates of K increased. The Ca and Mg in leaf samples of the highest rate of K treatment were reduced by 22-28% and 32-34% from the control for cultivars BRS1010 and BRS1003, respectively.

The influence of one cation on another can be attributed to the competition or synergism during the uptake process (Ahmad and Maathuis, 2014). High K^+ activity can competitively inhibit Ca^{2+} and Mg^{2+} uptake. The preferential uptake of K^+ occurs because of its monovalent charge and smaller degree/radius of hydration, which results in a higher tendency for plant uptake. The lowest contents of Ca and Mg taken up, observed with the highest rate of K (Table 3), were probably related to the saturation of K in the exchange sites as indicated by the increase in K bioavailability shown by both extractants.

The K fertilizer (KCl) has a solubility of 0.34 g mL^{-1} (Silva and Lopes, 2011), so the rainfall usually occurring in the area (~550 L m^{-2}) might be enough to solubilize the highest rate of KCl applied (110 kg K ha^{-1}). Therefore, in the case of our experiment, in addition to the high dissolution of K^+ from the KCl applied, the bioavailability of K was higher due to the long-term continuous fertilization. Such an increase in the K activity due to annual and continuous fertilization narrowed its capability for electrostatic retention and favored the uptake by soybean root systems resulting in K luxury uptake.

Increased Ca/Mg ratio in the first layers of a clayey Oxisol were observed for rates of K up to 400 kg ha^{-1} (Alvarenga and Lopes, 1988). The same authors stated that the competition for exchangeable sites was higher between K and Mg than K and Ca with the same tendency for subsurface layers. Oliveira et al. (2001) also observed that the

increase of soil available K intensified its competitive effect over Ca and especially Mg uptake by soybean, in a Typic Hapludox.

Table 3. Elemental contents of soybean leaves of cultivars BRS1010 and BRS1003 as affected by K fertilization rates (treatments)

K	BRS1010		BRS1003		Mean		BRS1010		BRS1003		Mean	
kg ha^{-1}	……N (g kg^{-1})……						……P* (g kg^{-1})……					
0	59.4	aA	57.9	aA	58.7	a	3.7	aA	3.3	aA	3.5	a
40	59.7	aA	57.9	aA	58.8	a	3.4	aA	3.3	aA	3.3	a
75	60.5	aA	55.5	aA	58.0	a	3.8	aA	3.3	aA	3.5	a
110	55.3	aA	53.0	aA	54.1	a	3.2	aA	3.1	aA	3.2	a
Mean	58.7	A	56.1	A			3.5	A	3.2	B		
	……K** (g kg^{-1})……						……Ca** (g kg^{-1})……					
0	10.0	cA	9.8	cA	9.9	c	8.3	aA	7.8	aA	8.1	a
40	13.3	bB	15.4	bA	14.3	b	7.3	abA	7.0	abA	7.2	ab
75	19.0	aA	19.5	aA	19.2	a	6.2	bA	6.4	bA	6.3	b
110	19.2	aA	19.2	aA	19.2	a	6.0	bA	6.1	bA	6.1	b
Mean	15.4	A	16.0	A			7.0	A	6.8	A		
	……Mg** (g kg^{-1})……						……S** (g kg^{-1})……					
0	6.0	aA	5.3	aB	5.6	a	1.9	aB	2.1	aA	2.0	a
40	5.0	bA	4.1	bB	4.6	b	2.0	aB	2.2	aA	2.1	a
75	4.4	bcA	3.8	bB	4.1	bc	2.0	aB	2.1	aA	2.1	a
110	4.1	cA	3.5	bB	3.8	c	2.0	aA	2.1	aA	2.0	a
Mean	4.8	A	4.2	B			2.0	B	2.1	A		
	……Zn (mg kg^{-1})……						……Mn* (mg kg^{-1})……					
0	37.5	a*A	28.2	aB**	32.9	a	112.5	aA	135.8	aA	124.1	a
40	38.0	aA	29.9	aB	33.9	a	93.8	aA	110.7	aA	102.2	a
75	32.9	bA	30.0	aA	31.4	a	89.8	aB	126.8	aA	108.3	a
110	35.1	abA	27.9	aB	31.5	a	106.9	aA	105.0	aA	106.0	a
Mean	35.9	A	29.0	B			100.7	B	119.6	A		
	……Fe (mg kg^{-1})……						……B (mg kg^{-1})……					
0	93.5	aA	103.5	aA	98.5	a	56.5	a**A	51.9	aA*	54.2	a
40	96.0	aA	102.8	aA	99.4	a	52.9	aA	45.9	abB	49.4	b
75	94.4	aA	91.2	aA	92.8	a	43.5	bA	43.4	bA	43.5	c
110	89.9	aA	89.5	aA	89.7	a	42.9	bA	40.9	bA	41.9	c
Mean	93.4	A	96.7	A			48.9	A	45.5	B		

Different low case letters in the same column (within cultivar) or capital letters in the same row (same K fertilizer rate) are significant at **p<0.01 and *p<0.05 (Tukey)

The long-term annual application of KCl, as in this study, was not enough to raise the K saturation to levels that would be able to significantly reduce the exchangeable contents of Mg given the Mg content in the tissue (Table 3). According to Harger (2008), the Mg content is considered adequate for soybean trifoliate leaflets (4.9 and 4.2 g kg^{-1}, on average, for BRS1010 and BRS1003, respectively), but low for Ca (7.0 and 6.8 g kg^{-1}, on average, for BRS1010 and BRS1003, respectively), as presented in Table 3.

The soybean cultivars receiving low K fertilizer rates had higher Ca/K, Mg/K and Ca+Mg/K ratios than plants growing under higher rates of K. The reduction in such ratios was accentuated as the rates of K application reached 75 kg ha^{-1}. The Ca+Mg/K ratios reached a minimum of 0.53 and 0.50 at rate of 110 kg K ha^{-1} for BRS1010 and BRS1003, respectively. The lack of difference observed between 75 and 110 kg K ha^{-1} can be explained by the high K saturation of the soil, probably as a consequence of continuous application during the experiment. The biggest antagonistic effect on Mg uptake was evidenced by the increasing Ca+Mg/K ratios of 35.3 and 34.4% comparing the control (0 kg K ha^{-1}) and the highest rate (110 kg K ha^{-1}) for BRS1010 and BRS1003, respectively.

The concentrations of these basic cations in soybean tissues are a direct consequence of their abundances on the exchangeable sites of the soil. The lowest Ca+Mg/K ratio was observed when the exchange resin was used for K extraction due to the higher amounts of K extracted in comparison to Mehlich-1 for the lower rates of K applied (Fig. 2). Some authors reported that the highest yield was obtained with Ca+Mg/K values between 23 and 31 in soils (Rosolem and Nakagawa, 1985). On the other hand, Oliveira et al. (2001) found that when the ratios of Ca+Mg/K were higher than 30, the nutritional imbalance was evident. In addition, NT increases dissolved

organic carbon (DOC) and its components can complex Ca^{2+} more strongly than Mg^{2+} resulting in Ca-DOC removal from the system by leaching more easily than Mg-DOC (Antonangelo et al., 2017). In the case of Mg, the adequate levels observed can be attributed to a synergistic effect between P and Mg in terms of root uptake since P was adequately supplied for all treatments with a fixed rate of 20 kg P ha^{-1} (Antonangelo et al., 2019).

Differences of B were found among all treatments ($p<0.01$) and the behavior was similar to that observed for Ca ($p<0.01$) regardless of the cultivar (Table 3). It may be related to the biostructural functions performed by the B in association to Ca, as denoted by the high correlations obtained between these elements for both cultivars (Fig. 3). Boron plays an important role in meristem growth, hemicellulose and cell wall biosynthesis, plasmatic membrane functioning, carbohydrates metabolism and auxins mobilization. Calcium enhances the formation of calcium pectates, which are fundamental for the formation and stability of the cell wall, besides promoting the growth of the pollen tube, membrane stabilization, and is essential for balancing cations and anions, osmoregulation, cellular extension and biological signaling. Calcium and B are generally located in the same cellular compartment leading to similar structural functions. Therefore, it is possible that the higher Ca^{2+} absorption, as demonstrated by plants under lower rates of K, promoted B uptake.

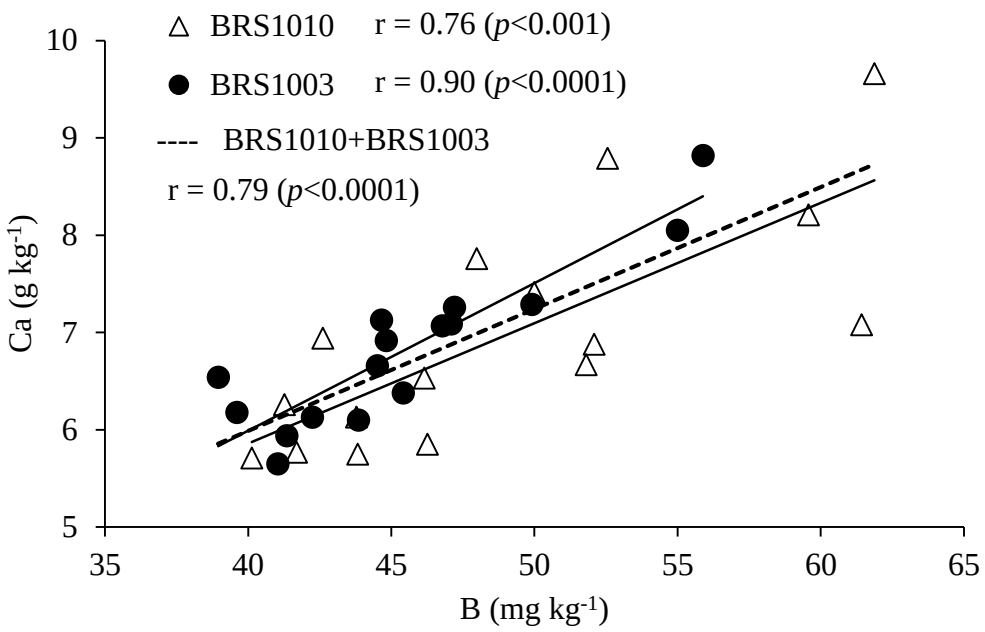

Fig. 3. Correlation between boron (B) and calcium (Ca) of soybean diagnostic leaves for cultivars BRS1010, BRS1003 and both combined

The contents of other micronutrients in soybean diagnostic leaves were not different among treatments (Table 3). Both Zn and Mn are considered adequate for soybean Harger (2008). However, Fe was below the 137 mg kg^{-1} critical level and considered low. The high contents of Mn probably inhibited the uptake of Fe even at a low soil pH. No-till systems tend to accumulate organic matter in the surface soil and result in more DOC, which enhances the preferential complexation of Fe ions resulting in losses from the root zone. It is also possible that free phosphate anions precipitate with free Fe ions in the soil solution further reducing iron bioavailability (Zambrosi et al., 2008). In the case of sulfur (S), the contents in soybean diagnostic leaves were, on average, 2.0 and 2.1 g kg^{-1} for BRS1010 and BRS1003, respectively, and both are considered low according to Harger (2008). It is possible that Rhizobium, responsible for

N biological fixation, consumed S in the surface layers, where the nodulation takes place, since S is a nutrient required in the process. The lack of significant S differences observed among treatments was probably an effect of NT since 95% of sulfate-S originates from organic decomposition.

Maximum responsive levels of soil test K with respect to tissue K concentration

Both K_{M-1} and K_{resin} were strongly correlated ($p<0.01$) with K_{Tissue} for both cultivars ($r = 0.82$ and $= 0.86$, for BRS1010; $r = 0.70$ and $= 0.78$, for BRS1003, respectively). The same trend was observed when both cultivars were combined ($r = 0.76$ and 0.82, $p<0.0001$, for K_{M-1} and K_{resin}, respectively). The relationship of our data was linear and quadratic until a plateau point (joint) (Fig. 4). Therefore, the joint is defined as the maximum responsive value (Fig. 3) by the linear plateau (LP) and quadratic plateau (QP) models, as done by Stammer and Mallarino et al. (2018).

Both LP and QP of K_{M-1} converged for BRS1010 and BRS1003 combined ($p<0.001$). Therefore, a range of maximum responsive K_{M-1} values was defined (1.72 ± 0.26 to 2.36 ± 0.35 $mmol_c$ K dm^{-3}). A range of maximum responsive K_{resin} was also obtained from both LP and QP (2.58 ± 0.22 to 3.11 ± 0.33 $mmol_c$ K dm^{-3}). The joint between K_{resin} and K_{Tissue} was higher than that between K_{M-1} and K_{Tissue} because K_{resin} was higher than K_{M-1} for all treatments.

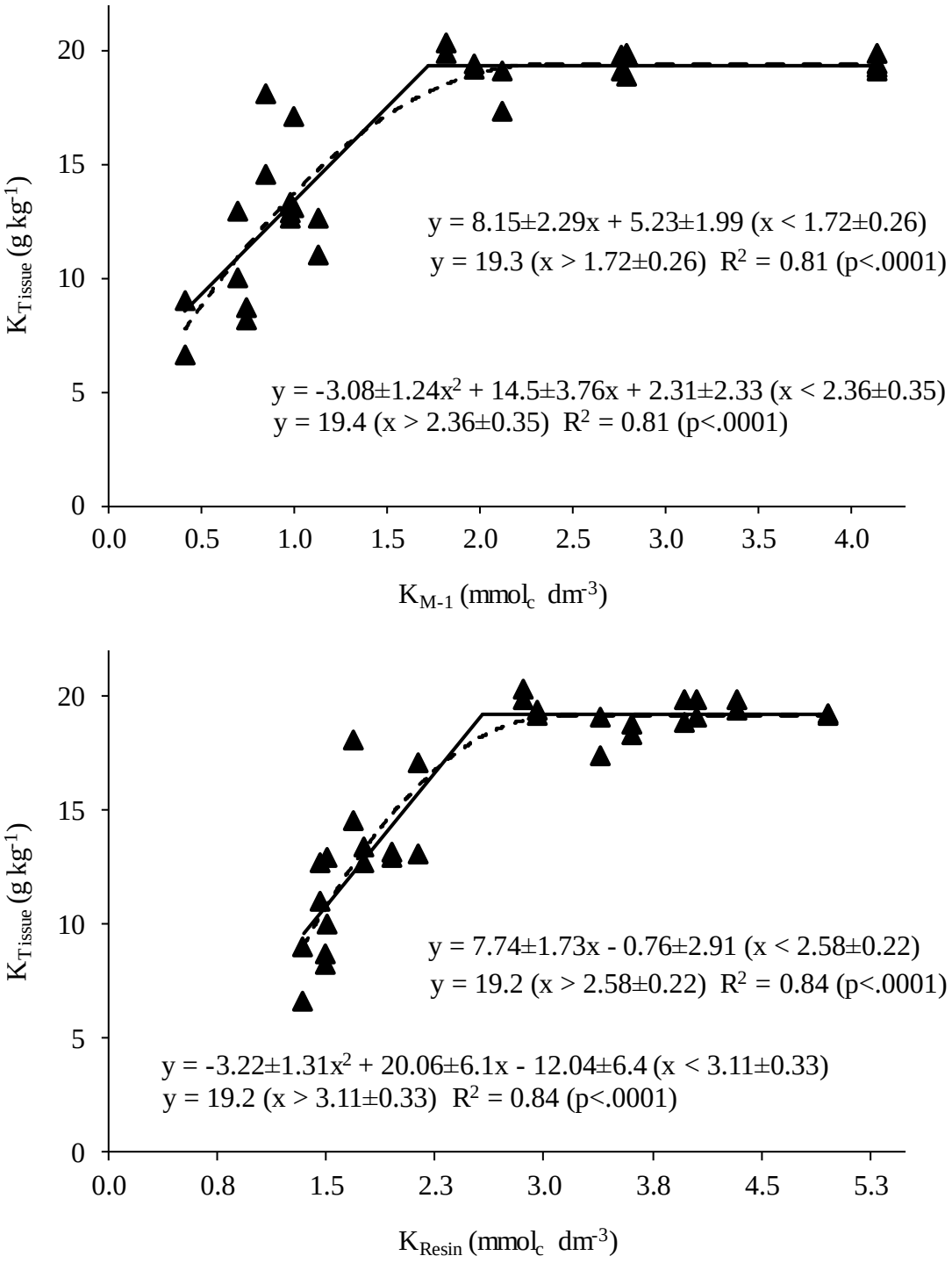

Fig. 4. Linear and quadratic plateau models between soybean leaf K content (K_{Tissue}) and Mehlich-1 (K_{M-1}) or resin (K_{Resin}) extractable plant available K in the soil for cultivars BRS1010 and BRS1003 combined. Values following ± are standard deviations

Soybean yield response to K fertilization

Soybean yields were affected by the rates of K applied (Table 4). On average, both cultivars had higher yields for treatments receiving K than the control. According to Zanon et al. (2016), the average yield of 2.6 Mg ha^{-1} for the treatment of 40 kg K ha^{-1} is already above the average soybean yield in Brazil at the time (2.5 Mg ha^{-1}). However, when considering the yield for each cultivar separately, BRS1010 showed a yield higher than 2.5 Mg ha^{-1} for the 40 kg K ha^{-1} treatment, whereas BRS1003 only showed the same at the rate of 75 kg K ha^{-1}. The results from Table 4 clearly show that BRS1010 yielded higher than BRS1003 on average.

As shown in Table 4, soybean yields were increased by 43% as the application rates of K increased up to 40 kg ha^{-1} and no further increase was observed with more K applied ($p<0.01$). The non-response to the rates higher than 40 kg K ha^{-1} can be explained by the adequate supply of K from previous applications evidenced by the high soil available K discussed earlier.

Table 4. Yields of soybean cultivars BRS1010 and BRS1003 as affected by K fertilization rates (treatments)

	BRS1010		BRS1003		Mean	
kg K ha^{-1}	……Yield (kg ha^{-1})……					
0	1975	bA	1670	bA	1823	b
40	2824	aA	2398	aB	2611	a
75	3098	aA	2874	aA	2986	a
110	2918	aA	2729	aA	2823	a
Mean	2704	A	2418	B	2561	

Different lower and capital letters in columns and rows, respectively, are significant at $p < 0.01$ and $p < 0.05$ (Tukey)

The recommendation for K fertilizer in Brazilian savannah and Sao Paulo state for an expected soybean yield between 2.5 and 3.0 Mg ha^{-1} is 40 kg ha^{-1} when K_{M-1} is between 0.6 – 1.3 $mmol_c$ dm^{-3} and 0.8 – 1.5 $mmol_c$ dm^{-3} in soils with clay content >20% and >40%, respectively (Sousa and Lobato, 1996; Sfredo et al., 2008). Therefore, the 40 kg K ha^{-1} was justified since the average K_{M-1} was about 1.0 $mmol_c$ dm^{-3} for this treatment. Although K content in the diagnostic leaves increased up to 75 kg K ha^{-1} of K (Table 3), soybean grain yields were increased only to 40 kg K ha^{-1}. No further response in the soybean yields for K rates higher than 40 kg ha^{-1} suggests K luxury consumption by plants or that climatic factors limited productivity (e.g. drought periods, high temperatures). This is supported by data shown in Fig. 5, which shows the LP models for soybean yields as affected by STK ($p<0.01$ and <0.05 for K_{M-1} and K_{resin}, respectively). The QP model failed to converge from this dataset; therefore, LP is used to derive the maximum responsive STK.

The maximum soybean yield responsive concentration of both K_{M-1} and K_{resin} (Fig. 5) is not different from those found between K_{Tissue} and STK when considering both LP and QP models (Fig. 4). The joint points or optimum STK levels for soybean yield were 2.16±0.58 for K_{M-1} and 3.42±0.91 for K_{resin} (Fig. 5).

The recommendation of K rates to be applied for soybean varies among regions. For instance, Sao Paulo state considers resin extractable K of 0-30, 31 to 60, 61 to 120, 121 to 240 and >240 mg dm^{-3} very low, low, moderate, high and very high, respectively (Ernani et al., 2007). While the Parana state treats values of <40, 40 to 80, 80 to 120 and > 120 mg dm^{-3} K_{M-1} as very low to high (Ernani et al., 2007).

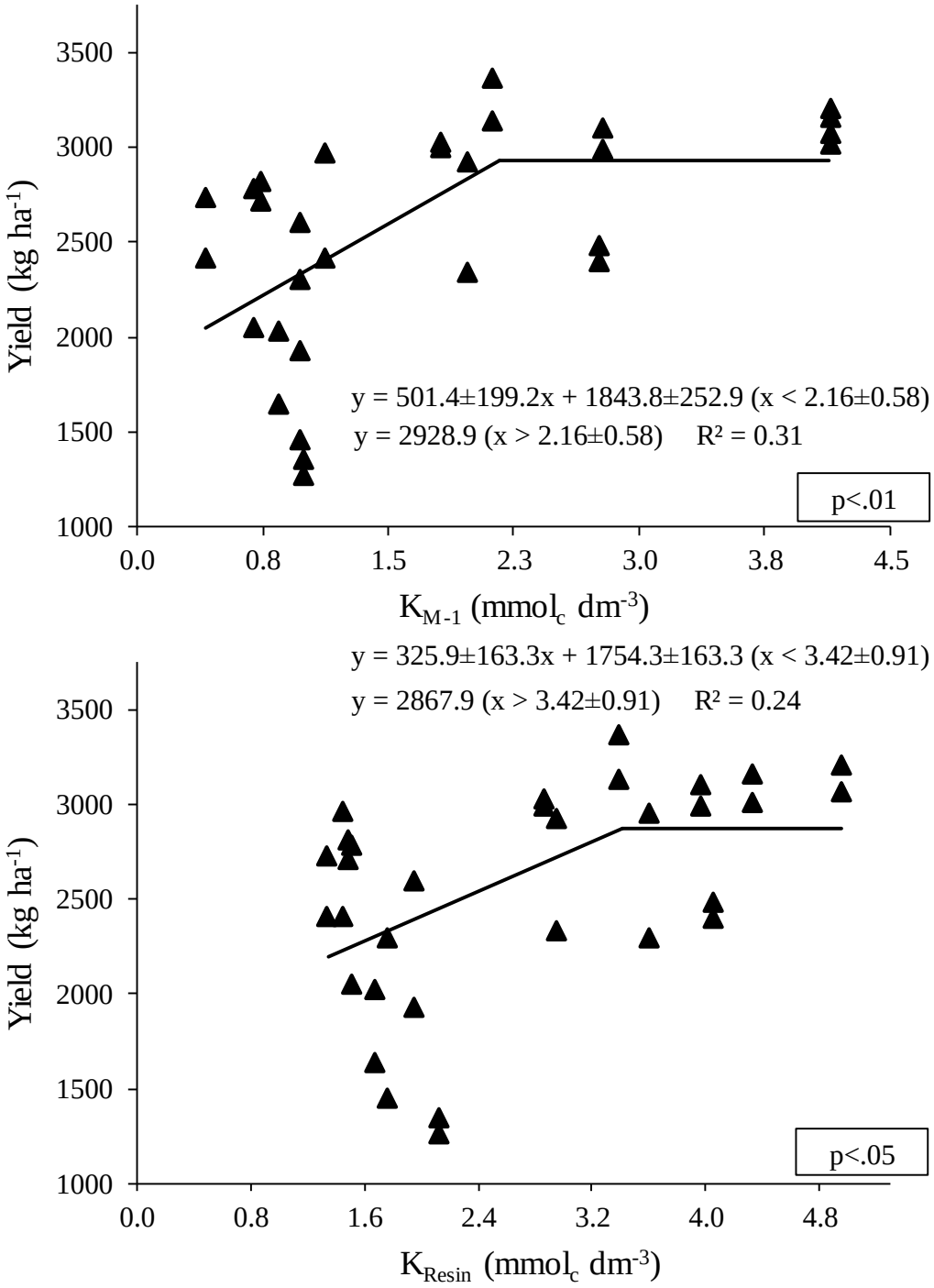

Fig. 5. Linear plateau models for soil test K levels with soybean yield for cultivars BRS1010 and BRS1003 combined. Values following ± were standard deviations

In our study, K_{resin} ranged from 54.6 (low) for the control (0 kg K ha^{-1}) to 163.8 mg dm^{-3} (high) for the treatment with 110 kg K ha^{-1} as lowest and highest levels of exchangeable K, respectively (Fig. 2). For K_{M-1}, it ranged from 27.3 (very low) to 144.3 mg dm^{-3} (very high) for the lowest and highest rates of K. Furthermore, LP and QP models were performed for K_{Tissue} *Vs* soybean yield in order to obtain the maximum responsive values of K_{Tissue} with respect to soybean yields (Fig. 6).

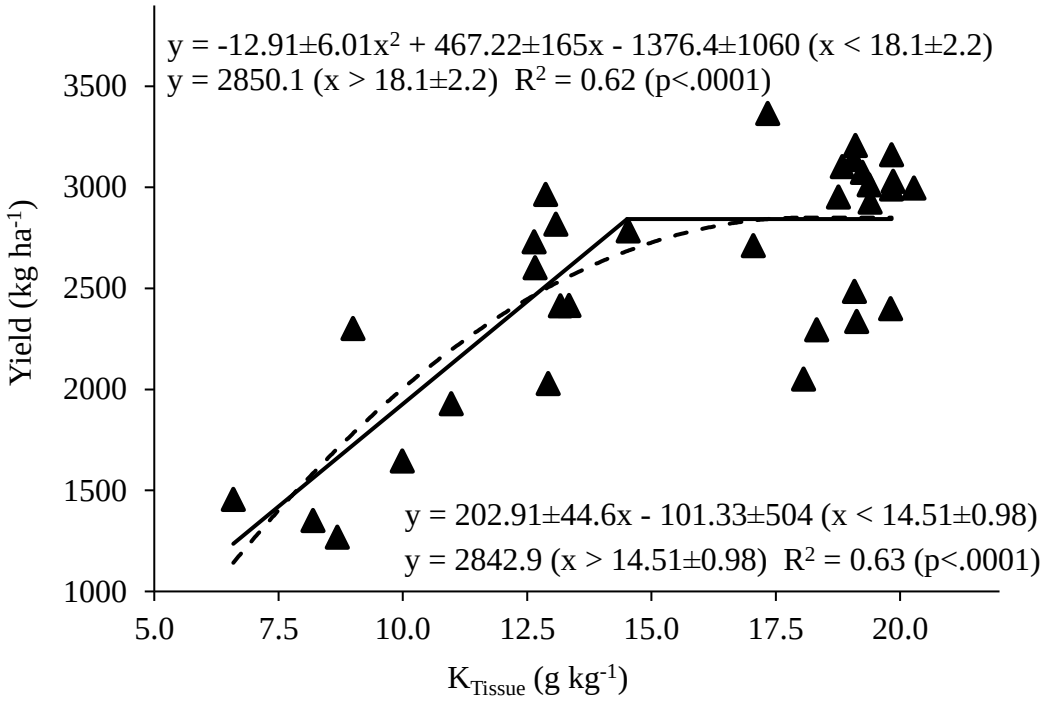

Fig. 6. Linear and quadratic plateau models for K content in trifoliate (K_{Tissue}) with soybean yield for cultivars BRS1010 and BRS1003 combined. Values following ± are standard deviations

The LP and QP converged successfully using the NLIN procedure of SAS software ($p<0.0001$) (Fig. 6). The range of the joints was 14.5±0.98 to 18.1±2.2 g K kg^{-1}, which is within the range of 15.6 to 19.9 g kg^{-1} found by Stammer and Mallarino (2018) for diagnostic leaves collected at the same soybean growth stages (R2), although their leaves were sampled with the petioles. The same authors emphasized that a K test of soybean leaves at the R2-R3 stage would be even more reliable than a test of young soybean plants at V5-V6. As a matter of fact, the maximum responsive concentration determined for leaves at the R2 stage was similar to other studies (Small and Ohlrogge, 1973; Parvej et al., 2016), but was lower than the 24.3 g K kg^{-1} critical concentration reported from Ontario (Yin and Vyn, 2004) and the 20.1 to 25 g K kg^{-1} sufficiency range suggested in Indiana, Michigan, and Ohio (Vitosh et al., 1995).

The increase in K bioavailability promoted increases in K uptake and nutrient content in the diagnostic leaves from 10 g kg^{-1} for the control (0 kg K ha^{-1}) to 19 g kg^{-1} for the highest rate (110 kg K ha^{-1}) of K fertilizer applied in both cultivars (Table 3). This change represents the transition from low (10 g kg^{-1}) to sufficient contents (19 g kg^{-1}) for trifoliate leaflets (Parvej et al., 2016). Contents between 13 and 17 g kg^{-1} in diagnostic leaves were related to higher yields of soybean grains (Borkert et al., 1993). However, modern cultivars with higher yield potential possibly have higher K requirements, as was the case of our experiment. Mallarino (2011) found that the critical concentrations varied between 20 and 23 g kg^{-1} of K in soybean tissue in Iowa. Mills and Jones (1996) suggested 17 to 25 g K kg^{-1} as sufficient. In contrast, the range of 15 to 17 g kg^{-1} for soybean cultivated in Mato Grosso and Mato Grosso do Sul was considered adequate in Brazil. Therefore, the nutritional requirement for soybean may vary as a function of

genetics, environmental factors and management practices, which makes it difficult to standardize the nutritional requirements for soybean growing in different regions.

As expected, the lowest yields were observed from the control of both cultivars (Table 4). The reduction of K content in soils and plant tissues followed by a decrease in soybean yields were also evidenced in long-term experiments with no K application (Rosolem and Nakagawa, 1985; Silva et al., 1995; Resende and Costa, 2014).

The mass of 300 grains for BRS1010 was significantly higher ($p<0.05$) at 75 kg K ha^{-1} than that of 40 kg K ha^{-1} and the control (data not shown). Therefore, mass of grains increased with K fertilizer rates up to 75 kg K ha^{-1}. The K application promoted a significant increase of around 19% in the mass of 300 grains for the 75 kg K ha^{-1} in comparison to the control. This increase contributed to 82% of ($p<0.01$) the grain yield increase for one of the cultivars (data not shown). However, a similar trend was not found for the other cultivar. The deficiency of K generally affects the quality of soybean seeds, but it also depends on soybean cultivar, as observed in our study. Petter et al. (2014) verified the increase in the mass of grains of soybean by increasing rates of K application, and found the rate of 133 kg K ha^{-1} was responsible for the maximum mass of thousand grains (150.7 g). Significant effects of K rates on the mass of soybean grains in a low STK Oxisol were also observed by Toledo et al. (2011).

According to Cakmak (2005), plants cultivated under soils with low K availability are more susceptible to reduced photosynthetic rates as well as to oxidative stress in the cell environment. Potassium deficient soybeans commonly produces small grain size and plants that are more susceptible to insects and diseases. This partially explains why BRS1010 had higher grain mass with the 75 kg K ha^{-1}. Borkert and Costa (1988)

observed that the sanitary, physical and physiological quality of seeds were superior for the treatments that received rates higher than 65 kg K ha^{-1}. The positive correlation between the mass of grains and soybean yield for BRS1010 (data not shown) supports the findings of Khan et al. (2004) and Moterle et al. (2016).

Conclusions

Although strongly correlated, resin extracted more K than Mehlich-1, but the difference decreased as K rates or STK increased. Soil test K levels from both extraction methods were correlated with K contents in soybean tissue samples, with higher positive correlation coefficient for K_{resin} than K_{M-1} ($r = 0.82$ and 0.76 with $p<0.0001$, respectively). The maximum responsive concentration of K_{M-1} and K_{resin} for K_{Tissue} was in the range of 1.72±0.26 to 2.36±0.35 and 2.58±0.22 to 3.11±0.33 $mmol_c$ K dm^{-3}, respectively, and was not different from those between STK and soybean yield. In our case, a general range of 14.5±0.98 to 18.1±2.2 g K kg^{-1} in the plant tissue is the maximum responsive concentration for the optimum soybean yields. The ratio of Ca+Mg/K in the diagnostic leaves was decreased as K application rates increased. Soybean yields were increased up to 40 kg K ha^{-1} applied. The additional K applied annually beyond 40 kg ha^{-1} partially contributed to soil K pool but not soybean yields. Therefore, our findings emphasize the need to recommend K based on either soil test and/or plant tissue analysis, in order to optimize yields and minimize cost and K losses.

References

Adeli, A., K.R. Sisani, D. Rowe, and H. Tewolde. 2005. Effects of broiler litter on soybean production and soil nitrogen and phosphorus concentrations. Agron. J. 97:314–321.

Ahmad, I., and F.J.M. Maathuis. 2014. Cellular and tissue distribution of potassium: Physiological relevance, mechanisms and regulation. J. Plant Physiol. 171(9): 708–714.

Alvarenga, I.M, and A.S. Lopes. 1988. Influence of potassium fertilization on the cations equilibrium of a dystrophic dusky red latosol, under "cerrado" vegetation. Pesquisa Agropecuária Brasileira 23:347–355.

Antonangelo, J.A., R.F. Firmano, L.R.F. Alleoni, A. Oliveira Junior, and H. Zhang. 2019. Soybean yield response to phosphorus fertilization on an Oxisol under long-term no-till management. Soil Sci. Soc. Am J. doi: 10.2136/sssaj2018.07.0251

Antonangelo, J.A., J.F. Neto, C.A.C. Crusciol, and L.R.F. Alleoni. 2017. Lime and calcium-magnesium silicate in the ionic speciation of an oxisol. Scientia Agricola 74:317–333.

Araújo, H.S., M.X.O. Junior, F.O. Magro, and A.I.I. Cardoso. 2013. Potassium top dressing levels on fruit yield of summer squash. Revista de Ciências Agrárias (Portugal) 36:303-309.

Araujo, D.F.S., A.M.R.B. Silva, L.L.A. Lima, M.A.S., Vasconcelos, S.A.C. Andrade, and L.A. Sarubbo. 2014. The concentration of minerals and physicochemical

contaminants in conventional and organic vegetables. Food Control 44:242-248.

Bertsch, P.M., and P.R. Bloom. 1996. Aluminum. In D.L. Sparks (ed.), Methods of Soil Analysis Part 3—Chemical Methods, p. 517-550. SSSA, Madison, WI.

Borkert, C.M., and N.P. da Costa. Potassium fertilization reduces disease and insect damage in soybeans. 1988. Potash review/Intern. Potash Inst. Subject 3. Crop quality and plant health, CH 3048 Worblaufen, Bern/Switzerland; Suite 1.

Borkert, C.M., G.J. Sfredo, and D.N. Silva. 1993. Calibration of potassium in soybean leaves in dystrophic Oxisol. Revista Brasileira de Ciência do Solo 17:227–230.

Cakmak, I. 2005. The role of potassium in alleviating detrimental effects of abiotic stresses in plants. J. Plant Nutrition Soil Sci. 168:521–530.

Clover, M.W., and A.P. Mallarino. 2013. Corn and soybean tissue potassium content responses to potassium fertilization and relationships with grain yield. Soil Sci. Soc. of Am. J. 77:630–642.

Deuschle, D., Minella, J. P., de AN Hörbe, T., Londero, A. L., & Schneider, F. J. (2019). Erosion and hydrological response in no-tillage subjected to crop rotation intensification in southern Brazil. Geoderma, 340, 157-163.

Edmeades, D.C., Wheeler, D.M., Clinton, O.E. 1985. The chemical composition and ionic strength of soil solutions from New Zealand topsoils. Australian Journal of Soil Research. 23:151-165.

Ernani, P.R., J.A., Almeida, and F.C. Santos. 2007. Potassium. In Novais et al. (Eds.), Soil Fertility. Brazilian Soil Science Society, Viçosa, p.1017.

Franchini, J.C., M. Miyazawa, M.A. Pavan, and E. Malavolta. 1999. Dynamic of ions in acid leached with green manure residues extracts and pure solutions of organic

acids. Pesquisa Agropecuaria Brasileira 34:2267–2276.

Fuentes-Llanillo, R., T.S. Telles, B. Volsi, D.S. Júnior, S.L. Carneiro, and M. de Fátima Guimarães. 2018. Profitability of no-till grain production systems. Semina: Ciências Agrárias 39:77-86.

Harger, N. 2008. Sufficiency ranges for foliar contents of nutrients in soybean, defined by the use of the DRIS method, for soils of basaltic origin. Ph.D. diss., Londrina State Univ. Londrina, 88p.

Helmke, P.A., and D.L. Sparks. 1996. Lithium, sodium, potassium, rubidium, and cesium. In D.L. Sparks (ed.), Methods of Soil Analysis Part 3—Chemical Methods, 5.3:551-574.

Holthusen, D., S. Peth, and R.F. Horn. 2010. Impact of potassium concentration and matric potential on soil stability derived from rheological parameters. Soil and Tillage Research 111:75–85.

Khan, H. Z., M. Asghar Malik, M. Farrukh Saleem, and I. Aziz. 2004. Effect of different potassium fertilization levels on growth, seed yield and oil contents of canola (Brassica napus L.). Intern. J. Agric. Biol. 6:1153–1155.

Kolar, J.S., and H.S. Grewal. 1994. Effect of split application of potassium on growth, yield and potassium accumulation by soybean. Fertilizer Research 39:217–222.

Maathuis, F.J. 2009. Physiological functions of mineral macronutrients. Curr. Opin. Plant Biol. 12(3): 250–258.

Mallarino, A.P., R.R. Oltmans, J.R. Prater, C.X. Villavicencio, and L.B. Thompson. 2011. Nutrient uptake by corn and soybean, removal, and recycling with crop residue. doi: https://doi.org/10.31274/icm-180809-269

Marschner, P., and Z. Rengel. 2011. Nutrient Availability in Soils, Marschner's Mineral Nutrition of Higher Plants: Third Edition. Elsevier Ltd.

Medeiros J.D., Oliveira F.H., Arruda J.A., Vieira M.D., and M.P. Fontes. 2010. Efficiency of available potassium extractants in soils of Paraiba state with different degrees of pedogenetic development. Revista Brasileira de Ciencia do Solo 34:183–194.

Mehlich, A. 1984. Mehlich 3 soil test extractant: A modification of Mehlich 2 extractant. Commun. Soil Sci. Pl. Anal. 15:1409-1416.

Mills, H.A., and J.B. Jones. 1996. Plant analysis handbook: A practical sampling, preparation, analysis, and interpretation guide, 2nd ed. MicroMacro Publishing, Athen.

Moreira A, Moraes L.A., and Fageria N.K. 2015. Variability on Yield, Nutritional Status, Soil Fertility, and Potassium-Use Efficiency by Soybean Cultivar in Acidic Soil. Commun. Soil Sci. and Pl. Anal. 46:2490–2508.

Moterle, D.F., J. Kaminski, D. Santos Rheinheimer, L. Caner, and E.C. Bortoluzzi. 2016. Impact of potassium fertilization and potassium uptake by plants on soil clay mineral assemblage in South Brazil. Plant and Soil 406:157-172.

Murphy, J.A.M.E.S., and J.P. Riley. 1962. A modified single solution method for the determination of phosphate in natural waters. Analytica chimica acta. 27:31-36.

Oliveira, F.A., Carmello, Q.A.C., Mascarenhas, H.A.A., 2001. Potassium availability and its relation to calcium and magnesium in greenhouse cultivated soybean. Scientia Agricola 58, 329–335.

Oliveira Junior, A., C. Castro, F.A. Oliveira, and L.T Jordão. 2013. Potassium

fertilization in soybean: nutrient balance care. IPNI Agronomic Informations 143:1–10.

Parvej, M.R., N.A. Slaton, L.C. Purcell, and T.L. Roberts. 2016. Critical trifoliolate leaf and petiole potassium concentrations during the reproductive stages of soybean. Agron. J. 108:2505-2518.

Petter, F.A., A.U. Alves, J.A. Silva, J.A., E.A. Cardoso, T.F. Alixandre, F.A Almeida, and L.P. Pacheco. 2014. Productivity and quality of soybean seeds as a function of potassium application. Semina: Ciências Agrárias 35:89-100.

Pettigrew, W.T. 2008. Potassium influences on yield and quality production for maize, wheat, soybean and cotton. Physiologia Plantarum 133:670–681.

Prado, R.M., L.F. Braghirolli, W. Natale, M.C.M. Corrêa, and E.V. Almeida. 2004. Potassium application on the nutritional status and dry matter production of passion fruit cutting. Revista Brasileira de Fruticultura 26:295–299.

Resende, G.M., and N.D. Costa. 2014. Effects of levels of potassium and nitrogen on yields and post-harvest conservation of onions in winter. Revista Ceres 61:572–577.

Rosolem, C.A., and J.C. Calonego. 2013. Phosphorus and potassium budget in the soil-plant system in crop rotations under no-till. Soil and Tillage Research 126:127–133.

Rosolem, C., and J. Nakagawa. 1985. Potassium uptake by soybean as affected by exchangeable potassium in soil. Communications in Soil Science and Plant Analysis 16:707–726.

Ruiz, H.A., J. Miranda, J.C.S. Conceição. 1999. Contribution of mass flow and diffusion mechanisms for suppying K, Ca and Mg to rice plants. Revista Brasileira de Ciencia do Solo 23:1015–1018.

SAS Institute. 2011. SAS system for Windows. Version 9.3. SAS Institute, Inc., Cary, NC.

Scherer, E.E. 1998. Soybean response to potassium fertilizer on a haplohumox soil over a 12-year period. Revista Brasileira de Ciência do Solo 22:49–55.

Sfredo, G.J. 2008. Soybean in Brazil: Liming, fertilization and mineral nutrition. (In Portuguese). Londrina, Parana, BR. 147 p.

Silva, D.N.E.J., M.N. Kaempf, and C.M. Borkert. 1995. Mineralogy and forms of potassium and its relationship with plant. Revista Brasileira de Ciencia do Solo 19:433-440.

Silva D.R.G., and Lopes A.S. 2011. Basic principles for formulation and mixing of fertilizers (In Portuguese). Lavras: Universidade Federal de Lavras, 24 p.

Small, H.G., and A.J. Ohlrogge. 1973. Plant analysis as an aid in fertilizing soybeans and peanuts. In: L.M. Walsh and J.D. Beaton, editors, Soil testing and plant analysis. SSSA, Madison, WI. p. 315–327.

Sousa, D.M.G., and E. Lobato. 1996. Correcao do solo e adubacao da cultura da soja. Embrapa Cerrados-Circular Técnica (INFOTECA-E). *In portuguese*.

Stammer, A.J., and A.P. Mallarino. 2018. Plant tissue analysis to assess phosphorus and potassium nutritional status of corn and soybean. Soil Sci. Soc. Am. J. 82:260–270. doi:10.2136/sssaj2017.06.0179

Toledo, M., G. Castro, C. Crusciol, R. Soratto, J. Nakagawa, and C. Cavariani. 2011. Physiological quality of soybean and wheat seeds produced with alternative potassium sources. Revista Brasileira de Sementes 33:363–371.

Urano, E.O.M., C.H. Kurihara, S. Maeda, A.C.T. Vitorino, M.C. Goncalves, and M.E.

Marchetti. 2007. Determination of optimal nutrient contents for soybean by the mathematical chance, diagnosis and recommendation integrated system and compositional nutrient diagnosis methods (In Portuguese, with English abstract). Rev. Bras. Ciencia do Solo 31:63–72.

van Raij, B. 1998. Bioavailable tests: alternatives to standard soil extractions. Commun. Soil Sci. Pl. Anal. 29:1553–1570.

van Raij, B., J.A. Quaggio, and N.M. da Silva. 1986. Extraction of phosphorus, potassium, calcium, and magnesium from soils by an ion-exchange resin procedure. Commun. Soil Sci. Plant Anal. 17:547–56.

Vitosh, M.L., J.W. Johnson, and D.B. Mengel. 1995. Tri-state fertilizer recommendations for corn, soybeans, wheat, and alfalfa. Ext. Bull. E-2567. Michigan State Univ. Ext., East Lansing. https://www.extension.purdue.edu/extmedia/AY/AY-9-32.pdf (verified 27 Nov. 2017).

Yin X., and T.J. Vyn. 2004. Residual effects of potassium placement for conservation-till corn on subsequent no-till soybean. Soil Tillage Res. 75:151–159.

Zambrosi, F.C.B., L.R.F. Alleoni, and E.F. Caires. 2008. Liming and ionic speciation of an oxisol under no-till system. Sci. Agric. 65:190–203.

Zanon, A.J., N.A. Streck, T. Schmitz, C.M. Alberto, A.C. Bartz, G.M. De Paula, R. Tomiozzo, L. Camargo, C. Augusto, E.L. Tagliapietra, A.P. Cardoso, P.S. Weber, and K.P. Bexaira. 2016. Growth habit effect on development of modern soybean cultivars after beginning of bloom in Rio Grande do Sul. Bragantia 75:446–458.

CHAPTER IV

PHOSPHORUS SPECIATION BY P-XANES IN AN OXISOL UNDER LONG-TERM NO-TILL CULTIVATION

Abstract: In highly weathered soils with low phosphorus (P) and high P fixing capacity, long-term application of P fertilizers may influence P speciation. The combined use of macro- and microscopic techniques is capable of providing important information on P distribution and reactivity in soils, which is the key to determining its loss potential into the environment. In this study, we aimed to evaluate the effects of P application rates under no-till (NT for 26 years) on solid-state P speciation on a highly weathered agricultural soil developed on a basalt spill in Brazil. Soil samples were collected from experimental plots that received 0, 20, 40 or 50 kg ha^{-1} P annually. X-ray fluorescence microanalysis (µ-XRF), X-ray absorption near edge structure (XANES) and extended X-ray absorption fine structure (EXAFS) spectroscopies were used along with soil mineralogy and conventional chemical analyses. Phosphorus availability increased as the applied P rates did. On the basis of our µ-XRF analysis, higher Pearson correlation coefficients (r) were obtained for P *Vs* Al, Si and Fe ($r = 0.77$-0.98, $p<0.0001$). Our P-XANES data showed that the proportions of P sorbed to goethite (Gt), hematite (Hm) and kaolinite (Kln) changed overtime with increases in P availability. The formation of non-

crystalline iron (Fe) minerals was favored under higher production availability as a consequence of the higher rates of P applied and utilization by the crops. The long-term continuous application of P fertilizers beyond plant uptake capacity favored P build-up in soils, resulting not only in poor P use efficiency, but also in exacerbated risk of P loss to the environment.

Keywords: P K-edge XANES; Fe oxides changes; Long-term P fertilization; P sorption to clay minerals.

Introduction

Tropical agriculture is key to secure current and future worldwide food supply to meet population growth. One way of achieving higher crop yields is by intensifying agriculture in these areas, which is likely to lean on the expense of large fertilizer inputs and improved management, particularly of soil P. Therefore, a thorough understanding of P chemical forms and their associations with soil mineral components is crucial to predict the fate and improve the efficiency of applied P fertilizers in soils.

Highly weathered soils of the tropics strongly sorb P due to the abundance of Al- and Fe-(hydr)oxide minerals in the clay fraction, which are the greatest scavengers for soluble P in acidic soils. As a result, P fertilization efficiency in these areas is generally low, in the order of 10% or less (Fageria & Baligar, 2007). Many attempts to increase P use efficiency (PUE) in tropical agricultural soils have been attempted including the use of P-rich animal wastes as P sources (Abdala et al., 2012; Boitt et al., 2018), application of organo-mineral P fertilizers (Corrêa et al.; 2018; Borges et al., 2019), improved P fertilizer placement (Vandamme et al., 2018; Williams et al., 2018) and by adopting soil

cultivation practices that could lower P retention in soils, such as no-tillage (NT) system (Abdala et al., 2015a; Caires et al., 2017; Tiecher et al., 2017).

Among the strategies to increase P availability in soils, and thus its use efficiency by plants, the adoption of NT is certainly the one that is more feasible to most farmers. Adoption of no-tillage in Brazil began in the early 1970's, and today, it represents ~80% of the land area cultivated with grains in the country (61 million hectares). The efficiency of P fertilization under NT is ~16% higher than that of conventional tillage, which relies on land plowing that enhances soil organic matter (SOM) loss and P fixation (Caires et al., 2017; Janegitz et al., 2016). Rodrigues et al. (2016) investigated the impact of NT and conventional tillage (CT) agriculture on accumulated soil P (legacy P) and P forms in four long-term trials in the Brazilian savanna (Cerrado) and found that NT system increased organic P cycling in these tropical soils. Studies addressing the distribution and chemical speciation of P in soils under NT, which favors the stabilization and increase of SOM content over time, are still scarce, especially in long-term trials carried out under tropical humid conditions. Improving the understanding on solid-state speciation of P as well as its distribution in tropical farmlands is of utmost importance to guide and to help establish soil management practices that are more likely to increase the efficiency of P fertilizers.

It has been observed that the adoption of NT promotes an increase in soil quality, carbon (C) inputs and sequestration, mitigating global warming effects (Aziz et al., 2013; Boddey et al., 2010; Ogle et al., 2012). Research has shown that in NT systems the content of SOM, microbial biomass and organic acids biosynthesis increased. This increase may reduce the crystallinity of Al- and Fe-(hydr)oxides, which occurs due to

partial degradation and/or coating by organic compounds in these minerals (Abdala et al., 2015a; Camargo et al., 2012; Kleber et al., 2005; Roden & Zachara, 1996). This change in crystallinity may promote a variation in P dynamics over time in NT because the crystallinity of Al and Fe minerals influences P lability (Abdala et al., 2018, 2015b) and thus its availability to plants (Igwe et al., 2010).

Chemical speciation of P relying on synchrotron radiation has become an important ally for soil scientists aimed at gaining insights into the sorbed forms of P present in soils, particularly, those bound to metal components, such as Al-, Fe- and Ca-P. Phosphorus K-edge X-ray absorption near edge structure (XANES) has been successfully employed in a number of agri-environmental studies to assess the chemical species of P present in soils that received long-term application of manures (Abdala et al., 2015a; Sato et al., 2005), organo-mineral fertilizers (Corrêa et al., 2018), or to study the effects of different fertilization schemes and management systems on soil P (Liu et al., 2015). Imaging techniques, as those accessed by X-ray fluorescence microanalysis (µ-XRF) have been used considerably to study the elemental distribution in soils and sediments as reported by Majumdar et al. (2012), but are restricted by their inability to probe and identify phosphorus chemical species. Therefore, the use of X-rays absorption spectroscopy (XAS) interestingly becomes associated with imaging techniques. More recently, the combined use of wet chemistry analysis, µ-XRF and synchrotron-based XAS has represented a successful means not only to chemically speciate P in soils, but also to assess its distribution and associations with soil constituents (Abdala et al., 2018; Kizewski et al., 2011; Liu et al., 2014; Lombi and Susini, 2009).

In this study, we combined P K-edge XANES, Fe K-edge extended X-ray absorption fine structure (EXAFS), μ-XRF and conventional chemical analysis to evaluate the effects of P rates on P speciation in highly weathered agricultural soils of Brazil over twenty-six years of NT cultivation. We hypothesize that long-term mineral phosphate fertilizer application may lead to P stabilization in soils under more thermodynamically stable forms, such as P-Fe and P-Al, in spite of the effects that abundant SOM under NT might have on P reactivity.

Material and methods

Soil attributes and experimental setting

A long-term field experiment has been conducted on a Rhodic Hapludox (*Soil Survey Staff*, 2014) since 1989 in Londrina, state of Parana, Brazil (23º 11' S; 51º 10' W, 613 m a.s.l.). The top soil layer (0-0.2 m) had clay content of 760 g kg^{-1}, pH (0.01 mol L^{-1} $CaCl_2$) of 4.5; 39 $mmol_c$ dm^{-3} Ca and 12 $mmol_c$ dm^{-3} Mg (extracted with 1 mol L^{-1} KCl); 9 mg dm^{-3} P and 4 mg dm^{-3} K (extracted by Mehlich-1) at the beginning of the experiment. The climate at the experimental area, according to Köppen's classification system is Cwa subtropical humid, with rainfall in all seasons and possible dry period during the winter. The average temperature of the hottest month is 25.5 ºC and 16.4 ºC in the coldest month. The experimental area has been managed under NT since the 1995/96 cropping season. The experimental design was a randomized block with four P rate treatments (0, 20, 40 and 50 kg ha^{-1}) with four replications (Table 1). A flat rate of K (40 kg ha^{-1}) was applied over the experiment annually.

Table 1. Phosphorus (P) application rates in a Rhodic Hapludox under NT prior to soybean sowing (adapted from Antonangelo et al., 2019)

P (kg ha^{-1})	Fertilization			P (kg ha^{-1})[2]
	....Summer....	....Winter....	....Whole year....	
	.....P[1] kg ha^{-1}.....			
0	0	0	0	0
20	0	20	20	515
40	20	20	40	889
50	30	20	50	1249

[1]Triple Superphosphate (~190 g P kg^{-1}) was the P source
[2]Sum of applications for all crops since 1989

The experiment has been predominantly cultivated with soybean (*Glycine max* L.) in the summer and wheat (*Triticum aestivum* L.), oat (*Avena strigosa* L.) or corn (*Zea mays* L.) in the fall/winter period. The plots were 160 m^2 (8 wide x 20 long m). The field was amended with dolomitic lime or calcium carbonate lime. Lime rates were calculated to raise the base saturation to 70%: 1.5 t ha^{-1} for the 1996/97, 2.0 t ha^{-1} for the 2001/02, 1 t ha^{-1} for the 2010/11 and 2 t ha^{-1} for the 2012/13. In addition, 1 t ha^{-1} gypsum was applied in the 2012/13 season, and 2.5 t ha^{-1} applied in the 2014/15 season to increase Ca and S availability in the soil and to reduce exchangeable Al in the subsoil (below 0.2 m in the soil profile). The last P and K fertilizations were performed in October 2014 for soybean and in February 2015 for oat prior to soil sampling (September 2015) for this investigation. Rates of applied P and K fertilizers were very similar throughout the 26 years of the experiment with slight differences due to changes in the application recommendations over the years.

Soil samples were collected in September 2015 with an auger after oat harvesting and prior to the soybean sowing (October 2015). Five subsamples from the 0-0.1 m layer per plot were collected as a composite sample. Soil samples consisted of 10 subsamples

from a native forest near (1 km) the experiment site were collected from 0-0.1 m layer for comparison. The collected samples were oven dried at 45 ºC and then were ground and sieved (< 2 mm). Soil attributes such as pH, organic carbon (OC), P, Ca, Mg, Al, exchangeable acidity (H+Al) and total cation exchange capacity (CEC_t) were determined according to van Raij (1998) and Bertsch and Bloom (1996). The exchangeable Al^{3+} was extracted by 1 mol L^{-1} KCl in a 1:10 (v/v) soil/solution ratio followed by titrimetric method (Bertsch e Bloom, 1996). Plant available P were extracted by Mehlich-1 (M1) solution (HCl 0.05 mol L^{-1} + H_2SO_4 0.0125 mol L^{-1}) (Silva, 2009), with ion exchange resin and sodium bicarbonate ($NaHCO_3$) (van Raij, 1998). P contents in the extracts were quantified by UV-vis spectroscopy.

The remaining P in the soil (P_{rem}) was determined by equilibrating 2.5 g of soil with 25 mL 0.01 mol L^{-1} $CaCl_2$ solution containing 60 mg L^{-1} of P (as KH_2PO_4) (Alvarez et al., 2000). This measurement allowed us to observe variations of the adsorption capacity of P that the Rhodic Hapludox exhibits. The total phosphorus of the soil was obtained by acid digestion.

The quantification of the total P content in samples (particle size < 0.1 mm) were also done by Energy Dispersive X-ray fluorescence (EDXRF) using a Shimadzu EDX-720/800HS equipped with a rhodium X-ray tube generator, a silicon detector with 10 mm collimator and 20 keV of voltage (Peate et al., 1992; USPEA, 1996). The soil matrix itself was used as a standard by the addition of P via monopotassium phosphate (KH_2PO_4) in two known concentrations, which were then served as the calibration curve for the determination of the actual P contents in the samples.

The Fe and Al contents in crystalline oxides were determined after extraction with dithionite-citrate-bicarbonate (DCB) (Mehra and Jackson, 1960). Iron (Fe) and Al contents in less crystalline oxides were extracted with ammonium oxalate (AO) (Camargo et al., 2009). The Fe and Al concentration in the extracts were determined by an inductively coupled plasma optical emission spectrometry ICP-OES.

Mineralogy

Soil samples from the experimental site and from the reference site (native forest) were analyzed for mineralogical composition. Initially, hydrogen peroxide was added to remove organic matter. The clay fraction was separated by dispersion and centrifugation with NaCl followed by powder X-ray diffraction (XRD), without orientation. Analyses were performed on a computer-controlled X-ray diffractometer (Rigaku MiniFlex) using a copper tube (Cu), graphite monochromator, and CuKα radiation (40 kV and 15 mA) with 5.0º of Soller slit for qualitative study of mineral components of the fraction (Whitting and Allardice, 1986). The goniometer velocity was 0.02º2θ s^{-1}, with an amplitude of 3 to 80º2θ. The qualitative interpretation of spectra was then carried out according to Chen (1977).

µ-XRF analysis

Elemental distribution along with the X *Vs* Y scattering plots were performed to ground soil samples with particle size < 0.1 mm. The materials were ground in a ball-mill and spread on a kapton tape for analysis. Rock fragments of about 1 cm thick with flat surfaces were removed for analysis. An area with approximately 3 mm^2 was randomly

chosen for analysis. The equipment provides a high analytical sensitivity working under vacuum (no influence of O_2 on the absorption of the electromagnetic beam). Phosphorus μ-XRF was collected using an Edax Orbis PC equipped with Rh tube (working under constant vacuum), operating at 40 kV and 1000 μA. The images were recorded with 3200 pixels and 2s of dwell time. The XRF was detected using a 30 mm^2 silicon drift detector.

Phosphorus K-edge XANES analysis

Composite soil samples from four replicates of each treatment, and a soil sample from an adjacent forest were ground to pass through a 150 μm-screen. Some standards of P-sorbed to minerals were prepared by reacting K_2HPO_4 with Fe to produce $FePO_4*2H_2O$; and with gibbsite (Al_2O_3), goethite (α-FeOOH), hematite (α-Fe_2O_3), kaolinite, non-crystalline Al-(hydr)oxide/variscite ($AlPO_4*_2H_2O$) and non-crystalline Fe-(hydr)oxide/ferrihydrite to produce more P-sorbed minerals. Other compounds, such as amorphous calcium phosphate, beta-tri-calcium-phosphate, brushite ($CaHPO_4*2H_2O$), DNA, potassium dihydrogen phosphate (KH_2PO_4), lecithin, $(NH_4)_3PO_4$, octacalcium phosphate [$Ca_8H_2(PO_4)_6.5H_2O$], monetite ($CaHPO_4$), hydroxyapatite-[$Ca_5(PO_4)_3OH$] and Na-phytate ($C_6H_{18}O_{24}P_6$), were obtained from commercial suppliers. The standards were diluted with boron nitride (BN) to yield concentrations below 0.15% P to minimize self-absorption effects.

XANES data were collected under vacuum from the Soft X-Ray Spectroscopy (SXS) beamline at the Brazilian Synchrotron Light Laboratory (LNLS), using a Si(111) monochromator calibrated with a calcium phosphate standard (E_0 = 2151.7 eV). A thin layer of either samples or reference compounds were spread on double-sided carbon tape,

mounted on a sample holder and placed in the high-vacuum chamber for analysis. The electron beam energy was 1.37 GeV and the beam current varied between 250 and 110 mA. The P K-edge XANES (E_0 2145.5 eV) spectra were collected in fluorescence mode from 2120 to 2350 eV and the step sizes were 1 eV (2120-2145 eV), 0.2 eV (2145.2-2180 eV), 1 eV (2181-2220 eV), and 3 eV (2223-2350 eV). Twelve to 20 scans were collected and merged to reduce spectral noise. Data processing and linear combination fitting (LCF) were performed using the Athena software (Ravel & Newville, 2005). After merging, spectra were calibrated setting de edge reference energy (E_0) at the maximum of the first derivative and normalized, setting the background pre-edge range from E_0 -22 to E_0 -10 eV, and the normalization range from E_0 +35 to E_0 +55 eV.

Reference compounds or standards were selected firstly by visual inspection of the main features. Linear combination fitting was performed over the -10 to +30 eV energy range relative to E_0 and carried out according to Colzato et al. (2017), employing two approaches that converged to the same results.

Iron K-edge EXAFS analysis

Iron (Fe) K-edge EXAFS spectra were collected at the X-Ray Absorption and Fluorescence Spectroscopy (XAFS2) beamline of the Brazilian Synchrotron Light Laboratory (LNLS). Five composite soil samples (four replicates) from the treatments of 0, 20, 40 and 50 kg ha^{-1} P, and a native forest (as reference) were used. The Fe mineral standards used were ferrihydrite (Fh), hematite (Hm) and goethite (Gt). All samples and standards were milled on an agate mortar and passed through 10-µm mesh. After milling, 30 mg of the samples were added to 10 mL of isopropanol and dispersed by ultrasonic

vibration. Once the suspension was obtained, the material was deposited on a cellulose acetate membrane induced by a vacuum pump. Thereafter, the membrane was placed on a sample holder with Kapton tape. The EXAFS spectra were collected in transmission mode under ambient conditions. The calibration was performed using a Fe foil, setting E_0 at 7111.3 eV. Spectra were collected from 7250 to 8000 eV: 7000 to 7080 eV in a step of 1.0 eV, from 7080 to 7250 eV in a step of 0.2 eV and of 7250 to 8000 in a space k of 0.05, with acquisition time of 1 s for all intervals. The combined and calibrated spectra were normalized using the Athena software in the computer package IFEFFIT (Ravel & Newville, 2005). Fe-EXAFS data were normalized from each averaged, unsmoothed and energy calibrated spectrum after the subtraction of a polynomial pre-edge function. A cubic spline fit was used above the absorption edge in order to remove the background and the data were k^3-weighted to enhance the *k* values. Normalized EXAFS spectra were filtered over a *k* range of ~3.1 to ~14 $Å^{-1}$ (Abdala et al., 2015a).

Statistical analysis

Soil chemical attributes were subjected to the analysis of variance (ANOVA) and the average results of each treatment compared by Tukey test. The standard deviation of the mean was also used to compare results among treatments and was represented by the symbol "±". Pearson correlation and linear and multiple regression analyses were performed to variables obtained from µ-XRF, using all replicate data (n=60), in SAS version 9.4 (SAS Institute, 2011).

Results and Discussion

Soil attributes

Soil P treatments did not significantly affect the soil chemical attributes ($p>0.05$), except for CEC_t (Table 2). The lack of differences among treatments receiving P was probably due to previous lime applications aimed to raise the base saturation to the same level in all plots and treatments, which resulted in similar CEC across all treatments. Since the very last topdressing liming took place 3 years before the soil samples were collected on the surface, the BS% dropped to below 70%. In spite of the apparent high CEC_t, they were significantly influenced by the potential acidity (H+Al), which is reflected in the BS% values around 50% (Antonangelo et al., 2019). As expected, OC, CEC_t, Ca^{+2} and Mg^{+2} were higher in the soil from native forest than in the soil receiving the treatments. Generally, soil organic matter (SOM) provides more negative charge and a higher CEC, which is a result of the increase in the organic carbon (OC) overtime. Also, the soil surface area (49.8 m^2 g^{-1}) was approximately 9% higher in the native forest than in the soils collected in the experimental area, with a mean of 45.8±1.6 m^2 g^{-1}.

The total P contents were influenced by the annual P rates applied. The highest contents were observed at the 50 kg ha^{-1} P rate regardless of the method used (XRF or total chemical digestion) (Table 2). It is probably a consequence of P build up due to over application. Resin-P was not different between the control and the 20 kg ha^{-1} treatment, and the native forest. However, the higher P rates (40 and 50 kg ha^{-1}) had higher P_{resin} than in the other treatments. The P_{M1} was also higher for the two highest rates of P applied. Therefore, a saturation point can be reached overtime and then any further P applied can increase soil available P (Table 2). Such behavior was also reflected by the

remaining P (P_{rem}), which exhibited a greater recovery in the plots that received the highest P rate. This might be related to the greater amount of fixed forms of P in the clay minerals and their saturation over the years (Gérard, 2016). Although no significant changes were observed in Fe and Al contents extracted with AO and DCB, they were numerically different with higher values of Fe_{AO} returned from the native forest soil (Table 2).

Table 2. Soil attributes

Attribute	……. Treatment…….				
	native forest	control	20 kg ha^{-1} P	40 kg ha^{-1} P	50 kg ha^{-1} P
pH 0.01 M $CaCl_2$	5.0 a	5.2 a	4.9 a	5.0 a	4.9 a
[1]OC (g kg^{-1})**	26 a	15 b	15 b	16 b	15 b
[2]CEC_t ($mmol_c$ dm^{-3})**	125 a	77 c	80 bc	84 b	84 b
[3]H+Al ($mmol_c$ dm^{-3})	38 a	36 a	48 a	45 a	48 a
Ca^{2+} ($mmol_c$ dm^{-3})**	66.9 a	28 b	23 b	27 b	26 b
Mg^{2+} ($mmol_c$ dm^{-3})**	19.1 a	11 b	8 b	10 b	10 b
Al^{3+} ($mmol_c$ dm^{-3})	3.8 ab	5.1a	6.1 a	5.7 a	6.4 a
K^+_{M1} ($mmol_c$ dm^{-3})*	1.8 a	1.8 a	1.0 ab	1.1 ab	0.9 b
[4]surface area (m^2 g^{-1})	49.8	46.6	47.6	44.4	44.6
[5]total P (mg kg^{-1})	696	544	564	756	894
[6]total P (mg kg^{-1})	-	594	653	731	1103
P_{M1}	3±1	2±1	9±2	14±6	45±9
P_{resin}	15±3	13±3	19±4	46±12	123±20
P_{rem} (%)	-	21±2.7	25±2.9	35±6.2	43±8.9
Fe_{DCB} (g kg^{-1})	122±5.4	132±4.4	130±2.6	127±1.8	127±3.5
Fe_{AO} (g kg^{-1})	5.1±0.4	4.4±0.3	4.9±0.3	4.6±0.1	4.7±0.4
Al_{DCB} (g kg^{-1})	-	4.2±0.1	3.8±0.1	3.2±0.1	3.5±0.1
Al_{AO}(g kg^{-1})	-	3.0±0.1	3.0±0.1	3.2±0.1	3.5±0.2

**significant at $p<0.01$ and *at $p<0,05$ (n=4) from Tukey test; [1]organic carbon extracted with $K_2Cr_2O_7$; [2]total cation exchange capacity (Ca+Mg+[H+Al]+K_{M1}); [3]Potential acidity estimated by the pH of the SMP solution (Shoemaker et al., 1961); [4]Surface analyzer (TriStar II 3020): samples were degasified at 80 ºC for 2 hours followed by liquid nitrogen (N_2) addition, and surface area was calculated through the BET equation (Brunauer et al., 1938); [5]Acid digestion; [6]X-ray fluorescence (XRF); Fe_{DCB}: sodium dithionite citrate and bicarbonate extractable Fe; Fe_{AO}: acidic solution of ammonium oxalate extractable Fe; Al_{DCB}: sodium dithionite citrate and bicarbonate-extractable Al; Al_{AO}: acidic solution of ammonium oxalate-extractable Al

Mineralogy

The soil clay fraction was shown to be predominantly composed of kaolinite (d: 0.725; 0.234; 0.183; 0.169; 0.149 nm), hematite (d: 0.269; 0.250; 0.220 nm) and goethite (d: 0.269; 0.220 nm) (Fig. 1). Such results are consistent with Camargo et al. (2014) and Moterle et al. (2016) in clay fractions of Oxisols developed from basaltic rocks. No differences were observed in the mineralogical compositions and peak intensity between the experimental and native forest soils. The kaolinite (Kln) was expected to be the dominant phyllosilicate found in highly weathered soils from humid tropical regions (Fontes et al., 2001). Gt and Hm are Fe oxides commonly found in Oxisols. The dominance of Hm in the clay fraction was expected due to pedo-environmental conditions (Schwertmann and Murad, 1983), such as moderate desilication, high temperatures, rapid organic matter mineralization and pH close to neutrality with a high Fe content in the parent material. The presence of gibbsite (d: 0.483) is also common in Brazilian Oxisols (Melo et al., 2001), and is the representative aluminum oxide in tropical humid soils. The observed minerals are typical in highly weathered Oxisols due to pedogenic processes such as ferralitization, desilication and bioturbation.

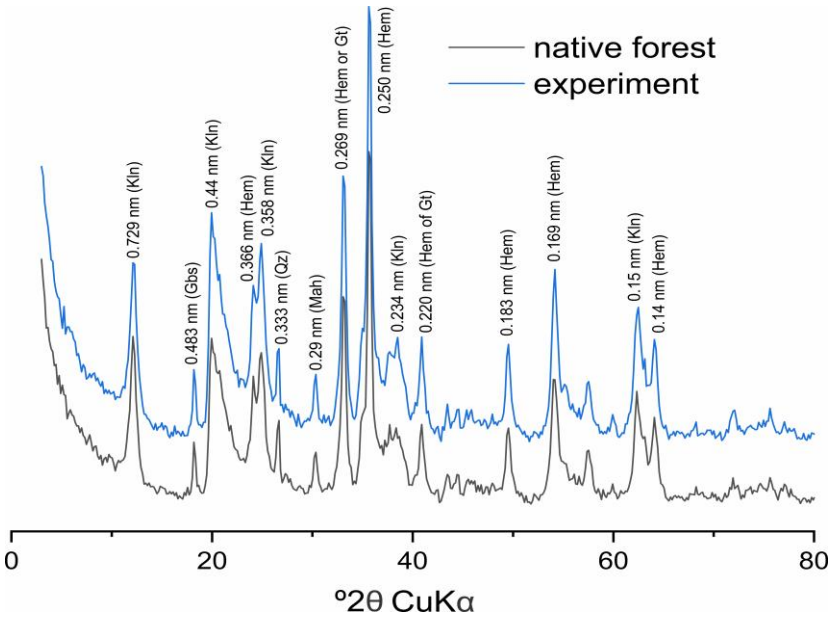

Fig. 1. X-ray diffraction of the experiment (blue) and native forest (black) soil clay fraction. Kln – kaolinite, Gb – gibbsite, Hm – hematite, Qz – quartz, Mah – maghemite, Gt – goethite

P analysis by µ-XRF

Our approach to investigating the distribution of P in bulk soil samples was similar to those performed by Eze et al. (2018). Aluminum, Si and Fe were chosen for the correlations due to the abundant presence of these elements in (hydr)oxides and phyllosilicates with high P fixation capacity (i.e., Fe as Gt and Hm; Al as Gb and Al and Si as Kln). Calcium was selected due to the liming practices over the years. It is evident that the association of P with Si, Al and Fe atoms is higher than P with Ca (Table 3). The better correlation between P and Ca observed for the 20 kg ha^{-1} P corroborates the higher HCl-*Pi* found in the soil chemical fractionation (SCF) for the same treatment (data not shown). The stronger association between P and Fe, Al and Si in all treatments is probably associated with the significant presence of Fe-oxides and kaolinite (Al and Si)

as highlighted by the XRD analysis (Fig. 1). Mappings of P distribution for the control and the highest rate of P applied are present in Fig. S1 (*Supplementary material*). The association of P with Fe-oxides and kaolinite species will be further discussed in the P-XANES and linear and multiple regression analyses.

Table 3. Pearson correlations (r) between the quantitative spatial distributions of Si, Al, Fe, Ca and P in samples from the native forest and experimental treatments determined by micro X-ray florescence.

Treatment	P *Vs* Al	P *Vs* Si	P *Vs* Fe	P *Vs* Ca
Native forest	0.97	0.91	0.80	0.60
p value	*<0.0001*	*<0.0001*	*<0.0001*	*<0.0001*
Control	0.97	0.85	0.85	0.34
p value	*<0.0001*	*<0.0001*	*<0.0001*	*0.009*
20 kg ha^{-1} P	0.98	0.80	0.91	0.80
p value	*<0.0001*	*<0.0001*	*<0.0001*	*<0.0001*
40 kg ha^{-1} P	0.97	0.89	0.86	0.76
p value	*<0.0001*	*<0.0001*	*<0.0001*	*<0.0001*
50 kg ha^{-1} P	0.94	0.62	0.77	0.42
p value	*<0.0001*	*<0.0001*	*<0.0001*	*<0.0001*

Phosphorus K-edge XANES analysis

The representative P species in solid-state found for the treatments are presented in Fig. 2. Most species were P-kaolinite, and P adsorbed to Fe minerals. It was expected considering that kaolinite is a dominant phyllosilicate found in Oxisols, so does the Fe oxides Gt and Hm, as previously emphasized in the XRD analyses. Ferrihydrite is a non-crystalline Fe mineral that occurs when the activity of organic matter over the crystalline Fe minerals is high, which is favored under NT conditions, as will be further discussed.

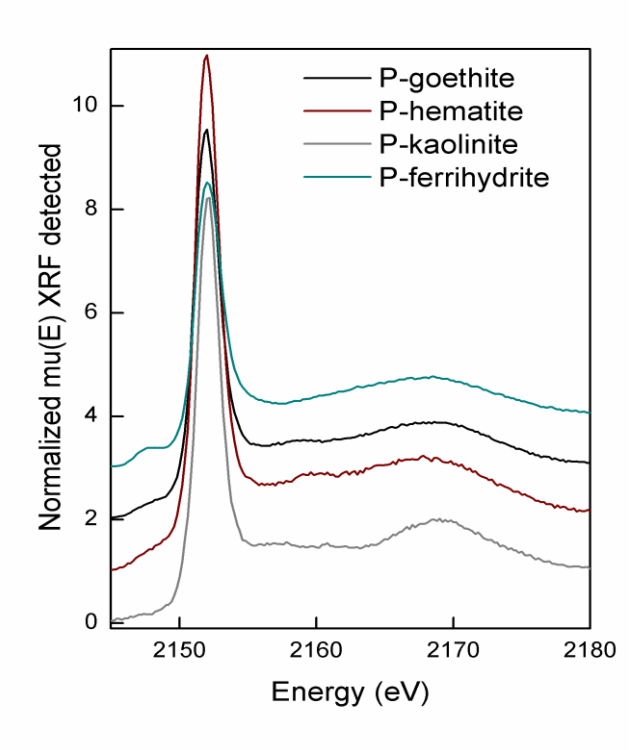

Fig. 2. P K-edge spectra of P sorbed to goethite (P-Gt), hematite (P-Hm), ferrihydrite (P-Fh) and kaolinite (P-Kln) used as reference compounds for linear combination fitting of XANES data

Best fitting results from LC analysis are shown in Fig. 3A. The pre-edge corresponds to 1s to 3d electronic transitions (Fig. 3B). Since Fe minerals are some of the most important sorbing phases for P in soils, particularly in highly weathered soils of the tropics, and its amount surpass by far the concentrations of other 3d metals, the presence of pre-edge in P-XANES spectra is an indication of P associated with Fe oxides. Dashed lines highlight differences in intensities and shapes of the main features of the spectra; therefore, the pre-edge was even more pronounced for the P-Fh spectra (Fig. 3). Similar characteristics were reproduced for all soil samples analyzed. Certainly, the standards we

prepared provided suitable fit, and the features of data and fit are consistent among the soil samples from the native forest and those receiving P application.

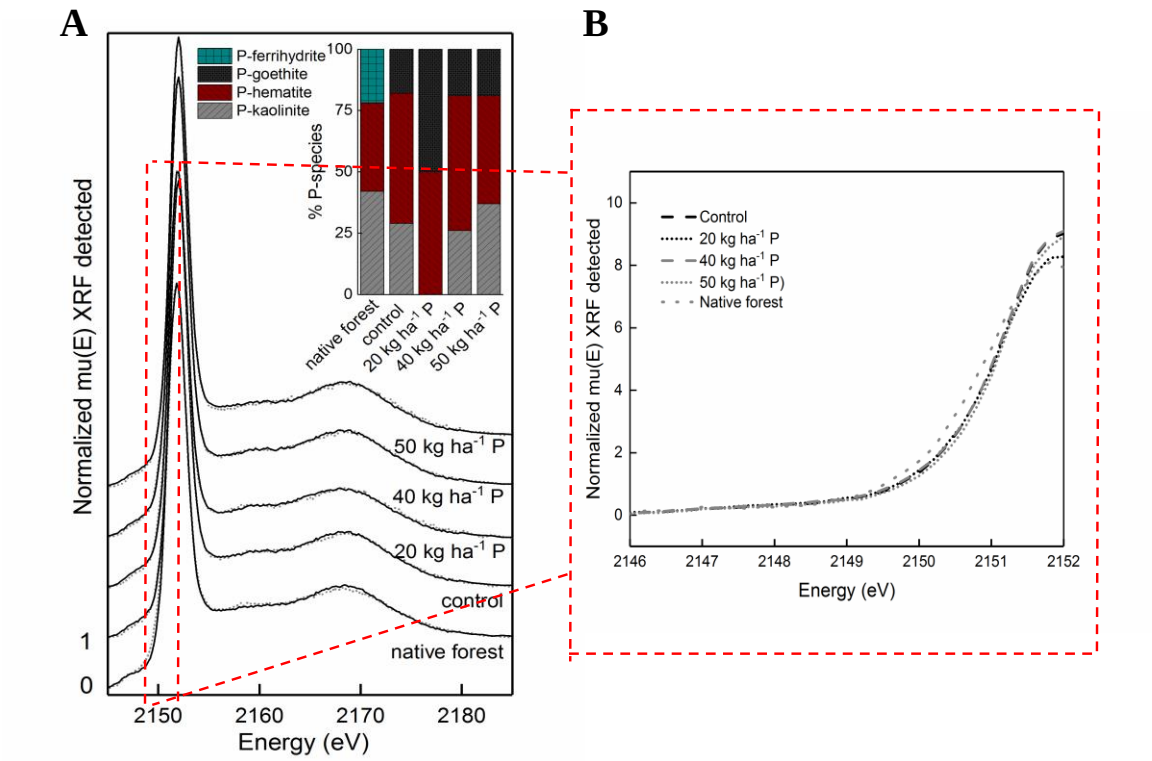

Fig. 3. (**A**) P K-edge XANES spectra (points) for native forest, control, 20 kg ha^{-1} P, 40 kg ha^{-1} P and 50 kg ha^{-1} P soil samples. Data are overlaid by LCF (lines). The bar graph reflects the fraction of the standards that best represented the sample spectra in the LCF. (**B**) the insert showing pre-edge crests of treated soils

Generally, P-Kln, P-Gt, P-Fh and P-Hm spectra were suitable to depict our set of soil samples in LCF with a pre-edge observed only for the Fe oxide minerals (Fig. 3B). These standards generally represent the main phosphate adsorbing oxide minerals typically found in Brazilian Oxisols. As a matter of fact, a pre-edge crest around 2148 eV

is characteristic of crystalline Fe phosphates (Abdala et al., 2015b; Hesterberg et al., 1999; Ingall et al., 2011; Khare et al., 2005). Although some authors stated that a pre-edge is more prominent in crystalline than in non-crystalline minerals (Abdala et al., 2015b; Hesterberg et al., 1999; Kruse e Leinweber, 2008), we found it more featured in the native forest soil sample, which was attributed to P-Fh, a non-crystalline P-Fe oxide association (Fig. 3A and 3B). Although the fitting has returned P-Fh as the primary P species, it is important to emphasize that this mineral was not identified in the soil clay fraction by XRD; however, this adjustment may have occurred due to the presence of Fe oxides (Hm) with a lower structural order, probably due to an amorphization process promoted by SOM. Along with P-Hm and P-Kln, P-Fh provided a good fit only in the native forest. Not only this P-non-crystalline species had a more prominent pre-edge than others, but also did the native forest soil sample, and it was reflected in the fitting (Fig. 3).

Out of all reference compounds used in the LCF analyses, the reference compounds that returned the best fitting results were those in which phosphate was sorbed to either Gt, Hem, Fh or Kln (Table 4). Linear combination fitting results and fit quality are shown in Fig. 3A. Overall, the fit results were consistently high, yielding relatively low R-factor values of 0.0005-0.0015 and low uncertainties, ≤2% (Table 4). In addition, the weighting factors summed to 96-103% (uncertainty below 3%) for all fits and were renormalized to 100%. Except for the 20 kg ha^{-1} P rate, P-XANES fitting results suggested a slight trend of increased phosphate bonding with $Fe_{(III)}$ oxide relative to the native forest and to the control with minor changes in P-XANES speciation (Table 4).

Table 4. Relative proportions of P-minerals based on linear combination analysis of P-EXAFS data

Soil sample	% P specie ± uncertainty				R-factor[1]
	P-ferrihydrite	P-goethite	P-hematite	P-kaolinite	
Native forest	22 ± 2	−	36 ± 2	42 ± 3	0.0025
Control	−	18 ± 1	53 ± 2	29 ± 2	0.0005
20 kg ha^{-1} P	−	50 ± 3	50 ± 2	−	0.0015
40 kg ha^{-1} P	−	19 ± 1	55 ± 2	26 ± 2	0.0005
50 kg ha^{-1} P	−	19 ± 3	44 ± 2	37 ± 2	0.0008

[1]R-factor=$\sum[(\text{data-fit})^2]/\sum(\text{data}^2)$ - (Kelly et al., 2008)

Abdala et al. (2015) observed more P was sorbed to crystalline minerals in the native (adjacent forest) than in soils cultivated for extended periods. However, in their study, soil samples were obtained from soils that received annual applications of manures, varying from 5 to 10 ton ha^{-1} $year^{-1}$, which caused an increase in the OC and Fe_{AO} contents in comparison to soils that did not receive manure applications. In our study, treatments received applications of mineral P, and the soil from our native forest presented a higher OC and a higher Fe_{AO} than soil samples from the experimental field. Therefore, since our native forest produced much more biomass and more SOM in comparison to the soils receiving mineral P, the presence of less crystalline Fe oxides was favored in the former. Abdala et al. (2015) attributed the same for soils received long-term organic sources of P input. According to Lovley (1987), OM associated with Fe^{3+} reduction is a thermodynamically favorable process that lead to the formation of amorphous $Fe_{(III)/(II)}$-containing minerals.

Regarding the percentages of P minerals in solid-sate presented in Fig. 3A, the distribution of P species is similar among the control, the highest rate of P applied, and

the soil from the native forest except for the P-Fh. While the control better represents a natural condition, the treatment receiving the highest P rate is more likely to have a similar distribution of P-sorbed to Fe oxide minerals as found for the native forest. Probably, the higher P pool attributed to increased P rate applied will contribute to the increase in biomass (Antonangelo et al., 2019) followed by the OC increase, which will influence the crystallinity of Fe oxides.

Except for the 20 kg ha^{-1} treatment, the P-Gt species were about the same for other treatments but absent in the native forest. Goethite, which is more reactive with phosphate than Hm, generally exists in low content in Oxisols. Therefore, Gt was probably saturated overtime and other Fe oxides served as P- adsorbing minerals. The P-Hm species showed an opposite trend to P-Kln. The P-Hm represented 36 to 55% of the spectra of all samples with its lower distributions found for the higher rates of P applied. The soil sample with 40 kg ha^{-1} P and the control had more intense white line than others and it was reflected by the amount of P represented by P-Hm in LCF (Fig. 3).

For the 20 kg ha^{-1} P treatment, we previously inferred that phosphate adsorption reactions begin immediately after P is added to the soil (Gérard, 2016), and P, therefore, will be preferentially adsorbed to more reactive Fe oxides, such as Gt and Hem although some authors have reported the strong association of P to Kln and 2:1 minerals rather than to oxides (Gérard, 2016). P-Kln did not provide good fitting for the 20 kg ha^{-1} P treatment, which was suitably represented by P-Hm and P-Gt. For our long-term continuous fertilization experiment, the soil test P pool was not increased by the low P rate (20 kg ha^{-1}) annually applied (Antonangelo et al., 2019). Therefore, the preferential reaction of P to Gt and Hm might be occurred after the current 20 kg ha^{-1} of P was added to the soil. In

addition, the 20 kg ha^{-1} P was similar to 40 and 50 kg ha^{-1} P with the main difference being the feature at the first post-edge. Such feature is related to the crystallinity and those higher rates of P applied returned a post-edge at 2169 eV, which is attributed to Kln. Indeed, using Kln instead of Gt outputs a better fit for those treatments of 40 and 50 kg ha^{-1} P applied. The R-factor was smaller and the first post-edge crest was better adjusted. The linear regression analyses performed for the quantitative spatial distribution of Al and Si from µ-XRF returned high and close to 1:1 Al:Si ratio, which indicates the possible presence of Kln (Table 5). Multiple regression analyses also returned high and significant relationship of P *Vs* Al and Si (Table 5) and the 3D surface area map (XYZ) for soil treatments is presented in Fig. 4. The results from Table 5 clearly show that all Multiple R ([Multiple R^2]$^{1/2}$: correlation coefficient of multiple regression) square values (0.94-0.98) were similar to R-values obtained between P and Al and were much higher than the R-values obtained between P and Si for all treatments (Table 3). Fig. 4 elucidates that P (dependent variable) increases as both Al and Si increase (independent variables); in addition, Al and Si are positively correlated presenting a 1:1 relationship, as previously mentioned. These results emphasize the greater P adsorption to kaolinite rather than other minerals. According to Gérard (2016), the capacity of Kln (1:1), or even other minerals such as montmorillonite and illite (2:1) to bind PO_4 may have been greatly underestimated by several studies. Depending on the crystallinity and specific surface area (SSA) of such minerals, the PO_4 binding capacity of clay minerals can even exceed that of Fe/Al oxides, particularly goethite and gibbsite. This also explains the better LCF of P-Kln in comparison to P-Gb obtained from P-XANES analyses.

Table 5. Linear and multiple regressions of the quantitative spatial distributions of Al *Vs* Si and P (dependent) *Vs* Al, Si (independents) in samples from the native forest and experimental treatments

Treatment	……....Al *Vs* Si…….....		P *Vs* (Al *Vs* Si)
	Equation	R^2	Multiple R^2
Native forest	Si = 0.03 + 0.91*x*Al	0.89	0.93
p value	*……..<0.0001……..*		*<0.0001*
Control	Si = 0.14 + 0.82*x*Al	0.8	0.94
p value	*……..<0.0001……..*		*<0.0001*
20 kg ha^{-1} P	Si = 0.15 + 0.94*x*Al	0.67	0.97
p value	*……..<0.0001……..*		*<0.0001*
40 kg ha^{-1} P	Si = 0.13 + 0.91*x*Al	0.86	0.94
p value	*……..<0.0001……..*		*<0.0001*
50 kg ha^{-1} P	Si = 0.01 + 0.45*x*Al	0.5	0.89
p value	*……..<0.0001……..*		*<0.0001*

Soils from tropical humid regions, especially those originated from basaltic rocks under several meters annual rainfall, present P depletion after millions of years undergoing weathering process, which is also responsible to originate highly reactive minerals, such as Fe oxides. The P-Fh provided good fitting, along with P-Hm and P-Kln, only in native forest soil sample, as highlighted by the most prominent pre-edge. Even with the greater SOM, the edaphic conditions that favor Fh formation are not common. This oxyhydroxide is a precursor of Hm formation and has low atomic order (Fink et al., 2016), presenting high SSA, usually up to 400 m^2 g^{-1} (Schwertmann and Taylor, 1989). Our hypothesis is that the soil of the native forest does not have Fh, but the Hm present in this soil has a lower structural order due to continuous contact with organic acids exuded by the roots active in the soil. These results in a better fit to the P associated with Fh, but probably P is also associated with Hm presenting a less organized three-dimensional structure. However, the

using of crystalline reference minerals for LCF and fingerprinting analysis is usually inadequate for describing heterogeneous mixtures, as soil minerals are often poorly crystalline, non-stoichiometric and variable in structure and composition (O'Day et al., 2004).

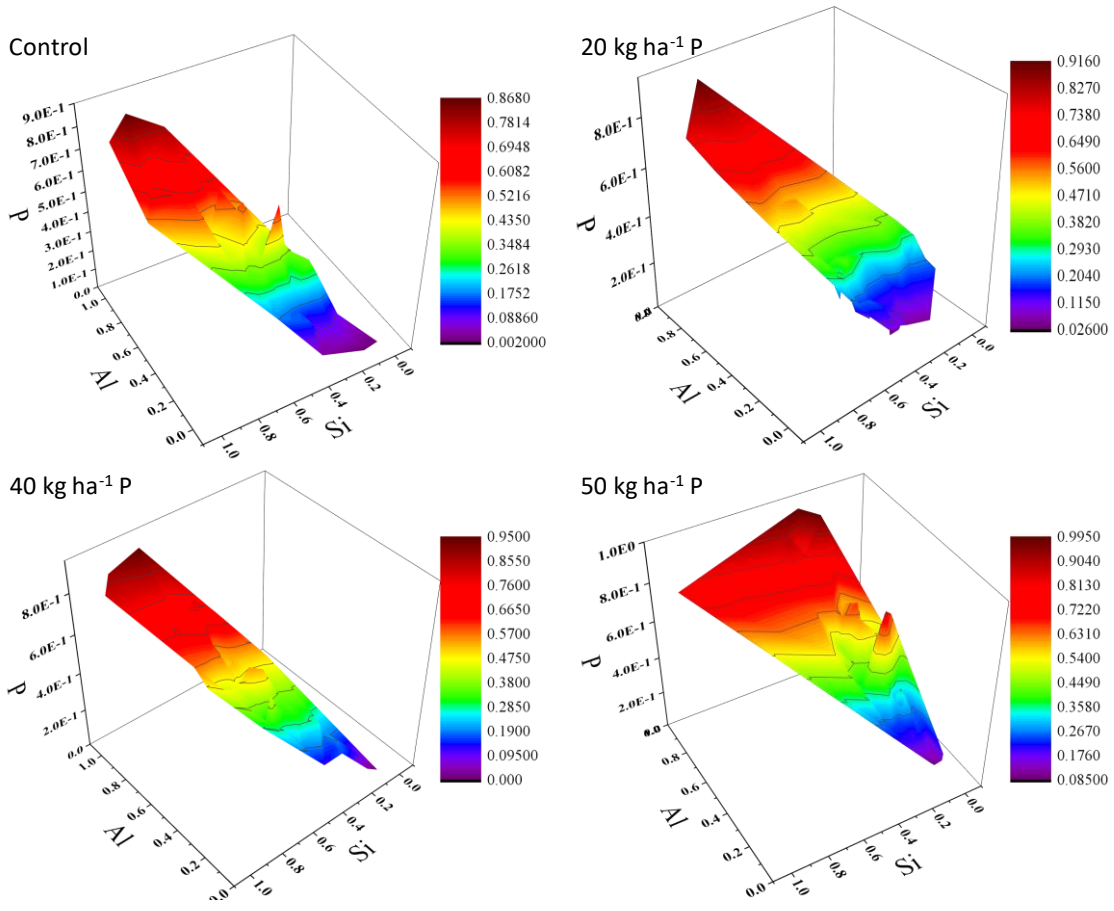

Fig. 4. 3D surface plot of the quantitative spatial distributions (counts s^{-1}) of Al/Si/P (XYZ) for experimental area treatments

Iron K-edge EXAFS analyses

Fe-(hydr)oxides was further investigated by means of Fe-XANES and Fe-EXAFS analyses. The results corroborated our previous findings about P-adsorbed to Fe oxides from P-XANES. Flattened signal after 10 $Å^{-1}$ is indicative of low crystallinity/non-stoichiometric, as denoted by the Fh standard in Fig. 5.

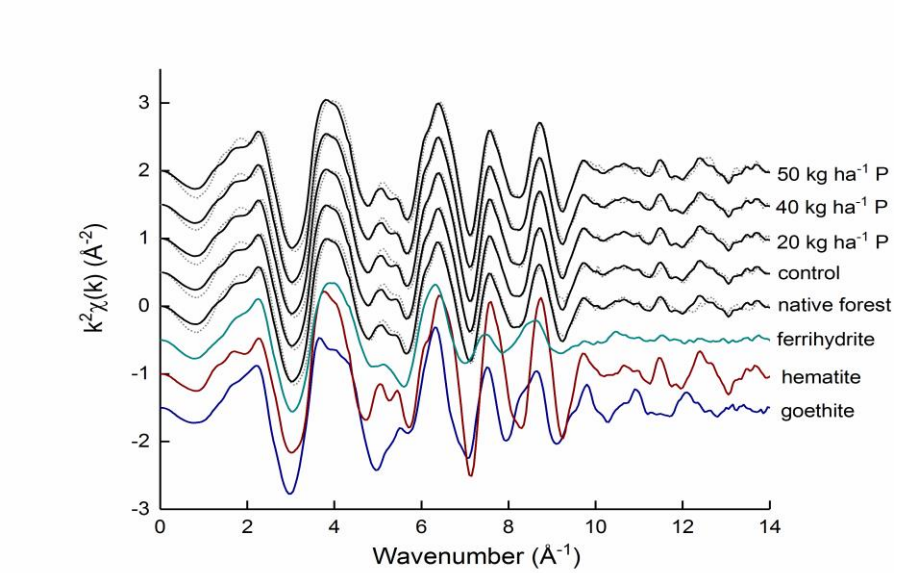

Fig. 5. Fe K-edge EXAFS spectra (points) for native forest, control, 20 kg ha^{-1} P, 40 kg ha^{-1} P and 50 kg ha^{-1} P soil samples and the standards Gt, Fh and Hm (colors). Sample data are overlaid by linear combination fits (lines)

Although results from Fe-EXAFS and Fe-XANES did not indicate better fit for Gt (as was indicated by P-XANES), the significant presence of Fh shows a trend of Fe-oxides with inconstant structure been formed overtime if more root activity and biomass is accumulated as a consequence of increased rates of P applied. There is still a lack of information regarding Fe speciation by EXAFS. Soil organic matter components, such as

dissolved organic carbon (DOC), play a big role in complexing Fe minerals, for example, hematite (Abdala et al., 2015) in native forests and systems under NT.

As for P-XANES, the Fe-EXAFS and Fe-XANES fitting results are summarized in Tables 6 and 7. Two of the standards used in the LCF analyses provided the best fit to the spectra of soil samples (Tables 6 and 7). Considering the errors, all samples and treatments are depicted by hematite and Fh standards in equivalent proportions from both Fe-EXAFS and Fe-XANES analyses, except by the native forest soil sample, which was predominated by Fh in the best fit (Tables 6 and 7). That corroborates our findings for the soil sample from the native forest, in which the P-XANES returned a significant distribution of P-Fh species in comparison to treatments receiving P. The quality of fits obtained by LCF was reflected by the similarity between Fe-EXAFS and Fe-XANES spectra and fits for soil samples receiving P rates (Fig. 5). The results are highlighted by consistently low R-factors of 0.005-0.05 and low uncertainties on fitted proportions of standards of ≤3%. In addition, the weighting factors summed up to 96-103% for all fits and were renormalized to 100%. Features between 5 and 6 $Å^{-1}$ of the standards provide reliable information about sample composition.

P-XANES, Fe-XANES and Fe-EXAFS results display the possibility of a reduction in the structural order of Fe-oxides in native forest samples, which probably contributes to the increase in surface area even more than crystalline forms of Fe-oxides. Only slight differences were observed among cultivated soil samples (Tables 6 and 7). However, there might be a tendency to increase the % Fe specie of Fh fitting in the future, if the experiment continues, mainly due to the greater input of available P, plant biomass and root action in the 50 kg ha^{-1} P treatment.

Table 6. Relative proportions of Fe-minerals based on linear combination analysis of Fe-EXAFS data

Soil sample	% Fe specie ± uncertainty						R-factor[1]	Chi-squared	Reduced Chi-squared
	ferrihydrite			hematite					
native forest	58	±	3	42	±	2	0.0427	1.7	0.008
control	50	±	3	50	±	2	0.0372	1.5	0.008
20 kg ha^{-1} P	47	±	3	53	±	2	0.0413	1.8	0.009
40 kg ha^{-1} P	50	±	2	50	±	2	0.0321	1.5	0.007
50 kg ha^{-1} P	48	±	3	52	±	2	0.0454	2.1	0.01

[1]R-factor=$\sum[(data-fit)^2]/\sum(data^2)$ (Kelly et al., 2008)

Table 7. Relative proportions of Fe minerals based on linear combination analysis of the first derivative of XANES data

Soil sample	% Fe specie ± uncertainty						R-factor[1]	Chi-squared	Reduced Chi-squared
	ferrihydrite			hematite					
native forest	62	±	3	38	±	3	0.02	0.013	0.000002
control	51	±	3	49	±	2	0.01	0.009	0.00003
20 kg ha^{-1} P	49	±	2	51	±	2	0.005	0.004	0.000008
40 kg ha^{-1} P	47	±	2	53	±	2	0.006	0.005	0.00001
50 kg ha^{-1} P	53	±	3	47	±	3	0.02	0.012	0.00003

[1]R-factor=$\sum[(data-fit)^2]/\sum(data^2)$ (Kelly et al., 2008)

Conclusions

The increased P application increases phytoavailable P and changes the proportions of P adsorbed to goethite, hematite and kaolinite. The kaolinite presents a great potential for the P adsorption, especially when more favored iron minerals to this purpose are already saturated by the excessive P application. Such over application

saturates soil with P and increases the possibility of P loss. Native forest and high rates of P application under NT seems to increase biomass production, which results in more soil organic carbon and decreases the crystallinity of Fe oxides.

References

Abdala, D.B., da Silva, I.R., Vergütz, L., Sparks, D.L., 2015. Long-term manure application effects on phosphorus speciation, kinetics and distribution in highly weathered agricultural soils. Chemosphere 119, 504–514.

Abdala, D.B., Ghosh, A.K., da Silva, I.R., de Novais, R.F., Alvarez Venegas, V.H., 2012. Phosphorus saturation of a tropical soil and related P leaching caused by poultry litter addition. Agric. Ecosyst. Environ. 162, 15–23.

Abdala, D.B., Moore, P.A., Rodrigues, M., Herrera, W.F., Pavinato, P.S., 2018. Long-term effects of alum-treated litter, untreated litter and NH_4NO_3 application on phosphorus speciation, distribution and reactivity in soils using K-edge XANES and chemical fractionation. J. Environ. Manage. 213, 206–216.

Abdala, D.B., Northrup, P.A., Arai, Y., Sparks, D.L., 2015b. Surface loading effects on orthophosphate surface complexation at the goethite/water interface as examined by extended X-ray Absorption Fine Structure (EXAFS) spectroscopy. J. Colloid Interface Sci. 437, 297–303.

Alvarez, V., Novais, R.F., Dias, L.E., Oliveira, J.A., 2000. Determination and use of remaining phosphorus. Inf. Bull. Brazilian Soil Sci. Soc. 25, 27–32.

Antonangelo, J., Firmano, R.F., Alleoni, L., Junior, A.O., Zhang, H., 2019. Soybean Yield Response to Phosphorus Fertilization in an Oxisol under Long-Term No-Till Management. Soil Science Society of America Journal. doi:10.2136/sssaj2018.07.0251

Aziz, I., Mahmood, T., Islam, K.R., 2013. Effect of long-term no-till and conventional tillage practices on soil quality. Soil Tillage Res. 131, 28–35.

Bertsch, P.M., Bloom, P.R., 1996. Aluminum, in: Sparks, D.L. (Org.), Methods of Soil Analysis Part 3 - Chemical Methods. p. 517–550.

Boddey, R.M., Jantalia, C.P., Conceiçao, P.C., Zanatta, J.A., Bayer, C., Mielniczuk, J., Dieckow, J., Dos Santos, H.P., Denardin, J.E., Aita, C., Giacomini, S.J., Alves, B.J.R., Urquiaga, S., 2010. Carbon accumulation at depth in Ferralsols under zero-till subtropical agriculture. Glob. Chang. Biol. 16, 784–795.

Boitt, G., Black, A., Wakelin, S.A., Mcdowell, R.W., Condron, L.M., 2018. Impacts of long-term plant biomass management on soil phosphorus under temperate grassland. Plant Soil, 427, 163–174.

Borges, B.; Abdala, D. B.; Souza, M.; Viglio, L.; Coelho, M.; Pavinato, P.; Franco, H., 2019. Organomineral phosphate fertilizer from sugarcane byproduct and its effects on soil phosphorus availability and sugarcane yield. Geoderma 339, 20-30.

Brunauer, S., Emmett, P.H., Teller, E. 1938. Adsorption of gases in multimolecular layers. Journal of the American Chemical Society 60(2), 309-319.

Caires, E.F., Sharr, D.A., Joris, H.A.W., Haliski, A., Bini, A.R., 2017. Phosphate fertilization strategies for soybean production after conversion of a degraded pastureland to a no-till cropping system. Geoderma 308, 120–129.

Camargo, L., Marques Júnior, J., Pereira, G., Alleoni, L., 2012. Catena Spatial correlation between the composition of the clay fraction and contents of available phosphorus of an Oxisol at hillslope scale. Catena 100, 100–106.

Camargo, L.A., Marques Júnior, J., Pereira, G.T., Bahia, A.S.R. de S., 2014. Clay

mineralogy and magnetic susceptibility of Oxisols in geomorphic surfaces. Sci. Agric. 71, 244–256.

Camargo, O.A., Moniz, A.C., Jorge, J.A., Valadares, J.M.A.S., 2009. Methods of Chemical, Mineralogical and Physical Analysis of Soil (in Portuguese), Boletim 10. ed. Agronomic Institute of Campinas, Campinas.

Chen, P.Y., 1977. Table of key lines in X-ray powder diffraction patterns of minerals in clays and associated rocks. Department of Natural Resources, Bloomington.

Colzato, M., Kamogawa, M.Y., Carvalho, H.W.P., Alleoni, L.R.F., Hesterberg, D., 2017. Temporal Changes in Cadmium Speciation in Brazilian Soils Evaluated Using Cd L –Edge XANES and Chemical Fractionation. J. Environ. Qual., 46, 1206-1214. https://doi.org/10.2134/jeq2016.08.0316

Corrêa, J.C., Rebellatto, A., Grohskopf, M.A., Cassol, P.C., Hentz, P., Rigo, A.Z. 2018. Soil fertility and agriculture yield with the application of organomineral or mineral fertilizers in solid and fluid forms. Pesquisa Agropecuária Brasileira 53(5), 633-640.

Eze, P.N., Madani, N., Adoko, A.C., 2018. Multivariate Mapping of Heavy Metals Spatial Contamination in a Cu – Ni Exploration Field (Botswana) Using Turning Bands Co-simulation Algorithm. Nat. Resour. Res. https://doi.org/10.1007/s11053-018-9378-3

Fageria, N.K., Baligar, V.C., 2007. Improving nutrient use efficiency of annual crops in Brazilian acid soils for sustainable crop production. Commun. Soil Sci. Plant Anal. 32, 1303–1319.

Fink, J.R., Inda, A.V., Tiecher, T., Barrón, V., 2016. Iron oxides and organic matter on soil phosphorus availability. Ciência e Agrotecnologia 40, 369–379.

Fontes, M.P.F., Camargo, O.A., Sposito, G., 2001. Electrochemistry of colloidal particles and its relationship with the mineralogy of highly weathered soils. Sci. Agric. 58, 627–646.

Gérard, F., 2016. Clay minerals, iron/aluminum oxides, and their contribution to phosphate sorption in soils — A myth revisited. Geoderma 262, 213–226.

Hesterberg, D., Zhou, W., Hutchison, K.J., Beauchemin, S., Sayers, D.E., 1999. XAFS study of adsorbed and mineral forms of phosphate. J. Synchrotron Radiat. 6, 636–638.

Igwe, C.A., Zarei, M., Stahr, K., 2010. Fe and Al oxides distribution in some Ultisols and Inceptisols of southeastern Nigeria in relation to soil total phosphorus. Environ. Earth Sci. 60, 1103–1111.

Ingall, E.D., Brandes, J.A., Diaz, J.M., De Jonge, M.D., Paterson, D., McNulty, I., Elliott, W.C., Northrup, P., 2011. Phosphorus K-edge XANES spectroscopy of mineral standards. J. Synchrotron Radiat. 18, 189–197.

Janegitz, M.C., Souza, E.A. De, Rosolem, C.A., 2016. Brachiaria as a Cover Crop to Improve Phosphorus Use Efficiency in a No-till Oxisol 1–9.

Kelly, S., Hesterberg, D., Ravel, B., 2008. Analysis of soils and minerals using X-ray absorption spectroscopy. Methods Soil Anal. Part 5 Mineral. Methods 387–464.

Khare, N., Hesterberg, D., Martin, J.D., 2005. XANES Investigation of Phosphate Sorption in Single and Binary Systems of Iron and Aluminum Oxide Minerals. Environ. Sci. Technol. 39, 2152–2160.

Kizewski, F., Liu, Y.-T., Morris, A., Hesterberg, D., 2011. Spectroscopic Approaches for Phosphorus Speciation in Soils and Other Environmental Systems. J. Environ. Qual.

40, 751-766.

Kleber, M., Mikutta, R., Torn, M.S., Jahn, R., 2005. Poorly crystalline mineral phases protect organic matter in acid subsoil horizons. Eur. J. Soil Sci. 56, 717–725.

Kruse, J., Leinweber, P., 2008. Phosphorus in sequentially extracted fen peat soils: A K-edge X-ray absorption near-edge structure (XANES) spectroscopy study. J. Plant Nutr. Soil Sci. 171, 613–620.

Liu, J., Hu, Y., Yang, J., Abdi, D., Cade-Menun, B.J., 2015. Investigation of soil legacy phosphorus transformation in long-term agricultural fields using sequential fractionation, P K-edge XANES and solution P NMR spectroscopy. Environ. Sci. Technol. 49, 168–176.

Liu, J., Yang, J., Cade-Menun, B., Liang, X., Hu, Y., Liu, C., Zhao, Y., Li, L., Shi, J., 2014. Complementary Phosphorus Speciation in Agricultural Soils by Sequential Fractionation, Solution 31 P Nuclear Magnetic Resonance, and Phosphorus K-edge X-ray Absorption Near-Edge Structure Spectroscopy. J. Environ. Qual. 1770, 1763–1770.

Lombi, E., Susini, J., 2009. Synchrotron-based techniques for plant and soil science: Opportunities, challenges and future perspectives. Plant Soil 320, 1–35.

Lovley, D.R., 1987. Organic matter mineralization with the reduction of ferric iron: a review. Geomicrobiol. J. 5, 375–399.

Majumdar, S., Peralta-videa, J.R., Castillo-Michel, H., Hong, J., Rico, C.M., Gardea-Torresdey, J.L., 2012. Analytica Chimica Acta Applications of synchrotron □ -XRF to study the distribution of biologically important elements in different environmental matrices : A review. Anal. Chim. Acta 755, 1–16.

Mehra, O.P., Jackson, M.L., 1960. Iron oxide removal from soils and clays by a dithionite–citrate system buffered with sodium bicarbonate, in: Clays and clay minerals: proceedings of the Seventh National Conference. p. 317–327.

Melo, V., Singh, B., Schaefer, C.E.G.R., Novais, R.F., Fontes, M.P.F., 2001. Chemical and Mineralogical Properties of Kaolinite-Rich Brazilian Soils. Soil Sci. Soc. Am. J. 65, 1324.

Moterle, D.F., Kaminski, J., Santos Rheinheimer, D., Caner, L., Bortoluzzi, E.C., 2016. Impact of potassium fertilization and potassium uptake by plants on soil clay mineral assemblage in South Brazil. Plant Soil 1–16.

O'Day, P.A., Rivera Jr, N., Root, R., Carroll, S.A. 2004. X-ray absorption spectroscopic study of Fe reference compounds for the analysis of natural sediments. American Mineralogist 89(4), 572-585.

Ogle, S.M., Swan, A., Paustian, K., 2012. No-till management impacts on crop productivity, carbon input and soil carbon sequestration. Agric. Ecosyst. Environ. 149, 37–49.

Peate, D.W., Hawkesworth, C.J., Mantovani, M.S., 1992. Chemical stratigraphy of the Paraná lavas (South America): classification of magma types and their spatial distribution. Bull. Volcanol. 55, 119–139.

Ravel, B., Newville, M., 2005. ATHENA, ARTEMIS, HEPHAESTUS: data analysis for X-ray absorption spectroscopy using IFEFFIT. J. Synchrotron Radiat. 12, 537–541.

Roden, E.E., Zachara, J.M., 1996. Microbial Reduction of Crystalline Iron (III) Oxides : Influence of Oxide Surface Area and Potential for Cell Growth Microbial Reduction of Crystalline Iron (III) Oxides : Influence of Oxide Surface Area and Potential for

Cell Growth.

Rodrigues, M., Pavinato, P.S., Withers, P.J.A., Teles, A.P.B., Herrera, W.F.B. 2016. Legacy phosphorus and no tillage agriculture in tropical oxisols of the Brazilian savanna. Science of the Total Environment 542, 1050-1061.

SAS Institute. 2011. SAS system for Windows. Version 9.3. SAS Institute, Inc., Cary, NC

Sato, S., Solomon, D., Hyland, C., Ketterings, Q.M., Lehmann, J., 2005. Phosphorus Speciation in Manure and Manure-Amended Soils Using XANES Spectroscopy. Environ. Sci. Technol. 39, 7485–7491.

Shoemaker, H.E., Mclean, E.O., Pratt, P.F. 1961. Buffer methods for determining the lime requirement of soils with appreciable amounts of extractable aluminum. Soil Sci. Soc. Am. Proc. 25, 274-277.

Schwertmann, U., Murad, E., 1983. Effect of pH on the formation of goethite and hematite from ferrihydrite. Clays Clay Miner. 31, 277–284.

Schwertmann, U., Taylor, R.M., 1989. Iron oxides, in: Dixon, J.B., Weed, S.B. (Orgs.), Minerals in soil environments. Soil Science Society of America, Madison, p. 379–438.

Silva, C.S., 2009. Manual of chemical analyzes of soils, plants and fertilizers, Second. ed. Embrapa technological information.

Soil Survey Staff, 12th ed., 2014. . USDA - Natural Resources Conservation Service, Lincoln.

Tiecher, T., Tiecher, T.L., Joel, F., Mallmann, K., Zafar, M., 2017. Chemical, Biological, and Biochemical Parameters of the Soil P Cycle After Long-Term Pig Slurry

Application in No-Tillage System 1–16.

USPEA, 1996. Soil screening guidance: technical background document, 2º ed. United States Government Publishing Office, Washington, United States of America.

van Raij, B., 1998. Bioavailable tests: alternatives to standard soil extractions. Commun. Soil Sci. Plant Anal. 29, 1553–1570.

Vandamme, E., Ahouanton, K., Mwakasege, L., Mujuni, S., Mujawamariya, G., Kamanda, J., Senthilkumar, K., Saito, K., 2018. Field Crops Research Phosphorus micro-dosing as an entry point to sustainable intensification of rice systems in sub-Saharan Africa. F. Crop. Res. 222, 39–49.

Whitting, L.D., Allardice, W.R., 1986. X-ray diffraction techniques, in: Klute, A. (Org.), Methods of soil analysis: Part 1 - Physical and mineralogical methods. American Society of Agronomy, Madison.

Williams, M.R., King, K.W., Pease, L.A., King, K.W., Duncan, E.W., Pease, L.A., Penn, C.J., 2018. Fertilizer placement and tillage effects on phosphorus concentration in leachate from fine-textured soils. Soil Tillage Res. 178, 130–138.

Supplementary material

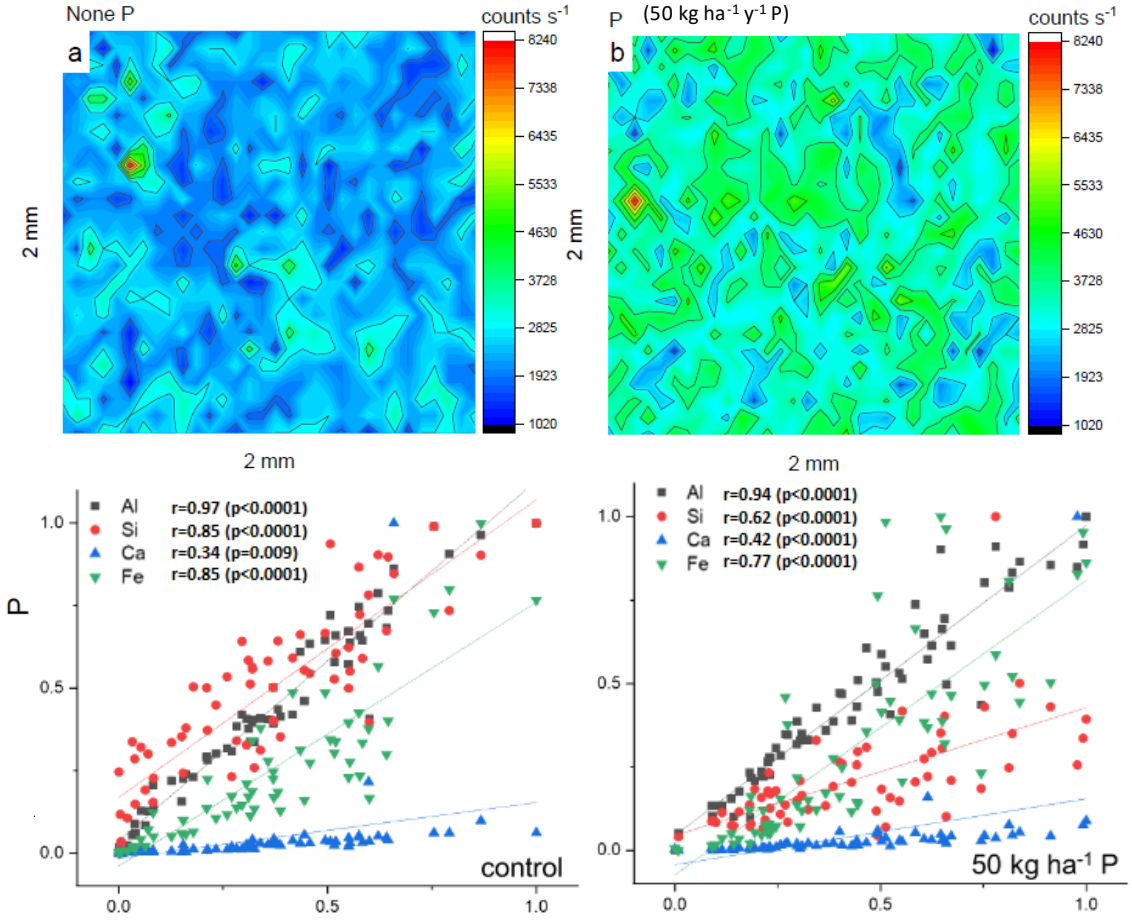

Fig. S1. (**a**, **b**) Quantitative spatial distribution of P, and scattering plots from elements distribution maps for Al, Si, Ca and Fe *Vs* P

CHAPTER V

PHYSICOCHEMICAL PROPERTIES AND MORPHOLOGY OF BIOCHARS AS AFFECTED BY FEEDSTOCK SOURCES AND PYROLYSIS TEMPERATURES

Abstract: Feedstock sources and pyrolysis temperatures affect the physicochemical and morphological properties of biochars. We evaluated biochars derived from switchgrass (SGB) and poultry litter (PLB) pyrolyzed at 350 ^{o}C (SGB350, PLB350) and 700 ^{o}C (SGB700, PLB700) to identify their potential ability in improving soil health. Except for SGB350, the pH of biochars was high (>10.0) and can be used as an amendment in acid soils. PLB700 had higher mineral content and nutrient availability due to its higher ash content (tenfold higher) and electrical conductivity. Surface functional groups responsible for metal retention were evidenced in all biochars. Cation exchange capacity (CEC), specific surface area (SSA) and microporosity more than doubled by increasing pyrolysis temperature. From 350 to 700 ^{o}C. The pH-buffering capacity measured through acid titration curve was better than that calculated with acid/alkali additions. Biochars pyrolyzed at 700 ^{o}C have much higher pH, CEC, SSA, and stronger buffering capacity thus are more promising to improve soil health and reduce contaminant bioavailability.
Keywords: biochars, switchgrass, poultry litter, physicochemical properties, pyrolysis.

Introduction

Pyrolyzed biochars are produced by thermal decomposition process (pyrolysis) in low or zero oxygen (O) environment using renewable feedstocks, such as crop residues or livestock manures (Dai et al., 2013). Biochars are applied with the intent of sequestering carbon and improve soil quality (Cantrell et al., 2012; Lehmann and Joseph, 2015; Spokas et al., 2012). However, there are few studies comparing morphological and physicochemical properties of biochars produced from different feedstock sources and at different slow pyrolysis temperatures as their effectiveness to be used as soil amendments.

Pyrolysis processes have a great impact on biochar properties (Brewer et al., 2011; Cantrell et al., 2012). Slow pyrolysis has been shown to retain the highest biomass carbon content in the char (Qian et al., 2013). The high organic C concentration associated with a porous structure, high pH, and high adsorption capacity makes biochar incorporation into soil a feasible and effective way to improve soil fertility and quality (Dai et al., 2013; Singh et al., 2010; Spokas 2010). The enhanced organic carbon provided by biochar addition contributes to raise pH in acid soils and decrease heavy metal availability by reducing metal solubility and bonding metals into more stable fractions (Xu et al., 2016; Zhang et al., 2017). The increase of both pH and organic carbon also contribute to a higher cation exchange capacity (CEC), then resulting in a higher heavy metal adsorption capacity (Bolan et al., 2014) thus improving soil quality (Qian et al., 2015).

The effectiveness of biochars on the immobilization of heavy metals also varies depending on biochar feedstocks and pyrolysis temperature. Biochars produced at higher

pyrolysis temperature enhances the immobilization of heavy metals (Uchimiya et al., 2011). Switchgrass-derived biochar (SGB) pyrolyzed at high temperature (500-700 ^{o}C) significantly contributes to the increased soil organic carbon (SOC) and pH (Kelly et al., 2015), thus also favoring heavy metal immobilization. Differently, SGB pyrolyzed at lower temperature (350 ^{o}C) increases the micronutrients availability in calcareous soils by slightly decreasing its pH (Ippolito et al., 2016). The application of poultry litter-derived biochar (PLB) strongly reduces the mobility of several metals in a contaminated soil (Gondeck and Mierzwa-Hersztek, 2016) as well.

Nevertheless, the biochars' effect on the mobility of heavy metals in soils is not only a function of the pyrolysis temperature and the feedstock used, but also the physical and electrochemical properties associated with them. The most important physicochemical properties of biochars responsible to reduce the bioavailability of heavy metals in soils and improve soil quality are the surface functional groups, specific surface area (SSA) and porosity (Gondeck and Mierzwa-Hersztek, 2016). Those properties, allied with alkalinity, pH-buffering capacity, CEC and electrical conductivity (EC) severely differ among biochars due to the several processing conditions (Azargohar et al., 2014; Sun et al., 2018; Yuan et al., 2011). However, literature is limited to elucidate biochar properties by specifically assessing elemental composition, functional groups, porosity and SSA. Except for a few works (e.g., Sun et al., 2016; Qian et al., 2015), there is still a lack of research focusing on the effects of different feedstocks and pyrolysis temperatures on other important properties of biochars (e.g., buffering capacity, CEC and nutrients availability). Therefore, it is necessary to completely assess biochars' physical, chemical, and morphological properties to elucidate their potential value as soil amendments.

We produced biochars using two feedstocks, switchgrass (SGB) and poultry litter (PLB), and two slow pyrolysis temperatures, 350 ^{o}C (SGB350 and PLB350) and 700 ^{o}C (SGB700 and PLB700) for this study. Our objectives were to investigate the impact of feedstock sources and pyrolysis temperatures on several biochar chemical–physical, structural and morphological characteristics.

Material and methods

Feedstocks used to produce Biochars

The biochars studied were converted from poultry litter (PL) and switchgrass (SG) biomass. Switchgrass (*Panicum virgatum*) was harvested from an established field at Clemson University Pee Dee Research and Education Center in Darlington County, SC. The switchgrass was hammer milled to approximately 6 mm particle size. The moisture content of milled switchgrass prior to pyrolysis was measured to be 6.45 ± 0.21 wt%. Poultry litter was collected from the top 5.0-7.5 cm depth from 10 locations in a commercial poultry house in Orangeburg County, SC. Poultry litter was ground (Wiley Mill equipped) to 2 mm particle size, and overnight oven dried at 105 ^{o}C. The moisture content of PL was determined to be 6.49%.

Biochar production and analysis

Switchgrass and Poultry litter-derived biochar (SGB and PLB, respectively) were produced at 350 and 700 ^{o}C by slow pyrolysis. Before pyrolysis, 0.5 to 1.5 kg of prepared samples were loaded onto a stainless steel tray and placed into a Lindburg electric box furnace equipped with a gas tight retort (Model 51662; Lindburg/MPH, Riverside, MI),

as described by Cantrell et al. (2012). The feedstock materials were pyrolyzed as following: 1h equilibration hold at 200 ^{o}C under an industrial-grade N_2 flow rate at 15 L min^{-1}; the temperature was increased to the desired temperature within 1 h at 2.52 ^{o}C min^{-1} for 350 ^{o}C; and at 8.33 ^{o}C min^{-1} for 700 ^{o}C. The maximum temperature was held for 2 h under N_2 flow at 1 L min^{-1}. The samples were cooled down to 100 ^{o}C (4.25 ^{o}C min^{-1}). The resulting biochars were allowed to cool to room temperature in an inert atmosphere N_2 (preparation of biochar was described by Cantrell et al. (2012). The coarse materials of the produced biochar were ground with a mortar and pastel gently before sieved by 2, 1, 0.25 and 0.053 mm mesh screens for specific analyses. The biochars with size less than 1 mm were used for most analyses.

Moisture, ash content and particle size distribution

The moisture content of biochars was determined by oven drying previously weighed biochar samples overnight at 105 ^{o}C (Ahmedna et al., 1997) and ash content by using the method of Novak et al. (2009) with weight loss after heating to 760 ^{o}C in air for 6 h by using conventional resistance muffle furnace (CMF) (Zhang and Dotson, 1994) (Table 1). Particle size distribution of biochars was obtained separately by using US standard sieve with 0.25 mm (sieve No. 60), 1.0 mm (sieve No. 18) and 2.0 mm (sieve No.10) mesh size (Table 1).

Elemental composition

Biochars (<1 mm fraction) were analyzed similarly to the manure/compost tests for total P, K, secondary nutrients, micronutrients (Recommended Methods for Manure

Analysis, 2003). Total nitrogen (TN) and total carbon (TC) were determined using a dry combustion Carbon/Nitrogen Analyzer (NFTA, 1993).

Table 1. Ash, moisture and particle size distribution of biochars

	SGB350	SGB700	PLB350	PLB700
		%		
Proximate analyses[§]				
Ash	2.7	4.4	29.8	45.9
Moisture	1.4	1.7	2.7	3.9
Particle size (% by weight)				
< 0.25 mm	1.40	2.30	10.2	7.00
0.25 - 1 mm	26.3	20.1	30.6	36.1
1 - 2 mm	59.0	71.3	28.8	54.8
>2 mm	13.3	6.30	30.4	2.10
Total	100	100	100	100

[§] Data showed on oven-dry basis

Surface functional groups

Surface functional groups (phenolic-OH, COOH, C=O, etc.) of the biochars were analyzed using Fourier Transform Infrared Spectroscopy - FTIR (Nicolet FT-IR 6700, Thermo Electron Corporation, Madison, WI, USA) with an attenuated total reflectance (ATR) accessory. A diamond crystal was used on the ATR accessory. The ATR-FTIR technique has been chosen because it shortens the analysis time and improves the quality of char spectra in comparison with the traditional infrared techniques.

Biochars with four different sizes (<2, <1, <0.25 and <0.053 mm) were scanned 8 (standard procedure), 64 (Chia et al., 2012; Ding et al., 2014; Uchimiya et al., 2010) and 256 (Azargohar et al., 2014; Qian et al., 2013) times at 4 cm^{-1} resolution from 4000 to 650 cm^{-1}. The average of 64 scans was settled as the best experimental procedure. All samples without pretreatments were scanned in absorbance mode. The collected spectra

were subjected to baseline correction manually (after auto-correcting peaks at 'order 6') followed by maximum smoothing (25). Air background was collected before each sample run in order to avoid any possible strong peak of carbon dioxide-CO_2 arising between 2300-2400 cm^{-1}. The spectra of the fine fraction were chosen to represent the peaks of functional groups for all biochars because of higher homogeneity in finer samples. The FTIR spectrum peaks were identified and analyzed by comparing the peak position with already known peaks found elsewhere in the literature.

Chemical attributes and specific surface area (SSA)

Biochar NO_3-N and NH_4-N were extracted with 1 M KCl solution and quantified by a Flow Injection Autoanalyzer (LaChat Flow Injection Auto-analyzer). Plant available P, K, Ca and Mg were extracted using Mehlich 3 solution (Mehlich, 1984). Phosphorus, K, Ca and Mg in the extracts were quantified by a Spectro ICP spectrometer (Soltanpour et al., 1996). Biochar sulfate was extracted by 0.008 M $Ca_3(PO_4)_2$ and analyzed by a Spectro ICP. Available Zn, Fe, Mn and B were extracted by DTPA-Sorbitol and quantified by ICP (Gavlak et al., 2005). The pH of each biochar was determined according to Yuan et al. (2011) in DI water at a 1:5 (w/w) ratio. The biochar samples were each thoroughly mixed with DI water in 50 mL centrifuge tubes and shaken at 220 rpm for 1 h. The pH was then measured using an Orion Star A221 pH electrode (Thermo Scientific). For the EC, a ratio of 1:20 (biochar:deionized water) was used and determined after 90 min-shaking with an electrical conductance cell (Rajkovich et al., 2012).

SSA of coarse fraction of biochars was determined on a Quantachrome Autosorb1 using N_2 sorptometry. Each biochar SSA was calculated using multi-point adsorption data from the 0.01–0.3 P/Po linear segment of the N_2 adsorption isotherms made at 77.35 K according to the Brunauer, Emmet, and Teller (BET) theory (Brunauer et al., 1938). Biochar samples were degassed under vacuum (200 °C for 12 h) prior to nitrogen adsorption at liquid nitrogen temperature (−196 °C).

Cation exchange capacity (CEC)

Cation exchange capacity of biochars were performed based on American Standard Test Method (ASTM-D7503–10, 2010). Briefly, 3.0 g of ground biochar sample was weighed into 50 ml centrifuge tube with a screw cap. Twelve ml of 1.0 M ammonium acetate solution (NH_4OAc) was added to the tube before shaken for 5 min on an orbital shaker at 220 rpm. Then, the tube was static for 24 h before shaken for another 15 min. The suspension in the tube was transferred into a funnel lined with Whatman No.2 filter paper on a filtering flask and filtered with vacuum. During filtration, 20 ml of 1.0 M NH_4OAc was used to wash the biochar each time for four times. The NH_4OAc washed biochar was then washed with 20 ml of isopropanol each time for three times to remove access NH_4OAc. The isopropanol washed biochar was then washed using 20 ml of 1.0 M KCl solution each time for four times. The biochar was not allowed to dry between additions of the same solution. The KCl extracts were transferred into 100 ml volumetric flask, which was then filled, to the volume of 100 mL with DI water. The KCl extracts were analyzed for nitrogen (NH_4-N) concentration (mg L^{-1}) using LaChat Flow Injection Auto-analyzer. CEC was calculated based on formula: CEC = N × 1(cmol)/140

(mg) × 0.10 (L)/3.0 (g) × 1000 (g kg^{-1}), where N = concentration of nitrogen (NH_4^+, in mg L^{-1}). Total soluble and bound cations were also measured according to ASTM-D7503–10 (2010).

pH-buffering capacity and acid titration curve

The pH-buffering capacity of biochars was determined according to Xu et al. (2012). In the process, 1.0 g of biochar sample was weighed into each of eight 50 mL centrifuge tube and appropriate amount of water was added such that a final volume after addition of acid or alkali was 20 mL. Additions of 0, 0.1 0.25, 0.5, 1.0, 2.0, 4.0 and 8.0 mL of 0.04 M HCl or NaOH were used based on initial pH of SG biochars used in this study. Chloroform (about 0.25 mL) was added to each tube after addition of acid or base to inhibit activity of microorganisms. Addition of 1.0 mL of 0.05 M $CaCl_2$ was made to each tube to minimize variations in ionic strength. The mixture was shaken at 220 rpm on an orbital shaker at 25℃ for 24 h and then left to equilibrate statically for an additional 6 days at 25℃. The mixture was shaken for 2 min each day to re-suspend the biochar. After equilibration, the pH of the mixture was measured by an Orion Star A221 pH meter (Thermo Scientific). The pH-buffering capacity was calculated as pH change per mmol of acid/alkali added for each kilogram of biochar.

Acid-base titration was based on Yuan et al. (2011) aiming to evaluate the proton neutralization capacity of each biochar. Half a gram (0.5 g) of biochar samples was placed in 125 mL serum bottles. Then, 20 mL of DI water (1:40 biochar to solution ratio) was added to each bottle, and each of the bottles was stirred on a magnetic stirrer for 2 h at 25℃. The samples were then titrated with 0.1 M HCl at 25℃ to the end point at pH 2.0

using an automatic titration instrument (TIM840 Titration Manager, Hach Company, Loveland, CO, USA) with continuous stirring. The titration rate was kept at 0.5 mL min^{-1} with data collected every 6 s.

Scanning Electron Microscopy (SEM)

The structure and surface morphology of the coarse fraction (>2mm) were examined by a field-Emission Environmental Scanning Electron Microscope (SEM). In order to obtain a clear image, the biochar particles were coated with gold. Images were viewed at the accelerating voltage of 15 kV.

Statistical analyses

Biochars chemical attributes were subjected to ANOVA and the treatments average (triplicates, n=3) compared by Tukey test. Simple correlation (Pearson) for specific variables and linear regression of the results obtained from pH-buffering capacity measurements were performed.

Results and discussion

The pH and elemental composition of Biochars

Pyrolysis temperature and feedstock types are critical factors affecting the biochar properties. Table 2 shows the pH and elemental composition of the biochars SGB and PLB produced with slow pyrolysis at 350 and 700°C. Except for SGB350, all other biochars had high pH values. The SGB350 and PLB350 presented the lower pH than that of SGB700 and PLB700. Although the pH value of PLB700 was very similar to that found by Cantrell et al. (2012) for the same biochar, the pH of PLB350 was different by

one unit, probably because the authors determined the biochar pH in different methods. The lowest pH of 5.21 found for SGB350 agrees with the findings of Ippolito et al. (2016), who also stated that the pH of an alkaline soil decreased after incubation with switchgrass-derived biochar pyrolyzed at 350 ^{o}C. Pearson correlations were performed and the results clearly showed high correlation coefficients ($r = 0.97$ to 0.99, $p<0.01$) of ash contents (Table 1) with the contents of total P, Ca, K, Mg, Na, S, Fe, Zn, Cu and Mn presented in Table 2. Since the ash contents of PLBs are higher than SGBs, all elements analyzed in PLB350 and PLB700 were higher than those of SGB350 and SGB700. Among all four types of biochars, PLB700 had the highest ash and elemental contents. The difference in total C between SGB350 and PLB 350 (42.6 - 38.4 = 4.2) is not much different from the deference between SGB700 and PLB700 (31.4 - 27.75 = 3.65). Consequently, considering the high difference in ash content between SGB and PLB, there is no clear correlation between total C and ash content except a consistent decrease with pyrolysis temperature. As expected from the feedstock materials, PLBs also showed lower C/N ratios in comparison to SGBs (9.3 and 17.3, respectively, for PLB350 and PLB700, whereas 50.1 and 42.4 were observed, respectively, for SGB350 and SGB700).

The functional groups found on Biochars

The FTIR analysis of fine SGB and PLB biochar samples (<0.053 mm) provided better spectra with more pronounced peaks and less noise spectrum than the spectra of coarser sizes (Fig. 1). The same peaks were also found in other biochar particle sizes (coarser), but these were not as distinct as those from the finest fraction.

Table 2. pH, total nutrient contents, total carbon (TC) and total nitrogen (TN) of switchgrass and poultry litter-derived biochars pyrolyzed at 350 and 700 ^{o}C

Variable		SGB350	SGB700	PLB350	PLB700	LSD[§]	CV (%)[£]
pH		5.21 ± 0.05 c	10.1 ± 0.2 a	7.43 ± 0.18 b	10.2 ± 0.05 a	0.36	1.6
P	%	0.1 ± 0.003 c	0.2 ± 0.02 c	2.6 ± 0.11 b	3.9 ± 0.08 a	0.2	3.9
Ca		0.5 ± 0.02 c	0.8 ± 0.1 c	3.6 ± 0.5 b	5.4 ± 0.2 a	0.9	12.4
K		0.3 ± 0.03 c	0.4 ± 0.04 c	5.6 ± 0.2 b	7.8 ± 0.06 a	0.3	3.2
Mg		0.3 ± 0.004 d	0.3 ± 0.03 c	1.2 ± 0.03 b	1.9 ± 0.01 a	0.07	3
Na		0.02 ± 0.01 c	0.03 ± 0.01 c	2± 0.07 b	2.6 ± 0.06 a	0.1	4.1
S		0.07 ± 0.004 c	0.04 ± 0.01 c	1.2 ± 0.02 b	1.4 ± 0.06 a	0.1	5.2
Fe	mg kg^{-1}	95 ± 10 c	111 ± 20.1 c	3313 ± 1329 b	6903 ± 1295 a	2515	34.1
Zn		38.5 ± 1.3 c	53.6 ± 5.8 c	1018 ± 18.7 b	1477 ± 43 a	62	3.4
Cu		16.7 ± 2.5 c	23.2 ± 2.7 c	209 ± 5 b	253 ± 4 a	9.9	2.8
Mn		105 ± 1.6 d	143.6 ± 10.7 c	802 ± 19.1 b	1108 ± 2 a	34	2.2
B		<1.0[¥]	<1.0[¥]	104 ± 2.7 a	103 ± 1.7 a	6.3	1.7
Ni		<1.0[¥]	11.3 ± 0.5 c	17± 0.5 b	25.5 ± 1a	2.1	4.1
TN	%	0.9 ± 0.07 c	0.7 ± 0.00 c	4.1 ± 0.1 a	1.6 ± 0.1 b	0.2	3.7
TC		42.6 ± 1.1 a	31.4 ± 1.3 c	38.4 ± 1.9 b	27.75 ± 1.4 c	4.2	4.2

[¥] <DL = Detection limit; Values after ± are the standard deviation (n=3)

[§] Least Significant Difference; Means followed by the same letter, in the row, are not significantly different

[£] Coefficient of Variation; ** Results are significant at p<0.01 (n=3) from Tukey test

The C=O stretching and aromatic C=C vibrations were visible at 1554.37 cm^{-1} band of SGB700. Peaks around 1560 cm^{-1} are related to the C=O stretching of carboxyl anions (Zhang and Luo, 2014), or aromatic C=C bending, especially for switchgrass-derived biochars (Qian et al., 2013; Cantrell et al., 2012; Keiluweit et al., 2010; Silverstein et al., 2014). The peaks in the range of 873.71-814.69 cm^{-1} for all biochars represent the out-of-plane deformation produced by aromatic C-H atoms (Behazin et al., 2015; Tatzber et al., 2007; Uchimiya et al., 2011). The peak at 796.47 cm^{-1} for SGB700 is also assigned to C-H bending of aromatic out of plane deformation and for biochars pyrolyzed at high temperatures (Uchimiya et al., 2011). Such peak is certainly much more pronounced than the peak at 782.01 cm^{-1} for SGB350 (Fig. 1).

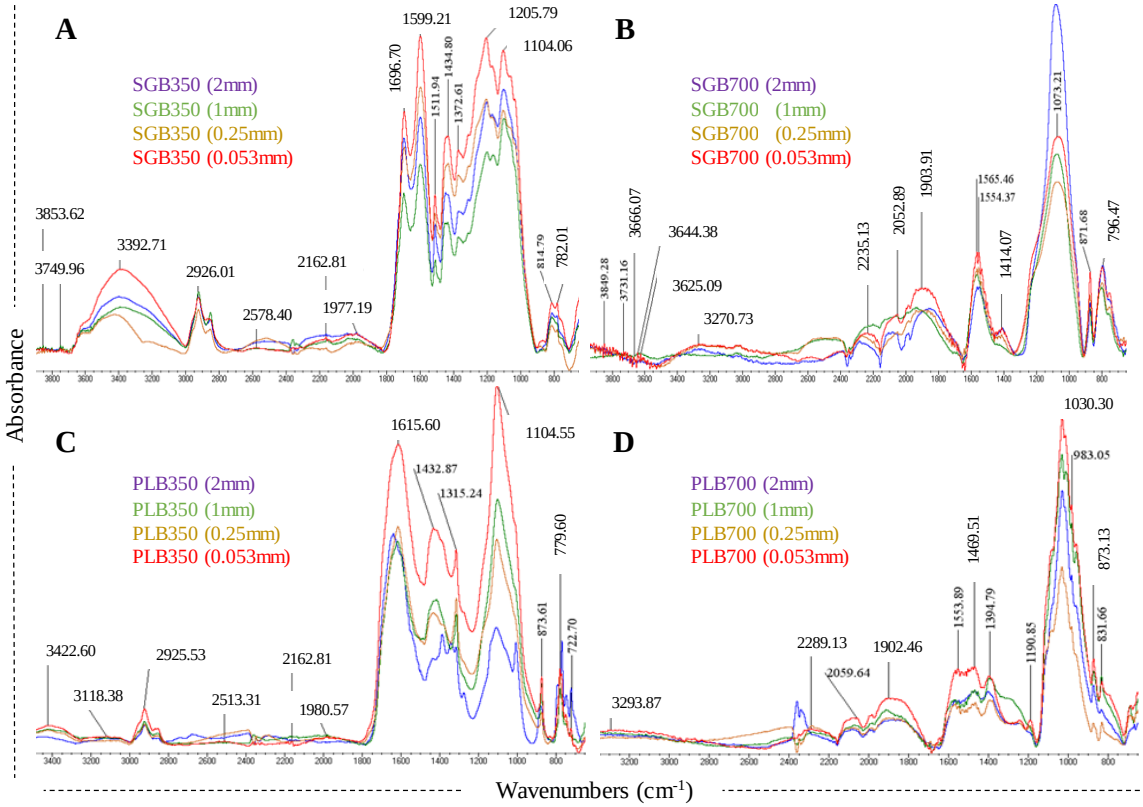

Fig. 1. FTIR spectra of switchgrass (SGB) and poultry litter-derived (PLB) biochars pyrolyzed at 350 (A, C) and 700 ºC (B, D), respectively, and sieved by 2, 1, 0.25 and 0.053 mm

The intense broad band at 1030.30 cm^{-1} for PLB700 was likely resulted from P-containing functional groups, mostly P-O bond of phosphate functional group such as phosphines and phosphine oxides. Woldetsadik et al. (2016), studying poultry litter-derived biochars, reported the same functional groups at 1038 cm^{-1} band. High P contents are observed for fecal and manure derived biochars, as found for PLB700 (Table 2). However, a pronounced peak found at 1073.21 cm^{-1} for SGB700 is more likely related to silicon oxide and C-O-C stretching of different types of oxygenated compounds such as

alcohols, phenols and ethers than phosphates functional group (Qian et al., 2013; Cantrell et al., 2012; Keiluweit et al., 2010; Silverstein et al., 2014) since the total phosphorus is about 24 times lower than that found in PLB700 (Table 2).

Peaks at ~1470 cm^{-1} possibly indicate deformation vibration from alkanes (Strezov et al., 2012). According to Azargohar et al. (2014), the intensity of such peaks in biochars decreased by increasing the pyrolysis temperature due to the improvement of aromatic structure, as observed for the 1434.80 (SGB350) to 1414.07 cm^{-1} (SGB700) and 1432.87 (PLB350) to 1469.51 cm^{-1} (PLB700) bands (Fig. 1).

Jiang et al. (2012) showed a number of pronounced peaks at 3419, 1614, 1103 and 795 cm^{-1} assigned to the hydroxyl (–OH) stretching, $–COO^-$ anti-symmetric stretching, bands of the out-of-plane bending for carbonates ($-CO_3^{2-}$) and to carboxylate ($–COO^-$) deviational vibration and symmetric stretching, respectively, for rice straw-derived biochar pyrolyzed at 300 ^oC, and attributed such functional groups to the ability in forming surface complexes with Pb(II). In our study, similar peaks were found at ~3600, ~1600 (1565.46-1554.37 cm^{-1} for SGB700 and 1553.89 cm^{-1} for PLB700), 1000-1100 and ~680-860 cm^{-1} for both SGB700 and PLB700; and very similar peaks were found at 3392.71, 1599.21, 1104.06 and 182.01 cm^{-1} for SGB350 and 3422.60, 1615.60, 1104.55 and 779.60 cm^{-1} for PLB350 (Fig. 1). According to Chia et al. (2012), the reduced peak at 3644.38 cm^{-1} (~3640 cm^{-1}) of SGB700 could be assigned to organic O-H stretching. Such reduced OH peak and the increased C=C peak around 1600 cm^{-1} (1565.46-1554.37 cm^{-1}) is attributed to the depolymerization and dehydration of materials due to pyrolysis, then resulting in the formation of C=C double bonds, carbonyl, and carboxylic functional groups (Lange, 2007).

There is a possibility of the ~2080 cm^{-1} (2052.89 cm^{-1} for SGB700 and 2059.64 cm^{-1} for PLB700 in the case of our study) peak arising from an organic azide group (-N=N=N) or a ketene group (>C=C=O). The azide group functional group is supported by the >1.0% of nitrogen found for PLB700 (Table 2) (Chia et al., 2012). However, the poor stability of azides at the high temperature used for pyrolysis suggests that a ketene may be a more likely candidate for this peak (Chia et al., 2012).

In summary, the peaks in the range of 3118.38-3853.62 cm^{-1} found for all biochars are probably from hydroxyl groups (Park et al., 2011). Peaks found at 1554.37 and 1553.89 cm^{-1} (SGB700 and PLB70, respectively) correspond to the stretching vibrations of conjugated C=O bonds in aromatic rings (Cao and Harris, 2010). Bands at 796.47 cm^{-1} for SGB700 and 873.13 cm^{-1} for PLB700 are probably due to the contribution from C–H bond vibration in aromatic compounds (Park et al., 2011; Moreno-Castilla et al., 2000). The presence of such surface functional group play important role in the adsorption of heavy metals such as Pb, Cd and Zn (Park et al., 2011). FTIR analyses suggest that the differences in the composition of surface functional groups are also attributed to the type of feedstocks, which could further influence the metal retention capacity of biochars. However, in the case of our study, the surface functional groups of all biochars seem to be promising as far as heavy metal adsorption is concerned. Therefore, physicochemical and morphological analyses are necessary to decide which biochars can provide a higher potential as a soil amendment.

Physicochemical properties of Biochars

The major physicochemical properties of the biochars are summarized in Table 3. As observed for the elemental composition, the available nutrient contents were generally higher for PLB700 in comparison to other biochars, which is reflected in its high EC value as well (Table 3). Pearson correlation also showed high correlation coefficients between available nutrients and ash contents ($r = 0.97$ to 0.99, $p<0.01$), except for Fe and Cu ($p>0.05$), and the EC was also highly correlated with the ash content ($r = 0.99$, $p<0.01$). Despite the fact that the ash content of PLBs were very similar to those found by Cantrell et al. (2012), using a similar method, the EC values were different, much higher for PLB700 in the case of our experiment, probably because of different methods used for EC measurements when comparing both works. In the case of Cantrell et al. (2012), the authors used a ratio of 1% (w v-1) and stirred samples for 2 h., which could have led to different results. As expected, SSA of biochars from both feedstocks increased as the pyrolysis temperatures increased (Table 3). The same trend was observed by Cantrell et al. (2012) in the case of PLBs. Although their SSA was higher than ours because different sizes were used by those 2 studies.

The high pH of all biochars except for SGB350 (Table 2) was probably due to the release of alkali cations. Bound cations include precipitated ions, such as oxides and carbonates. According to Sun et al. (2018), the CEC is an inherent characteristic of biochar, represents the ability to hold on nutrients, and provides buffering against acidification. CEC values of SGB350 and PLB350 were similar to biochars derived from canola straw, corn straw, soybean straw and peanut straw (Yuan et al., 2011), and biochars derived from switchgrass, forage sorghum and red cedar (Sun et al., 2018).

However, the CEC of SGB350 and PLB350 were 1.98 and 1.60 times lower than SGB700 and PLB700, respectively. Biochars pyrolyzed at 700 ^{o}C exhibited higher pH, SSA, CEC (inside the ranges found for humus: 200-500 cmol kg^{-1}), and total soluble and bound cations than those pyrolyzed 350 ^{o}C, indicating the higher potential of using SGB700 and PLB700 for heavy metal immobilization and soil health enhancement (Qian et al., 2015). CEC and SSA of biochars were highly correlated as well ($r = 0.98$, $p<0.01$).

Table 3. Extractable nutrients and other selected physicochemical properties of biochars

Physicochemical properties	Method	SGB350	SGB700	PLB350	PLB700
		……..……mg kg^{-1}……..……			
NO_3^-	KCl	0.00	0.59	0.80	2.12
NH_4^+	KCl	0.98	0.80	6.87	2.79
P	Mehlich-3	120	254	6293	8425
K	Mehlich-3	193	616	24428	54504
Mg	Mehlich-3	202	541	3616	6869
Ca	Mehlich-3	323	1575	4862	5690
Na	Mehlich-3	<0.3[§]	10.9	5058	11252
Fe	DTPA	1.0	2.7	2.7	122.4
Mn	DTPA	4.7	17.6	66.1	94.6
Cu	DTPA	0.6	1.2	10.7	9.8
Zn	DTPA	1.0	3.8	22.8	29.8
B	DTPA	<0.2[§]	<0.2[§]	8.4	5.6
EC (µS cm^{-1})	Rajkovich et al. (2012)	191	240	7370	9150
SSA (m^2 g^{-1})	BET equation	1.043	22.9	1.862	9.278
		……..……cmol kg^{-1}……..……			
CEC[£]	ASTM (2010)	156.7	309.6	147.8	235.9
Soluble cations[¥]		939.8	12222	850.0	13982
Bound cations[¶]		311.5	11124	995.1	16351

[§] <DL = Detection limit

[£] Cation Exchange Capacity CEC = N × 1(cmol)/140 (mg) × 0.10 (L)/3.0 (g) × 1000 (g kg^{-1}), N = concentration of nitrogen (NH_4^+, in mg L^{-1});

[¥] Total soluble cations are the sum of total Na^+, K^+ ,Ca^{2+} and Mg^{2+} soluble in water

[¶] Total bound cations are the sum of total Na^+, K^+, Ca^{2+} and Mg^{2+} insoluble in water

Biochars pH-buffering capacities

Buffering curves for the biochars obtained according to Xu et al. (2012) and Aitken and Moody (1994) are presented in Fig. 2. The amount of acid and alkali added was linearly related to biochar pHs. For SGBs, the linear models were fitted in the pH ranges of 4.0-8.0 (SGB350) and 2.5–9.5 (SGB700) (Fig. 2). In the case of PLB350 and PLB700, the linear models were in the narrower pH ranges of 6.5-8.0 and 10.0-10.5, respectively. Since the narrow pH ranges obtained from PLB350 (6.5-8.0) and PLB700 (10.0-10.5) probably do not encompasses most poultry litter-derived biochars, the automatic titration with acid addition, until PLBs reach a pH 2.0, was further performed to better determine the pH-buffering capacity of PLB (Fig. 3).

All correlation coefficients (R^2) between pH and acid or alkali added were higher than 0.93 with $p<0.0001$. Therefore, the pH-buffering capacity of the biochars was calculated from the slope of regression lines (Fig. 2). There were large differences in pH-buffering capacity among biochars from different feedstock and pyrolysis temperatures ranging from the lowest of 45 mmol kg^{-1} pH^{-1} for SGB700 to the highest of 433 mmol kg^{-1} pH^{-1} for PLB700. This suggests that biochar properties greatly affected pH-buffering capacity.

Fig. 3 shows acid titration curves for the biochars. As stated by Sun et al. (2018), the acid titration curves represent Acid Neutralizing Capacity (ANC) or alkalinity of each biochar. The initial pH values of SGB350, SGB700, PLB350 and PLB700 in water matrix before titration were 5.74, 10.01, 8.02 and 10.68, respectively. To reach a pH of 2.0, PLB700 required the highest volume of 0.1M HCl (25.5 mL) followed by PLB350 (14.3 mL), SGB700 (3.3 mL), and SGB350 (2.9 mL). In this sense, biochars from the same

feedstock but processed at higher pyrolysis temperatures not only ameliorate soil acidity, but also increase soil pH-buffering capacity if applied to an acidic soil.

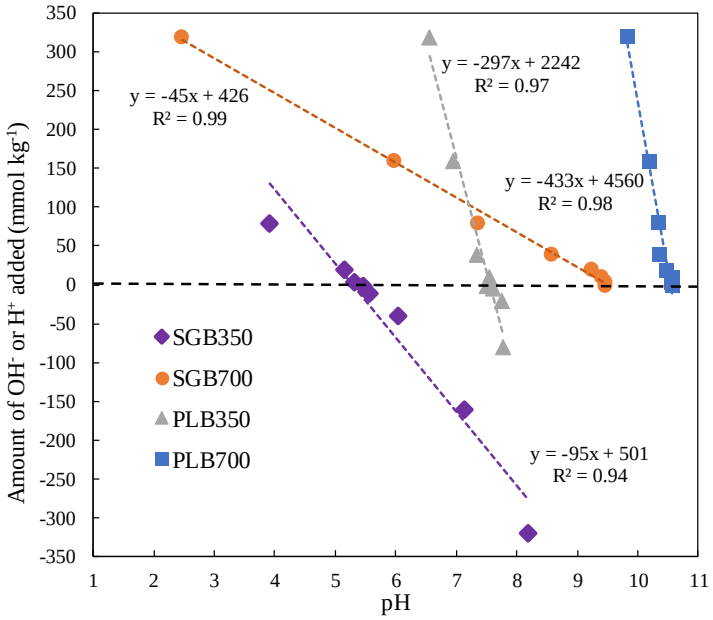

Fig. 2. Relationships between the amount of acid and basis added and the pH of biochars. Switchgrass-derived biochars pyrolyzed at 350 and 700 ºC (95 and 45 mmol kg^{-1} pH^{-1} for 0.04 M of HCl or NaOH added). Poultry litter-derived biochars pyrolyzed at 350 and 700 ºC (297 and 433 mmol kg^{-1} pH^{-1} for 0.04 M of HCl or NaOH added)

Despite Sun et al. (2018) used biochars produced from gasification process, their volumes of 0.1M HCl necessary to reach pH 2.0 of switchgrass and poultry litter-derived biochars were very similar to SGB700 and PLB700. The pH of PLB700 in water matrix decreased from 10.7 to 2.0 slower than other biochars did throughout the titration, indicating PLB700 possessed stronger alkalinity. During acid titration, the pH increased from 5.2 to 5.4 and from 3.6 to 4.1 in PLB350 and PLB700, respectively, indicating a

strong ANC within these ranges. SGB350 had the lowest ANC because its pH decreased faster than other biochars. Very similar results were observed by Sun et al. (2018) when comparing PLB with biochars produced from other feedstocks. Considering the wide range of 0.1M HCl (2.9-25.5 mL) necessary to reach pH 2.0, the automatic titration technique can be used to determine pH-buffering capacity of biochars pyrolyzed at different temperatures.

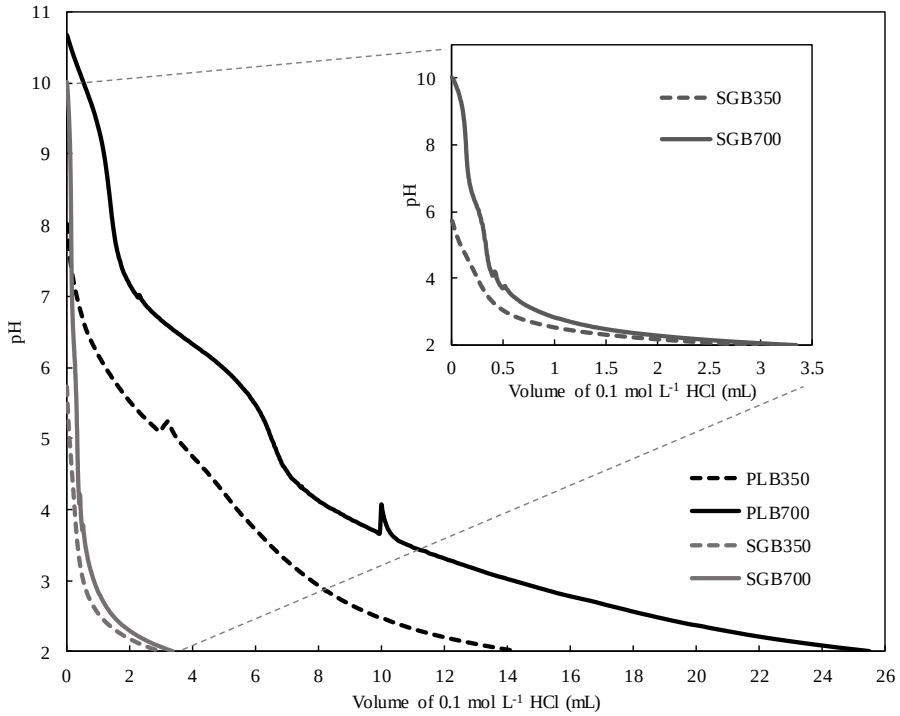

Fig. 3. Acid-base titration curves of switchgrass and poultry litter-derived biochars pyrolyzed at 350 and 700 ºC

For comparison, linear regression analyses were also performed for the dataset obtained from the automatic acid titration and the results are presented in Fig. 4. Although the p values are highly significant ($p<0.0001$), the pH-buffering capacity

calculated from the slope is different for biochars, which were 1.8, 2.2, 1.4 and 2.0 times lower than those obtained from the acid/alkali addition method for SGB350, SGB700, PLB350 and PLB700, respectively.

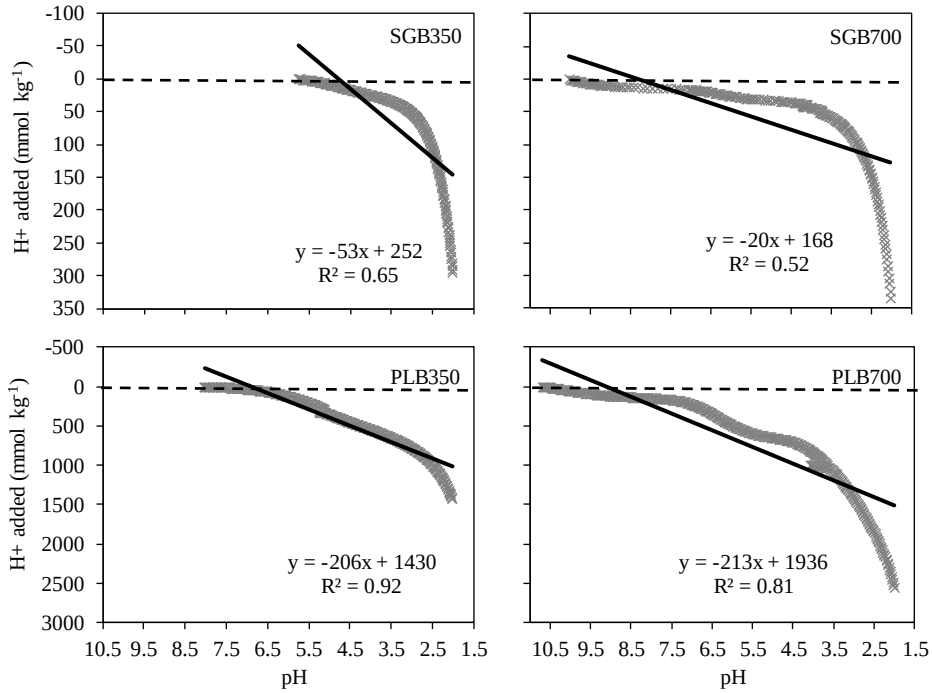

Fig. 4. Linear regression for acid-base titration curves of switchgrass and poultry litter-derived biochars pyrolyzed at 350 and 700 ^{o}C

The morphology of Biochars

The surface morphology of the biochars was examined by SEM (Fig. 5). For SGB350 and SGB700, part of the biomass fibrous structure was maintained and it was clearly porous in all of the SEM images (Fig. 5A and 5B). Because of the pyrolysis temperature, the SGB700 probably provided with more micropores than SGB350 (Fig. 5A, 5B), reflected by their SSA difference (Table 3), and the similar morphological and SSA differences were also observed when comparing PLB350 and PLB700 (Fig. 5C,

5D). While SGB350 presented a SSA of 1.0 m^2 g^{-1}, the SGB700 was 22.9 m^2 g^{-1} (Table 3); whereas those values were 1.9 and 9.3 m^2 g^{-1} for PLB350 and PLB700, respectively. Therefore, the observed higher microporosity of PLB350 than SGB350 (Fig. 5A, 5C) resulted in differences in their SSA as well.

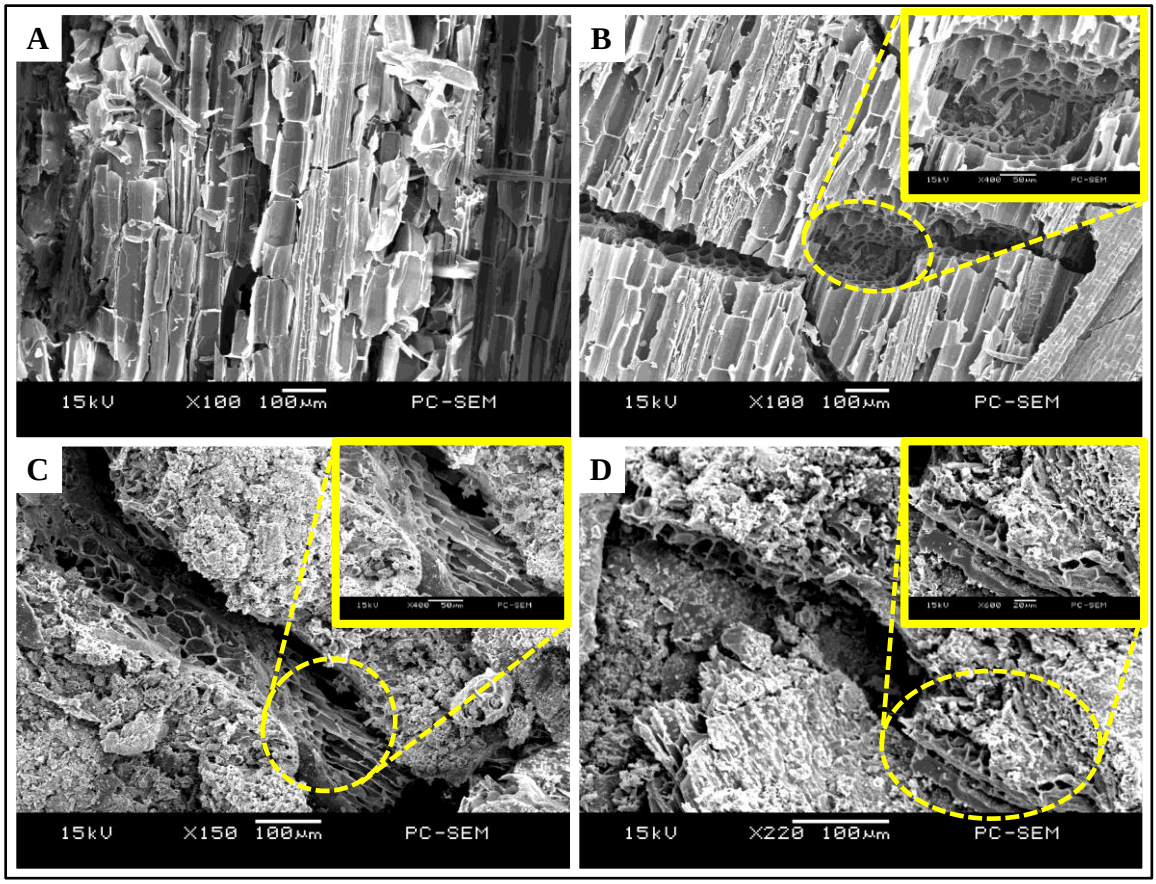

Fig. 5. SEM images of switchgrass (SGB) and poultry litter-derived (PLB) biochars pyrolyzed at 350 (A, C) and 700 ^oC (B, D), respectively

The appreciable surface porosity seen in biochars derived from switchgrass showed more pores with regular geometrical morphology than PLBs. The less pores obtained with biochars from low pyrolysis temperatures (350 ^oC) are related to their low

SSA as high SSA is indicative of high porosity. On the other hand, the higher porosity observed for biochars pyrolyzed at 700 ^{o}C is also associated with their higher CEC since SSA and CEC are highly correlated ($r = 0.98$, $p<0.01$). Moreover, the findings of Song et al. (2014) showed that high heating temperature rates during biochars processing will likely increase the pyrogenic nanopores in biochar resulting in higher microporosity. The increased microporosity and CEC enhance the ability of biochars to hold water, which could attribute to a higher soil moisture content if biochars are applied. The capacity of retaining more water also prevents heavy metals to be lost by leaching thus favoring the protection against groundwater contamination. These morphological features once more suggest biochars from pyrolyzed at higher temperatures (such as 700^{o}C) to be more promising as soil amendments.

Conclusions

The feedstock types and pyrolysis temperature affected the physical, chemical and morphological properties of biochars. The elemental compositions of PLBs were much higher than those of SGBs, attributed to the higher ash contents of PLBs. Functional groups changed from low to high pyrolysis temperature. The acid titration curve obtained from an automatic titration method proved more effective to determine pH-buffering capacity than simply adding acid and base approach. The buffering capacities decreased in the following order: PLB700> PLB350>SGB700>SGB350. The porous structures were more pronounced for SGB700 and PLB700, resulting in their higher CEC and SSA. In addition to their potential liming effect, SGB700 and PLB700 possess a greater potential to improve soil health and reduce heavy metal toxicity.

References

Ahmedna, M., Johns, M. M., Clarke, S. J., Marshall, W. E., Rao, R. M. (1997). Potential of agricultural by-product-based activated carbons for use in raw sugar decolourisation. Journal of the Science of Food and Agriculture, 75(1), 117-124.

Aitken, R. L., Moody, P. W. (1994). The effect of valence and ionic-strength on the measurement of pH buffer capacity. Soil Research, 32(5), 975-984.

ASTM-D7503–10. (2010). Standard Test Method for Measuring the Exchangeable Complex and Cation Exchange Capacity of Inorganic Fine-Grained Soils. ASTM International, West Conshohocken, PA.

Azargohar, R., Nanda, S., Kozinski, J. A., Dalai, A. K., Sutarto, R. (2014). Effects of temperature on the physicochemical characteristics of fast pyrolysis bio-chars derived from Canadian waste biomass. Fuel, 125, 90-100.

Behazin, E., Ogunsona, E., Rodriguez-Uribe, A., Mohanty, A. K., Misra, M., Anyia, A. O. (2015). Mechanical, chemical, and physical properties of wood and perennial grass biochars for possible composite application. BioResources, 11(1), 1334-1348.

Bolan, N., Kunhikrishnan, A., Thangarajan, R., Kumpiene, J., Park, J., Makino, T., Kirkham, M. B., Scheckel, K. (2014). Remediation of heavy metal(loid)s contaminated soils–to mobilize or to immobilize? Journal of Hazardous Materials, 266, 141-166.

Brewer, C. E., Unger, R., Schmidt-Rohr, K., Brown, R. C. (2011). Criteria to select biochars for field studies based on biochar chemical properties. BioEnergy Research, 4(4), 312-323.

Brunauer, S., Emmett, P. H., Teller, E. (1938). Adsorption of gases in multimolecular layers. Journal of the American Chemical Society, 60(2), 309-319.

Cantrell, K. B., Hunt, P. G., Uchimiya, M., Novak, J. M., Ro, K. S. (2012). Impact of pyrolysis temperature and manure source on physicochemical characteristics of biochar. Bioresource technology, 107, 419-428.

Cao, X., Harris, W. (2010). Properties of dairy-manure-derived biochar pertinent to its potential use in remediation. Bioresource Technology, 101(14), 5222-5228.

Chia, C. H., Gong, B., Joseph, S. D., Marjo, C. E., Munroe, P., Rich, A. M. (2012). Imaging of mineral-enriched biochar by FTIR, Raman and SEM–EDX. Vibrational Spectroscopy, 62, 248-257.

Dai, Z., Meng, J., Muhammad, N., Liu, X., Wang, H., He, Y., Brookes, P. C., Xu, J. (2013). The potential feasibility for soil improvement, based on the properties of biochars pyrolyzed from different feedstocks. Journal of soils and sediments, 13(6), 989-1000.

Ding, W., Dong, X., Ime, I. M., Gao, B., Ma, L. Q. (2014). Pyrolytic temperatures impact lead sorption mechanisms by bagasse biochars. Chemosphere, 105, 68-74.

Gavlak, R., Horneck, D., Miller, R. O., Kotuby-Amacher, J. (2003). Soil, plant and water reference methods for the western region. WCC-103 Publication, Fort Collins, CO.

Jiang, T. Y., Jiang, J., Xu, R. K., Li, Z. (2012). Adsorption of Pb (II) on variable charge soils amended with rice-straw derived biochar. Chemosphere, 89(3), 249-256.

Ippolito, J. A., Ducey, T. F., Cantrell, K. B., Novak, J. M., Lentz, R. D. (2016). Designer, acidic biochar influences calcareous soil characteristics. Chemosphere, 142, 184-191.

Keiluweit, M., Nico, P. S., Johnson, M. G., Kleber, M. (2010). Dynamic molecular structure of plant biomass-derived black carbon (biochar). Environmental Science & Technology, 44(4), 1247-1253.

Kelly, C. N., Calderón, F. C., Acosta-Martinez, V., Mikha, M. M., Benjamin, J., Rutherford, D. W., Rostad, C. E. (2015). Switchgrass biochar effects on plant biomass and microbial dynamics in two soils from different regions. Pedosphere, 25(3), 329-342.

Lange, J. P. (2007). Lignocellulose conversion: an introduction to chemistry, process and economics. Biofuels, Bioproducts and Biorefining, 1(1), 39-48.

Lehmann, J., Joseph, S., (2015). Biochar for Environmental Management: Science and Technology. Earthscan, Sterling, VA.

Mehlich, A. (1984). Mehlich 3 soil test extractant: A modification of Mehlich 2 extractant. Communications in Soil Science and Plant Analysis, 15(12), 1409-1416.

Moreno-Castilla, C., Lopez-Ramon, M. V., Carrasco-Marın, F. (2000). Changes in surface chemistry of activated carbons by wet oxidation. Carbon, 38(14), 1995-2001.

National Forage Testing Association. 1993. Forage Analyses Procedures.

Novak, J. M., Busscher, W. J., Laird, D. L., Ahmedna, M., Watts, D. W., Niandou, M. A. (2009). Impact of biochar amendment on fertility of a southeastern coastal plain soil. Soil Science, 174(2), 105-112.

Park, J. H., Choppala, G. K., Bolan, N. S., Chung, J. W., Chuasavathi, T. (2011). Biochar reduces the bioavailability and phytotoxicity of heavy metals. Plant and Soil, 348(1-2), 439.

Qian, K., Kumar, A., Patil, K., Bellmer, D., Wang, D., Yuan, W., Huhnke, R. L. (2013). Effects of biomass feedstocks and gasification conditions on the physiochemical properties of char. Energies, 6(8), 3972-3986.

Qian, K., Kumar, A., Zhang, H., Bellmer, D., Huhnke, R. (2015). Recent advances in utilization of biochar. Renewable and Sustainable Energy Reviews, 42, 1055-1064.

Rajkovich, S., Enders, A., Hanley, K., Hyland, C., Zimmerman, A. R., Lehmann, J. (2012). Corn growth and nitrogen nutrition after additions of biochars with varying properties to a temperate soil. Biology and Fertility of Soils, 48(3), 271-284.

Recommended Methods for Manure Analysis. 2003. University of Wisconsin-Extension.

Silverstein, R. M., Webster, F. X., Kiemle, D. J., Bryce, D. L. (2014). Spectrometric identification of organic compounds. John Wiley & Sons.

Singh, B., Singh, B. P., Cowie, A. L. (2010). Characterisation and evaluation of biochars for their application as a soil amendment. Soil Research, 48(7), 516-525.

Spokas, K. A. (2010). Review of the stability of biochar in soils: predictability of O:C molar ratios. Carbon Management, 1(2), 289-303.

Song, X. D., Xue, X. Y., Chen, D. Z., He, P. J., & Dai, X. H. (2014). Application of biochar from sewage sludge to plant cultivation: Influence of pyrolysis temperature and biochar-to-soil ratio on yield and heavy metal accumulation. Chemosphere, 109, 213-220.

Spokas, K. A., Cantrell, K. B., Novak, J. M., Archer, D. W., Ippolito, J. A., Collins, H. P., Boateng, A.A., Lima, I.M., Lamb, M.C., McAloon, A.J., Lentz, R. D. (2012). Biochar: a synthesis of its agronomic impact beyond carbon sequestration. Journal of environmental quality, 41(4), 973-989.

Soltanpour, P. N., Johnson, G. W., Workman, S. M., Jones, J. B., Miller, R. O. (1996). Inductively coupled plasma emission spectrometry and inductively coupled plasma-mass spectrometry. Methods of Soil Analysis Part 3—Chemical Methods, (methodsofsoilan3), 91-139.

Sun, X., Atiyeh, H. K., Kumar, A., Zhang, H., Tanner, R. S. (2018). Biochar enhanced ethanol and butanol production by Clostridium carboxidivorans from syngas. Bioresource Technology, 265, 128-138.

Strezov, V., Popovic, E., Filkoski, R. V., Shah, P., Evans, T. (2012). Assessment of the thermal processing behavior of tobacco waste. Energy & Fuels, 26(9), 5930-5935.

Uchimiya, M., Klasson, K. T., Wartelle, L. H., Lima, I. M. (2011). Influence of soil properties on heavy metal sequestration by biochar amendment: 1. Copper sorption isotherms and the release of cations. Chemosphere, 82(10), 1431-1437.

Uchimiya, M., Lima, I. M., Thomas Klasson, K., Chang, S., Wartelle, L. H., Rodgers, J. E. (2010). Immobilization of heavy metal ions (Cu^{II}, Cd^{II}, Ni^{II}, and Pb^{II}) by broiler litter-derived biochars in water and soil. Journal of Agricultural and Food Chemistry, 58(9), 5538-5544.

Tatzber, M., Stemmer, M., Spiegel, H., Katzlberger, C., Haberhauer, G., Mentler, A., Gerzabek, M. H. (2007). FTIR-spectroscopic characterization of humic acids and

humin fractions obtained by advanced NaOH, $Na_4P_2O_7$, and Na_2CO_3 extraction procedures. Journal of Plant Nutrition and Soil Science, 170(4), 522-529.

Woldetsadik, D., Drechsel, P., Keraita, B., Marschner, B., Itanna, F., Gebrekidan, H. (2016). Effects of biochar and alkaline amendments on cadmium immobilization, selected nutrient and cadmium concentrations of lettuce (Lactuca sativa) in two contrasting soils. SpringerPlus, 5(1), 397.

Yuan, J. H., Xu, R. K., Zhang, H. (2011). The forms of alkalis in the biochar produced from crop residues at different temperatures. Bioresource Technology, 102(3), 3488-3497.

Xu, P., Sun, C. X., Ye, X. Z., Xiao, W. D., Zhang, Q., Wang, Q. (2016). The effect of biochar and crop straws on heavy metal bioavailability and plant accumulation in a Cd and Pb polluted soil. Ecotoxicology and Environmental Safety, 132, 94-100.

Xu, R. K., Zhao, A. Z., Yuan, J. H., Jiang, J. (2012). pH buffering capacity of acid soils from tropical and subtropical regions of China as influenced by incorporation of crop straw biochars. Journal of Soils and Sediments, 12(4), 494-502.

Zhang, H., Dotson, P. (1994). The use of microwave muffle furnace for dry ashing plant tissue samples. Communications in Soil Science & Plant Analysis, 25(9-10), 1321-1327.

Zhang, R. H., Li, Z. G., Liu, X. D., Wang, B. C., Zhou, G. L., Huang, X. X., Lin, C. F., Wang, A. H., Brooks, M. (2017). Immobilization and bioavailability of heavy metals in greenhouse soils amended with rice straw-derived biochar. Ecological Engineering, 98, 183-188.

Zhang, Y., Luo, W. (2014). Adsorptive removal of heavy metal from acidic wastewater with biochar produced from anaerobically digested residues: kinetics and surface complexation modeling. BioResources, 9(2), 2484-2499.

CHAPTER VI

HEAVY METAL PHYTOAVAILABILITY IN A CONTAMINATED SOIL OF NORTHEASTERN OKLAHOMA AS AFFECTED BY BIOCHAR AMENDMENT

Abstract: High concentrations of heavy metals (HM) in soils have negative impacts on plants, human health and the environmental quality. The purpose of this study was to evaluate the effects of biochars on the phytoavailability of Zn, Pb and Cd in a contaminated soil in the Tar Creek area of NE Oklahoma, as well as on the growth and uptake of these elements by perennial ryegrass (*Lolium perenne*). Biochars were produced from switchgrass (SGB) and poultry litter (PLB) feedstocks at 700 °C and applied to the soil at 0.0, 0.5, 1.0, 2.0 and 4.0% (w/w), with three replications. Regardless of the feedstock, both soil organic carbon (SOC or OC) and pH increased as the rates of biochars increased, which significantly decreased the HM phytoavailability ($p<0.01$). The Zn, Pb and Cd extracted by DTPA were highly correlated ($p<0.0001$) with their concentration in ryegrass shoots and roots. Except for some significant positive correlations ($p<0.05$), HM concentration in ryegrass shoots and roots were not correlated with their biomass ($p>0.05$). The transfer factor (HM in roots to HM in shoots ratio) decreased as the rates of biochars applied increased, especially for Pb and Cd ($p<0.01$). Our results suggest it is beneficial to use biochars at Tar Creek as a soil amendment to

reduce HM phytoavailability and metal uptake by ryegrass.

Keywords: Contaminated soil, Biochars, Heavy metal phytoavailability, Transfer factor

Introduction

Biochar is a carbon-rich product produced from the pyrolysis of biomass feedstock under partial or total absence of oxygen (Lehmann 2015). Amending soil with biochar is not a new concept and has been practiced for a long time. In addition to the role of biochars in increasing the sequestration of carbon and influencing CO_2 emissions, biochars have been shown to enhance soil quality as well as to stabilize heavy metals (HM) (Ahumada et al. 2014; Sidhu et al. 2016). Also, biochar has a potential benefit for improving soil fertility (Chan et al. 2008; Novak et al. 2009) and other soil properties such as pH (Houben et al. 2013), cation exchange capacity (CEC) (Gondeck and Mierzwa-Hersztek, 2016) and water holding capacity (Streubel et al. 2011), thus enhancing plant growth (Peng et al. 2011) and reducing nutrient leaching losses (Laird et al. 2010). Therefore, biochars have the ability to immobilize HM such as Zn, Pb and Cd and thereby reduce their phytoavailability and toxicity to plants by increasing soil pH (Houben et al. 2013) and CEC (Gondeck and Mierzwa-Hersztek, 2016).

Fellet et al. (2011) reported that the application of orchard prune derived biochar to mine tailings reduced bioavailable (DTPA-extractable) contents of Zn, Pb and Cd. Rice straw-derived biochar reduced Cd concentration in the plant available soil fraction cultivated under greenhouse conditions (Zhang et al. 2017). Biochars reduced Cd and Pb accumulation in ryegrass shoot (Xu et al. 2016), which may be a viable option for safe production of forage in HM polluted soils. Therefore, phytoremediation combined with

biochar addition enhances soil biological activities (Houben et al. 2013). In another study, the concentrations of Cu, Pb and Zn had a direct reverse relationship with the concentration of biochars applied, with a significant effect for amendments >1% (w/w) applied (Gondeck and Mierzwa-Hersztek, 2016). According to the same authors, the application of poultry litter-derived biochar (PLB) reduced the mobility of Cu, Cd, Pb and Zn and the reduction of mobility increased as the rate of PLB applied increased in a HM contaminated soil. Similarly, the bioavailability of metals gradually decreased with time when the soil was amended with 5% or 10% of biochar (Houben et al. 2013). Ahmad et al. (2016) observed that biochars produced at high temperatures (700 ^{o}C) decreased Pb phytoavailability much more effectively than biochars produced at low temperatures (300-350 ^{o}C). However, depending on the type of biochar and the specie of HM, the increased amount of biochar applied can either significantly reduce HM availability or make no difference (Al-Wabel et al. 2015; Li et al. 2016; Lu et al. 2014; Puga et al. 2015; Zhang et al. 2016). Therefore, the efficiency of biochars from different feedstocks in immobilizing soil HM must be carefully evaluated for each specific site before large-scale application (Banik et al. 2018; Zhang et al. 2016). Although there are several reports on the application of biochar in neutral pH soils, only a few works have reported the effect of biochar application on the phytoavailability of HM to ryegrass in non-acidic soils (Rees et al. 2016; Zhang et al. 2016). Additionally, no work has been conducted in soils with slightly neutral pH located in the Tar Creek area.

The area now known as Tar Creek is a part of the Tri-state mining district (TSMD), located in the border region of Oklahoma, Kansas and Missouri (Neuberger et al. 2009). Due to rich deposit of Zn and Pb ore, this area was mined during the early

1900s to the 1970s. Because of mining and milling operations, large quantities of wastes (coarse material contaminated with Zn, Pb and Cd), locally referred to as chat, were left on ground surface in piles. The size and number of chat piles throughout of those communities resulted in Zn, Pb and Cd contamination outside the areas due to wind blowing and the chat materials used as gravel. In addition, chat accumulations in Tar Creek area have distorted the land, inhibited productive use, and affected human health (Zota et al. 2011; Hu et al. 2007). Reclamations of contaminated lands have been attempted by US Government and the Quapaw Tribe. Although the state of Zn, Pb and Cd contamination in the TSMD has been addressed in numerous studies (Brown et al. 2007; Beattie et al. 2017; Gouzie 2018), there is still a lack of research using different soil amendments, such as by-products produced from different feedstocks for HM remediation and phytoavailability reduction. Since current literature is deficient in addressing these needs, we believe that our research has the potential to expand from laboratory based small-scale tests to larger scale long-term studies (Wang et al. 2019). The objectives of this work were to investigate the effects of increased rates of switchgrass- and poultry litter-derived biochars pyrolyzed at high temperature (700 ^{o}C) application on the immobilization of HM in the Tar Creek contaminated soil; and to evaluate the impacts of these biochars on ryegrass growth and HM phytoavailability to shoots and roots.

Material and methods

Biochar preparation and characterization

The biochars studied were converted from poultry litter (PL) and switchgrass biomass. Switchgrass (SG; Panicum virgatum) was harvested from an established field at Clemson University Pee Dee Research and Education Center in Darlington County, SC. The switchgrass was hammer milled to approximately 6 mm particle size. The moisture content of milled switchgrass prior to pyrolysis was measured to be 6.45 ± 0.21 wt%. Poultry litter was collected from the top 5.0 - 7.5 cm depth from10 locations in a commercial poultry house in Orangeburg County, SC. Poultry litter was ground (Wiley Mill equipped) to 2 mm particle size, and overnight oven dried at 105 ^{o}C. The moisture content of PL was determined to be 6.49%. Switchgrass- and poultry litter-derived biochars (SGB, PLB, respectively) were produced at 700 ^{o}C by slow pyrolysis. The feedstock samples were pyrolyzed as following: 1h equilibration hold at 200 ^{o}C under an industrial-grade N_2 flow rate at 15 L min^{-1}; the temperature was increased to the desired temperature within 1 h at 8.33 ^{o}C min^{-1}. The maximum temperature (700 ^{o}C) was held for 2 h under N_2 flow at 1 L min^{-1}. The samples were cooled down to 100 ^{o}C (4.25 ^{o}C min^{-1}). The resulting biochars were allowed to cool to room temperature in an inert atmosphere N_2 (Cantrell et al. 2012). Biochars coarse materials were ground with a mortar and pastel gently before sieved through 1 mm for further analyses and 0.25 mm for pot experiment.

Moisture content was determined by oven drying previously weighted biochar samples overnight at 105 ^{o}C (Ahmedna et al. 1997) and ash content by using the method of Novak et al. (2009) with weight loss after heating to 760 ^{o}C in air for 6 h by using conventional resistance muffle furnace (CMF) (Zhang and Dotson, 1994). The pH of

each biochar was determined according to Yuan et al. (2011) in DI water at a 1:5 (w/w biochar:water) ratio. The biochar samples were each thoroughly mixed with DI water in 50 mL centrifuge tubes and shaken at 220 rpm for 1 h. The pH was then measured using an Orion Star A221 pH meter (Thermo Scientific). The electrical conductivity (EC) was determined in a 1:20 biochar to deionized water suspension after 90 min-shaking (Rajkovich et al. 2012). Biochars were analyzed similar to the manure/compost tests for total P, K, secondary nutrients, micronutrients. Total nitrogen (TN) and carbon (SOC) were determined using a dry combustion Carbon/Nitrogen Analyzer.

The biochars used in this study were characterized as their specific surface area (SSA) and surface functional groups. SSA of coarse fraction of biochars was determined on a Quantachrome Autosorb1 using N_2 sorptometry. Each biochar SSA was calculated using multi-point adsorption data from the 0.01–0.3 P/Po linear segment of the N_2 adsorption isotherms made at 77.35 K according to the Brunauer, Emmet, and Teller theory (BET). Biochar samples were degassed under vacuum (200 °C for 12 h) prior to nitrogen adsorption at liquid nitrogen temperature (−196 °C). Biochars with four different sizes (<2, <1, <0.25 and <0.053 mm) without pretreatments were scanned 64 times at 4 cm^{-1} resolution from 4000 to 650 cm^{-1} in absorbance mode. The collected spectra were subjected to baseline correction manually. Air background was collected to avoid any peak of carbon dioxide-CO_2 arising between 2300-2400 cm^{-1}. The spectra of the fine fraction were chosen to represent the peaks of functional groups for all biochars because of higher homogeneity in finer samples. The FTIR spectrum peaks were identified by comparing the peak position with already known peaks found elsewhere in the literature.

Soil sampling and physicochemical analysis

Multi-metal contaminated soil samples were collected with a shovel (0-15 cm) from a residential yard near chat piles located in Picher, Ottawa County, Oklahoma. The soils were homogenized, air-dried for 1 week, sieved with a 10-mm screen and stored in polyethylene containers before oven-dried at 65 ^{o}C for 24 h, and passed through a 2-mm sieve. Before and after the pot experiment, the 2 mm-sieved soil samples were analyzed for pH, (SOC) content, total and DTPA-sorbitol extractable Zn, Pb and Cd. The soil pH was determined in deionized water with a 1:1 soil to water ratio (Ahmad et al. 2012). The SOC and total nitrogen (TN) were determined by dry combustion using a LECO Truspec carbon and nitrogen analyzer (St. Joseph, MI). Total Zn, Pb and Cd were digested by concentrated HNO_3 and H_2O_2 using EPA method 3050B (Church et al. 2017), and quantified by an inductively coupled plasma – atomic emission spectroscopy (ICP-AES). Phytoavailable HM were analyzed by adding 20 ml of DTPA-sorbitol to 10 g of soil and shaken for 2 h. The SOC, TN, total and DTPA-extractable HM before the potting experiment are presented in Table 1. The total HM contents were about tenfold the maximum found for typical Oklahoma soils (Richards et al. 2012). Plant available P and K were extracted by shaking 2 g soil in 20 ml Mehlich-3 solution for 5 min (Mehlich 1984), and quantified by ICP-AES; and nitrate- and ammonium-N were extracted by 1.0 M KCl (Kachurina et al. 2000) and simultaneously measured on a flow-injection analyzer (Table 1). The sum of both nitrate and ammonium N characterized the amount of plant available N in the soil. After the pot experiment, electrical conductivity (EC) was measured in 1:1 soil to water extract.

Table 1. pH, SOC, extractable and total nutrients of Tar Creek soil before the experiment

		Extractable											
Tar Creek	pH	N	P	K	Ca	Mg	S	B	Fe	Cu	Zn	Pb	Cd
		mg kg^{-1}											
soil	6.4	1.5	25	117.5	2094	153.5	30.3	0.12	35.3	1.77	220.6	49.9	1.84
Stdev	0	0	1.3	1.3	31.3	2.3	0.36	0.01	1.6	0.06	9.3	1.7	0.03
	Total												
Tar Creek	SOC	N	P	K	Ca	Mg	S	Mn	Fe	Cu	Zn[§]	Pb[§]	Cd[§]
	%							mg kg^{-1}					
soil	2.1	0.17	0.03	0.09	0.39	0.12	0.08	242.4	13029	12.8	1765	233.7	9
Stdev	0.2	0.01	0	0.01	0.04	0.01	0.02	54.9	2076	0.3	220.5	10.8	0.6

Stdev: Standard deviation (n=3); Extractable N = NO_3^-+NH_4^+;

§The averages (and ranges) of Zn, Pb and Cd in typical Oklahoma soils are 55.2 (15.3–142), 14.9 (2.60–31.7) and 0.30 (0.13–0.80) mg kg^{-1}, respectively (Richards et al. 2012)

Potting experiment

Ryegrass was grown in biochar-amended soils contaminated by HM in an environmentally controlled growth chamber. Plastic pots (1/4 to 3/8" depth) were filled with 1200 g of 2 mm sieved soils and amended with 0.0 (control), 0.5, 1.0, 2.0 and 4.0% (w/w) of 0.25 mm-sieved (Park et al. 2011) SGB and PLB. The biochar-amended soils were incubated for ~30 days (Zhang et al. 2016) at 75% of field capacity before ryegrass seeds were sown in each pot at 30 kg ha^{-1} (~80% of germination). The grass grew from 04/08/2018 (planting) to 06/22/2018 (harvesting) in a growth chamber using a completely randomized design with three replications (n=3). Pots were rotated weekly to eliminate spatial variability in the chamber. The humidity was kept in a range of 75 to 95%. The temperature was set at 20 ^oC for the first 2 weeks, in the following weeks, daily conditions were switched to 14 ^oC with 14 h of light to simulate daytime and 10 ^oC with 10 h of dark to simulate nighttime. Daytime and nighttime simulations continued until

harvest. On 05/03/2018, each pot was supplied with the same amount of N based on soil test for grass production subtracting N supplied by biochars. Since biochars already provided adequate P and K, only the control received additional P and K. Pots were regularly watered with R.O. water (EC = 29.1 μS cm^{-1}) to maintain a water content near field capacity and prevent nutrient leaching. The number of germinated seeds was counted, and the germination rate was calculated. After harvesting plants, the shoots and roots were separated, washed with deionized water, oven dried to constant weight at 105 ^{o}C, and their weight were recorded. Dried plant materials were ground using a mechanical grinder for further analyses.

Heavy metal analysis in plants

Ground plant materials were analyzed for metals using nitric acid digestion, in which 0.5 g of ground plant materials were predigested for 1 h with 10 ml of trace metal grade HNO_3 in the HotBlock^{TM} Environmental Express block digester. The digestion products were then heated to 115 ^{o}C for 2 h and diluted with deionized water to 50 mL (Westerman et al. 1990). The digested samples were analyzed for Zn, Pb and Cd by an ICP-AES. Phytoavailability of HM and the heavy metal transfer factor were calculated as follows:

$$\text{Phytoavailability (\%)} = \frac{\text{HM concentration in shoots and/or roots (mg kg}^{-1}\text{) x Dry biomass (kg pot}^{-1}\text{)*100}}{\text{HM concentration in soil}_{DTPA}\text{ (mg kg}^{-1}\text{)}^{\S}\text{ x Soil mass (kg pot}^{-1}\text{)}}$$

(Woldetsadik et al. 2016) **Eq. 1**

$$\text{Phytoavailability (mg kg}^{-1}\text{)} = \frac{\text{HM concentration in soil}_{DTPA}\text{ (mg kg}^{-1}\text{)}^{\S}\text{ x Phytoavailability (\%)}}{100}$$

§DTPA-extractable HM after ryegrass harvesting. **Eq. 2**

$$\text{Transfer factor} = \frac{\text{HM concentration in shoots (mg kg}^{-1}\text{)}}{\text{HM concentration in roots (mg kg}^{-1}\text{)}}$$

(Ghosh and Singh, 2005) **Eq. 3**

Statistical analyses

The standard deviation was plotted to show significant differences among treatments by using the excel software. Ryegrass germination, biomass and heavy metal transfer factor results were subjected to ANOVA by following the completely randomized design and the treatments average compared by Tukey test at 1%. Only a few outliers were removed from the replication dataset of treatments by using IML and UNIVARIATE (ROBUSTSCALE) procedures of SAS program (SAS Institute 2011), and the statistical analyses were performed with n=2 for those specific treatments. Pearson simple correlations and multiple regression analyses were also performed for some variables, using all replicate data, and the graphs were created with the assistance of OriginPro 9.1 software.

Results and discussion

Characteristics of biochars

Table 2 shows proximate analyses, physicochemical properties and chemical composition of biochars. Ash content was clearly higher in PLB (45.9) than in SGB (4.4), probably due to the higher contents of total minerals in PLB, as well as higher EC in PLB than SGB (Table 2). The EC of the biochar can potentially increase the EC of the amended soil thus affecting plant growth mainly if soil EC>4.0 dS m^{-1} (Montoroi 2018), as observed in our experiment for the control, 2 and 4% of PLB applied (Table 2 and Fig. S1 and S2 – Supplementary material). The high soluble salts in PLB increased soil electrical conductivity (EC) up to 4% of PLB application and reduced ryegrass biomass by 79%. Regarding the SSA, the higher values obtained for SGB is probably a

consequence of the surface porosity with more pores presenting regular geometrical morphology than PLBs. The OC was 31.4±1% and 27.8±1.4% for SGB and PLB, respectively. The ash and OC contents in our experiment agree with Lu et al. (2017) and Zhao et al. (2016) who showed that manure-derived biochars had lower carbon content than green waste-derived biochars since the latter generally has a lower ash content (Table 2). The moisture content of PLB was higher than that of SGB suggesting the higher water holding capacity of the former. This observation was confirmed in the growth chamber given that all soils receiving PLB showed a higher soil moisture content when the same amount of water was applied, especially at the 4.0% amendment rate.

The FTIR spectra for the functional groups of SGB and PLB are provided in supplementary material (Fig. S3). The C=O stretching and aromatic C=C vibrations were visible at 1554.37 cm^{-1} band of SGB. The peak at 796.47 cm^{-1} for the same biochar is also assigned to C-H bending of aromatic out of plane deformation and for biochars pyrolyzed at high temperatures (Uchimiya et al. 2011).

The intense broad band at 1030.30 cm^{-1} for PLB was likely resulted from P-containing functional groups, mostly P-O bond of phosphate functional group such as phosphines and phosphine oxides. Woldetsadik et al. (2016), studying poultry litter-derived biochars, reported the same functional groups at 1038 cm^{-1} band. High P contents are observed for fecal and manure derived biochars, as found for PLB (Table 2). However, a pronounced peak found at 1073.21 cm^{-1} for SGB is more likely related to silicon oxide and C-O-C stretching of different types of oxygenated compounds such as alcohols, phenols and ethers than phosphates functional group (Qian et al. 2013; Cantrell

et al. 2012; Keiluweit et al. 2010; Feinstein 2018) since the total phosphorus is about 24 times lower than that found in PLB (Table 2).

Table 2. Ash, moisture, EC, SSA, total nitrogen (TN), OC, pH and total nutrient contents of switchgrass- and poultry litter-derived biochars pyrolyzed at 700 ^{o}C

		SGB	PLB
	Ash (%)	4.4	45.9
	Moisture (%)	1.7	3.9
	EC (µS cm^{-1})	240	9150
	SSA (m^2 g^{-1})	22.9	9.3
	TN (%)	0.74 ± 0.00	1.6 ± 0.10
	OC (%)	31.4 ± 1.28	27.8 ± 1.38
	pH	10.1±0.16	10.2±0.05
Macronutrients			
P		1.6 ± 0.2	38.7 ± 0.8
Ca		7.9 ± 1.0	54.2 ± 2.4
K		4.0 ± 0.4	78.0 ± 0.6
Mg	g kg^{-1}	3.4 ± 0.3	19.0 ± 0.1
Na		0.3 ± 0.1	25.8 ± 0.6
S		0.4 ± 0.1	13.5 ± 0.6
Micronutrients			
Fe		111 ± 20.1	6903 ± 1295
Zn		53.6 ± 5.8	1477 ± 43
Cu		23.2 ± 2.7	253 ± 4
Mn	mg kg^{-1}	144 ± 10.8	1108 ± 2
B		<1.0[§]	102 ± 1.7
Ni		11.3 ± 0.47	25.5 ± 1.02

§ <DL = Detection limit; Values after ± are the standard deviation (n=3)

Jiang et al. (2012) showed a number of pronounced peaks at 3419, 1614, 1103 and 795 cm^{-1} assigned to the hydroxyl (–OH) stretching, $–COO^-$ anti-symmetric stretching, bands of the out-of-plane bending for carbonates ($-CO_3^{2-}$) and to carboxylate ($–COO^-$) deviational vibration and symmetric stretching, respectively, for rice straw-

derived biochar, and attributed such functional groups to the ability in forming surface complexes with Pb(II). In our study, similar peaks were found at ~3600, ~1600 (1565.46-1554.37 cm^{-1} for SGB and 1553.89 cm^{-1} for PLB), 1000-1100 and ~680-860 cm^{-1} for both SGB and PLB. There is a possibility of the ~2080 cm^{-1} (2052.89 cm^{-1} for SGB and 2059.64 cm^{-1} for PLB in the case of our study) peak arising from an organic azide group (-N=N=N) or a ketene group (>C=C=O). The azide group functional group is supported by the >1.0% of nitrogen found for PLB (Table 2) (Chia et al. 2012). However, the poor stability of azides at the high temperature used for pyrolysis suggests that a ketene may be a more likely candidate for this peak (Chia et al. 2012).

In summary, the peaks in the range of 3270.73-3849.28 cm^{-1} found for all biochars are probably from hydroxyl groups (Park et al. 2011). Peaks found at 1554.37 (SGB) and 1553.89 cm^{-1} (PLB) correspond to the stretching vibrations of conjugated C=O bonds in aromatic rings (Cao and Harris, 2010). Bands at 796.47 cm^{-1} for SGB and 873.13 cm^{-1} for PLB are probably due to the contribution from C–H bond vibration in aromatic compounds (Park et al. 2011; Moreno-Castilla et al. 2000). FTIR analyses suggest that biochars produced with high pyrolysis temperatures can result in the formation of certain surface functional groups. Those found in our study seem to be promising as far as heavy metal adsorption is concerned since they play an important role in the adsorption of Pb, Cd and Zn (Park et al. 2011).

Ryegrass biomass and germination

Ryegrass germination rates and the biomass weight of shoots and roots are presented in supplementary material (Table S1). The highest germination rates and the

highest biomass produced were observed for the 0.5, 1.0 and 2.0% of PLB treatments. The other treatments had both poor germination and low biomass production. This could be attributed to metal toxicity, high salinity or other factors, which will be discussed in later sections.

Effects of biochars on the DTPA-extractable heavy metals in the soil

The phytoavailability of HM as affected by biochar amendment in the soil after the harvest of ryegrass was extracted by DTPA and is shown in Fig. 1. The phytoavailable HM extracted from the untreated soil (control, 0% biochar) varied in the following order: Zn (189.1±10 mg kg^{-1}) > Pb (47.7±5.2 mg kg^{-1}) > Cd (1.7±0.1 mg kg^{-1}). Generally, the DTPA-extractable HM contents were the highest for the control and decreased as the rates of biochars increased.

According to Zhang et al. (2016), previous studies suggested that the incorporation of biochars to soils effectively decreased the phytoavailability of HM assessed by strong extractants including DTPA (Al-Wabel et al. 2015; Li et al. 2016; Mohamed et al. 2015; Shen et al. 2016). However, a slight increase of Pb and Cd over the control was observed for the 0.5% SGB treatment in our study (Fig. 1). Probably at such rate, the significant decrease of Zn in comparison to the control was enough to increase Pb and Cd phytoavailability in comparison to the same treatment. In contrast to Zn, the increased rates of PLB was more efficient in reducing Pb and Cd phytoavailability in comparison to SGB, which can be attributed to the different effects of different feedstocks on SOC and soil pH.

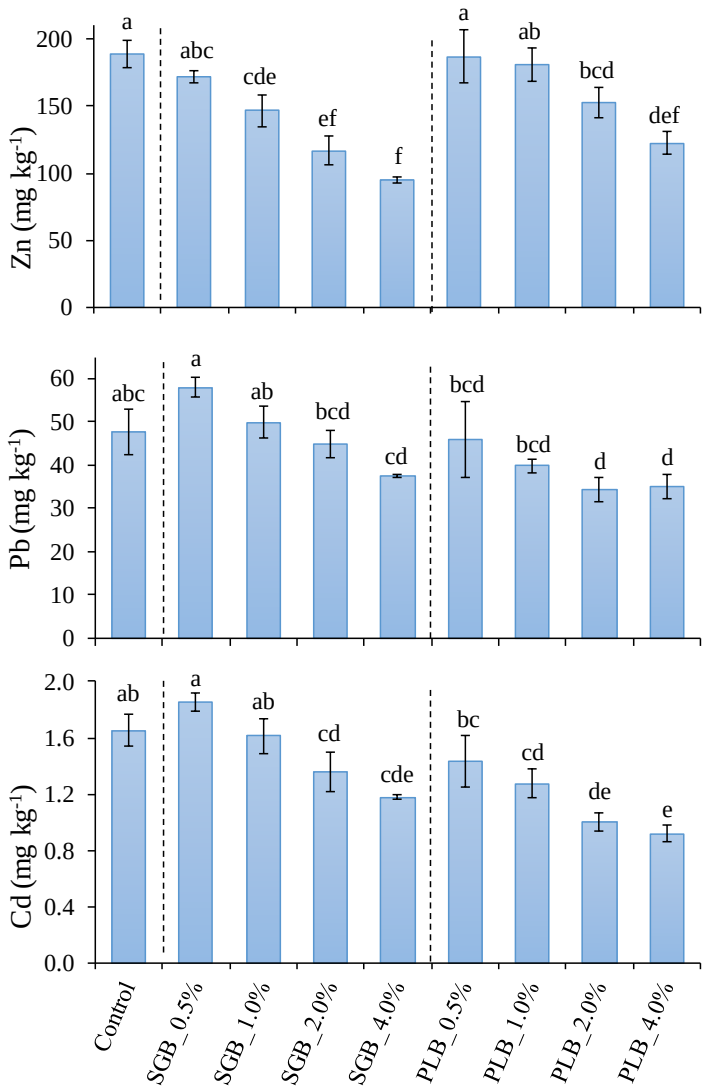

Fig. 1. Heavy metals extracted by DTPA as a function of biochar application rates. Bars are the average standard deviation ($p<0.01$)

The relationships between SOC or pH and heavy metal phytoavailability in the soil

The application of biochars significantly increased the SOC ($p<0.01$) for most treatments, as shown in supplementary material (Fig. S4), which was similar to the findings of Mohamed et al. (2015) and Zhang et al. (2016). The SOC in the soils treated with biochars was 1.17 to 2.50 (SGB) and 1.10 to 1.42 (PLB) times that of the control.

With the increasing rates of SGB and PLB, the SOC content increased correspondently. Similar trend was observed for soil pH (data not shown) as a result of biochar amendment. The SOC content of SGB treated soils increased more than that of PLB due to the higher SOC content of the former (Fig. S4 and Table 2).

Fig. 2 shows the significant negative correlations between SOC or pH and HM extracted by DTPA. All correlations were significant, except for pH Vs Pb in SGB treated soil. The alkaline pH generally reported for biochars (Lahori et al. 2017; Ahmad et al. 2016) agrees with our results, where SGB and PLB had a pH of 10.1±0.16 and 10.2±0.05, respectively. Therefore, by increasing soil pH biochars act as liming materials and precipitate HM as insoluble HM-hydroxides. Biochars with high CEC associated with a highly porous structure, high pH and the presence of carbon-based active functional groups are the main physicochemical properties responsible for HM adsorption, fixation and immobilization (Zhang et al. 2017; Park et al. 2011). Heavy metals are adsorbed by biochars primarily through cation exchange and ligand exchange reactions, which requires negatively charged and specific polar organic functional groups to be present on biochar surfaces (Banik et al. 2018). Therefore, the adsorption of the HM onto biochars through electrostatic and chemical interaction play a role in immobilization and is enhanced when SOC and soil pH are increased. Thus we conducted multiple regression analyses to evaluate how extractable HM was affected by the combination of both SOC and pH (Fig. 3). The multiple correlation coefficients (R^2) were higher in the case of Zn and Cd (Fig. 3) than observed for SOC and pH when plotted separately (Fig. 2). Although the R^2 for Pb was lower than Pb Vs SOC for PLB, it was significant

(p=0.0001) for SGB and presented a higher coefficient of correlation than Pb Vs SOC and Pb Vs pH for the same feedstock (R^2 = 0.88) (Fig. 3).

These results suggest that the decrease of HM phytoavailability is a consequence of increasing both SOC and soil pH as the rates of biochars increased. In addition, the correlation between SOC and pH is positive and significant for SGB (r=0.84, p=0.0001), PLB (r=0.90, p<0.0001) and the two biochar treated soils - SGB+PLB (r=0.70, p<0.0001).

The extractable Zn was more sensitive to pH changes when the two biochar treated soils were combined (r = -0.86, p<0.05, data not shown) even considering that the soil pH was not drastically changed by increasing biochar application rates (6.0 to 7.5) (Fig. 2). Also, in contrast to Pb and Cd, Zn also showed significant relationships with what? (R^2 = 0.88, p<0.0001) when both biochars were plotted together (data not shown) (Fig. 3). However, the small pH increase was important in immobilizing HM, although its immobilization was not as much as it was due to SOC increasing (2.0 to 5.5%).

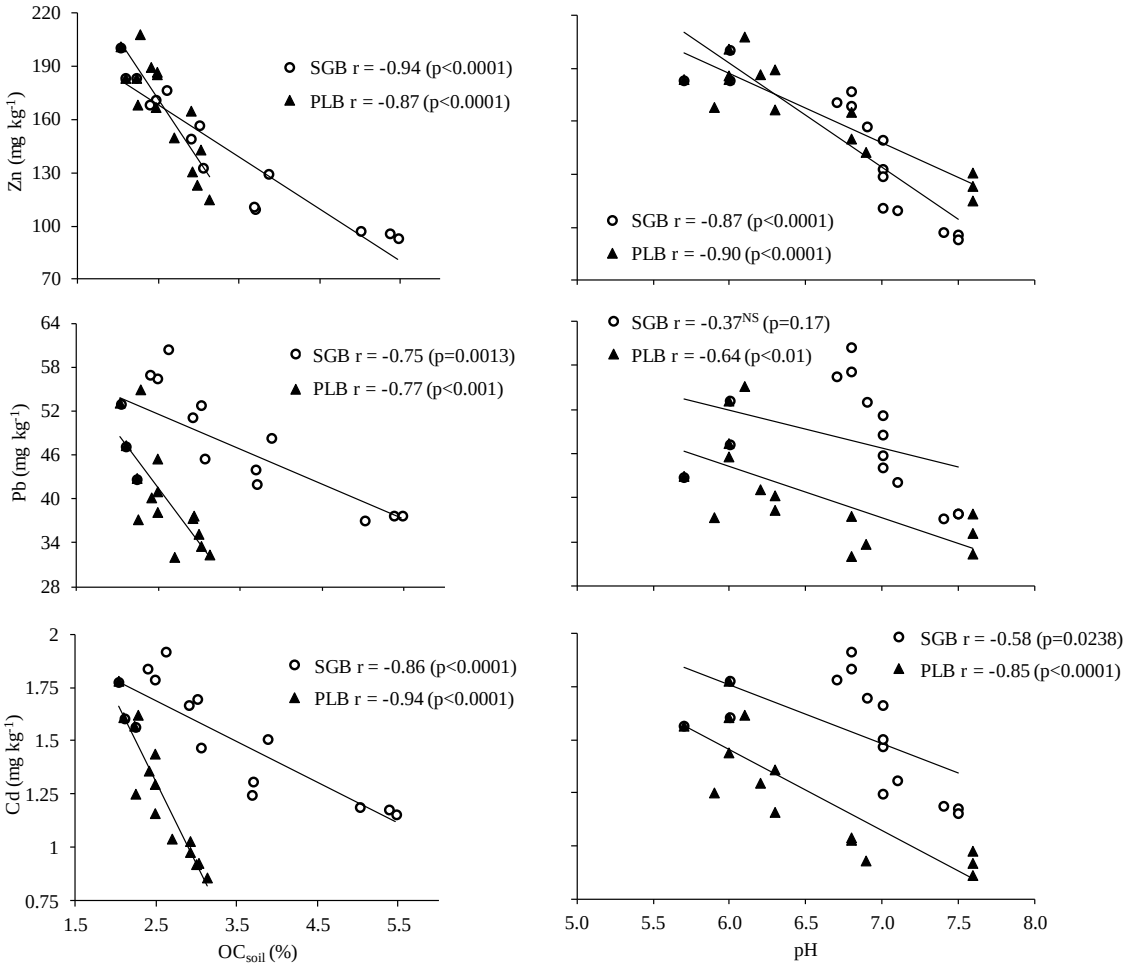

Fig. 2. Pearson correlations between soil heavy metal contents extracted by DTPA and organic carbon in the soil (OC_{soil}) or pH. NS=non-significant

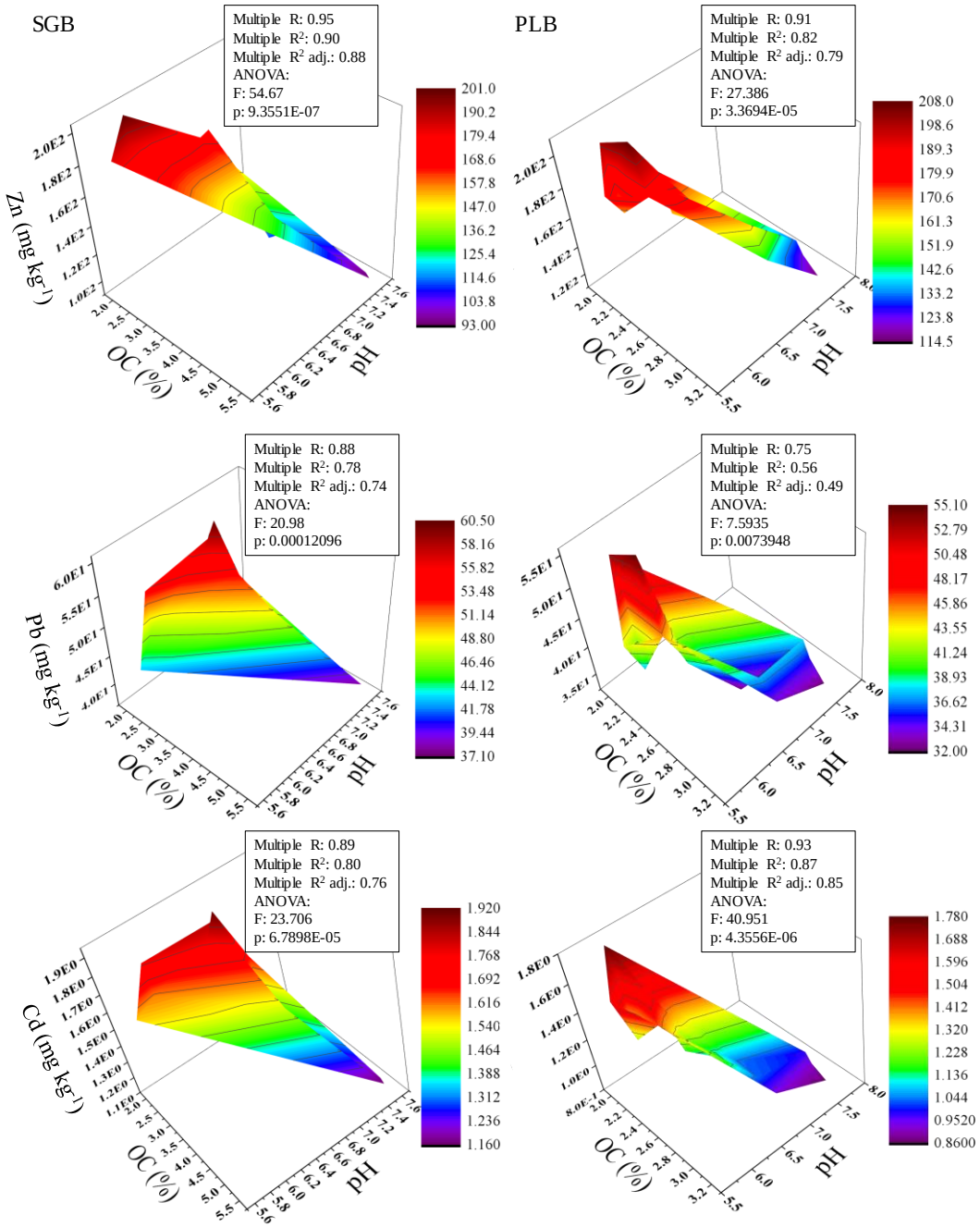

Fig. 3. 3D surface plot (XYZ) containing multiple regression analyses of heavy metal (Z) Vs soil organic carbon (X) and soil pH (Y)

Effects of biochars on the uptake of heavy metals by the ryegrass

The effect of biochars on HM phytoavailability (%) to ryegrass was calculated according to Equation 1 (Woldetsadik et al. 2016) and the results are presented in Fig. 4. The HM concentrations in ryegrass shoots of untreated soil followed the order: Zn (1521±4.6 mg kg^{-1}) > Pb (238±21.3 mg kg^{-1}) > Cd (5.44±0.6 mg kg^{-1}), and in the roots followed the order of Zn (1203±93.8 mg kg^{-1}) > Pb (141±16.3 mg kg^{-1}) > Cd (19±0.4 mg kg^{-1}). The patterns of metal phytoavailability agreed well with the DTPA-extractable HM, thereby favoring in establishing true phytoavailability assessments with DTPA extraction. On the other hand, Zhang et al. (2016) found no correlation when assessing HM phytoavailability by using EDTA.

The addition of biochars significantly reduced ($p<0.01$) the plant uptake of Zn, Pb and Cd in the shoots by 64.5 to 81.7%, 96.7 to 97.2% and 46.1 to 78.1% from SGB at 0.5% to SGB at 4.0%, and 67.9 to 85.8%, 96.7 to 97.5% and 35.5 to 80% from PLB at 0.5% to PLB at 4.0%, compared with the control, respectively. These results are consistent with previous similar studies (Al-Wabel et al. 2015; Gondeck and Mierzwa-Hersztek, 2016; Shen et al. 2016; Karami et al. 2011; Lu et al. 2014; Mohamed et al. 2015; Puga et al. 2015; Zhang et al. 2016).

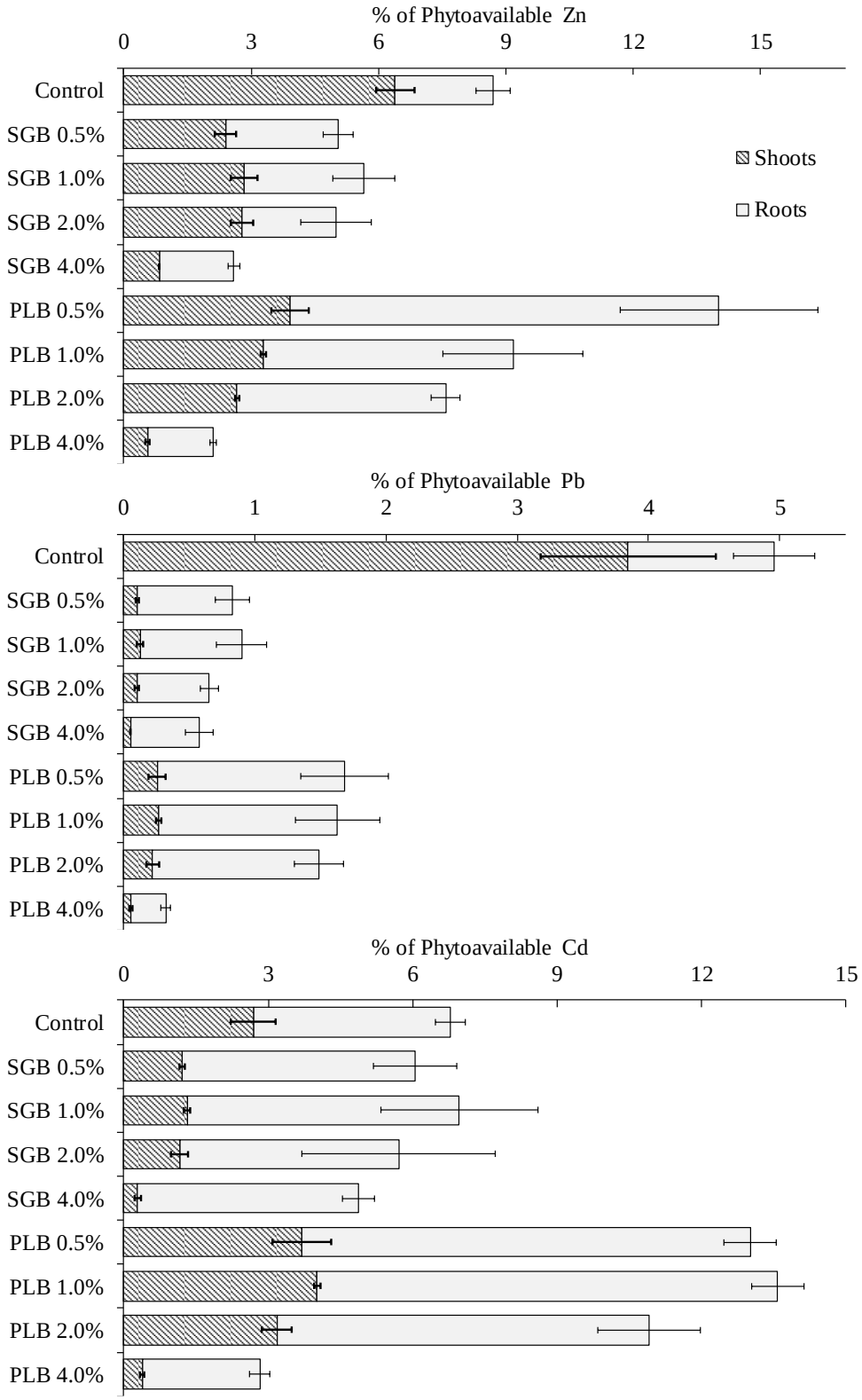

Fig. 4. Comparison of phytoavailable Zn, Pb and Cd of the ryegrass shoots and roots treated with various amount of biochars. Bars are the average standard deviation ($p<0.01$)

The HM concentrations in the roots were not different between the 0.5% treatment and the control. However, the reduction was significant for treatments with higher rates ($p<0.01$) ranging from 6.9% to 53.8% and 26% to 53.7% for Zn and Pb in SGB treated soils, respectively, and 28.5 to 72.7% for Pb in PLB treated soils. The only significant decrease from the control for Cd ($p<0.01$) was found for PLB at 2.0 and 4.0%, where the Cd was reduced by 30.9 and 51.2%, respectively. Other studies have also reported the preferential accumulation of Cd in the roots of grasses rather than shoots, such as ryegrass (Jarvis et al. 1976) and rice (Huang et al. 2019). In our study, it is evident that the phytoavailable Cd was higher in the roots of ryegrass than the shoots even for the control, which was not observed for Zn and Pb (Fig. 4).

The phytoavailability of HM in biochars assessed by several chemical extractants other than DTPA ($CaCl_2$, NH_4NO_3, HOAc, and EDTA) has failed to represent the uptake of most HM to plants cultivated in soils containing biochars (Farrell et al. 2013; Zhang et al. 2016). Therefore, we correlated the phytoavailable DTPA-extractable HM from the biochar-treated and –untreated soils with HM concentration in the ryegrass shoots and roots cultivated in the Tar Creek soil (Table S2 - Supplementary material). All phytoavailable HM in shoots, roots and shoots+roots were positively correlated with the DTPA extractable regardless of the type of biochars applied ($p<0.0001$).

Our findings suggest that the DTPA extraction used for routine micronutrient phytoavailability assessment by service soil testing labs is probably reliable for predicting the phytoavailability of HM in biochar-treated soils as well. The efficiency of SGB for reducing the uptake of HMs to ryegrass planted in the Tar Creek soil was significantly

higher than that of PLB. This trend is probably attributed to the clearly lower ash content and higher organic matter in SGB (Table 2) (Qiu et al. 2015) and consequently the surface functional groups that are carbon-based, further affecting the phytoavailability of HM.

Some studies revealed that the "dilution effect" caused by the increase of plant biomass also contributed to the decrease of HM concentrations in plants cultivated in biochar-treated soils (Zhang et al.; 2016; Lu et al. 2014; Park et al. 2011), which suggests that such decrease is probably not a consequence of biochar application. However, in the case of our study no correlations between the concentrations of Zn, Pb and Cd in the shoots of ryegrass and their biomass were observed ($p>0.05$), with some exceptions (Table S3 - Supplementary material). Similar results were observed by Zhang et al. (2016) when evaluating ryegrass shoots. In contrast, significant positive correlations were observed between the concentrations of Zn and Cd in the roots of ryegrass and their biomass for both SGB and PLB ($p<0.01$). The similar correlation was confirmed for Zn only when the two biochar treated soils were combined ($p<0.01$), which does not support the "dilution effect" but supports the reduction in HM uptake due to biochar addition.

The transfer factors of HM in the untreated soil were in the following order: Pb (1.96) > Zn (1.34) > Cd (0.29) (Table 3). A lower transfer factor indicates higher root concentrations and lower transferring to above ground plant parts, thus lower the risk to the primary consumer (Zhang et al. 2016; Karami et al. 2011). Compared with the control, the incorporation of SGB and PLB significantly reduced the average transfer factors of Zn, Pb and Cd ($p<0.01$) by 48 and 82% (Zn), 83 and 79% (Pb), and 62 and 43% (Cd), respectively (Table 3).

Table 3. Zinc, Pb, and Cd transfer factor as a function of biochar application rates. Transfer factor = metal concentration in shoots/metal concentration in roots (Ghosh and Singh, 2005)

Treatment	Zn		Pb		Cd	
	……...Transfer factor……					
Control	1.34	a	1.96	a	0.29	a
SGB 0.5%	0.45	bcd	0.07	c	0.12	cd
SGB 1.0%	0.50	bc	0.08	bc	0.12	cd
SGB 2.0%	0.62	b	0.09	bc	0.13	cd
SGB 4.0%	0.50	bcd	0.09	bc	0.07	d
PLB 0.5%	0.18	e	0.08	c	0.18	bc
PLB 1.0%	0.24	de	0.08	c	0.16	bc
PLB 2.0%	0.26	cde	0.08	c	0.20	b
PLB 4.0%	0.28	cde	0.17	b	0.12	cd
F value	29.95	**	735.6	**	23.40	**
Average	0.44		0.18		0.15	
Stdev	0.07		0.02		0.02	
CV (%)	16.7		12.9		14.7	

**p<0.01. Same letters in the column are not different from Tukey test at 1%
Stdev: Standard deviation; CV: Coefficient of variation

The effects of biochar feedstock types on transfer factors were similar to their effects on plant metal uptake. Generally, the transfer factors did not significantly differ among the soils treated with the same biochar, but the Zn transfer factor was slightly different between SGB and PLB for the same rates applied (Table 3). This lack in difference could be attributed to the fact that feedstocks only had a slight different impact on the uptake of HM to ryegrass. The significant decrease of the transfer factor from the control after addition of biochars was probably a result of their high efficiency in decreasing the HM uptake by ryegrass. The distribution of phytoavailable HM in ryegrass

shoots and roots presented in Fig. 4 clearly indicates that roots had higher concentrations of HM regardless of the feedstock, and only a small portion of them moved to the shoots.

Conclusions

A potting experiment was conducted to investigate the effects of biochars on the availability of Zn, Pb and Cd to ryegrass in the Tar Creek contaminated soil. Biochars significantly decreased the phytoavailability of HM extracted by DTPA, which resulted in less HM uptake. The highly positive correlations between the extractable HM and the plant uptake suggest that DTPA extraction is probably a reliable indicator of HM phytoavailability in contaminated soils. Negative correlations between HM and SOC or soil pH indicate that biochars converted from poultry litter and switchgrass at 700 ^{o}C had high efficiency in reducing the phytoavailability of the HM investigated. Such change in soil properties (especially in pH and SOC) could serve as main reason for the immobilization of HM in biochar-treated soils. Non-significant correlations between HM concentrations in the shoots and roots and their biomass indicate the reduction of metals in plants is not due to dilution but resulted from reduced uptake. The significant decrease of the transfer factor values from ryegrass roots to ryegrass shoots was probably a result of the high efficiency of biochars in decreasing HM uptake. Those findings are supportive for getting insights into the immobilization effects of biochars on HM to reduce their phytoavailability. Our observations will be helpful for designing biochars as soil amendments to reduce the bioavailability of HM to plants in soils since the results seem useful in the practice because the contaminated soil in the Tar Creek area of NE Oklahoma was tested.

References

Ahmad M, Lee SS, Yang JE, Ro H-M, Lee YH, Ok YS (2012) Effects of soil dilution and amendments (mussel shell, cow bone, and biochar) on Pb availability and phytotoxicity in military shooting range soil. Ecotoxicology and Environmental Safety 79:225–231. doi: 10.1016/j.ecoenv.2012.01.003

Ahmad M, Ok YS, Rajapaksha AU, Lim JE, Kim B-Y, Ahn J-H, Lee YH, Al-Wabel MI, Lee S-E, Lee SS (2016) Lead and copper immobilization in a shooting range soil using soybean stover- and pine needle-derived biochars: Chemical, microbial and spectroscopic assessments. Journal of Hazardous Materials 301:179–186. doi: 10.1016/j.jhazmat.2015.08.029

Ahmedna M, Johns MM, Clarke SJ, Marshall WE, Rao RM (1997) Potential of agricultural by-product-based activated carbons for use in raw sugar decolourisation. Journal of the Science of Food and Agriculture 75:117–124. doi: 10.1002/(sici)1097-0010(199709)75:1<117::aid-jsfa850>3.0.co;2-m

Ahumada I, Sepúlveda K, Fernández P, Ascar L, Pedraza C, Richter P, Brown S (2014) Effect of biosolid application to Mollisol Chilean soils on the bioavailability of heavy metals (Cu, Cr, Ni, and Zn) as assessed by bioassays with sunflower (Helianthus annuus) and DGT measurements. Journal of Soils and Sediments 14:886–896. doi: 10.1007/s11368-013-0842-8

Al-Wabel MI, Usman AR, El-Naggar AH, Aly AA, Ibrahim HM, Elmaghraby S, Al-Omran A (2015) Conocarpus biochar as a soil amendment for reducing heavy metal

availability and uptake by maize plants. Saudi Journal of Biological Sciences 22:503–511. doi: 10.1016/j.sjbs.2014.12.003

Banik C, Lawrinenko M, Bakshi S, Laird DA (2018) Impact of Pyrolysis Temperature and Feedstock on Surface Charge and Functional Group Chemistry of Biochars. Journal of Environment Quality 47:452. doi: 10.2134/jeq2017.11.0432

Beattie RE, Henke W, Davis C, Mottaleb MA, Campbell JH, Mcaliley LR (2017) Quantitative analysis of the extent of heavy-metal contamination in soils near Picher, Oklahoma, within the Tar Creek Superfund Site. Chemosphere 172:89–95. doi: 10.1016/j.chemosphere.2016.12.141

Brown S, Compton H, Basta N (2007) Field Test of In Situ Soil Amendments at the Tar Creek National Priorities List Superfund Site. Journal of Environment Quality 36:1627. doi: 10.2134/jeq2007.0018

Cantrell KB, Hunt PG, Uchimiya M, Novak JM, Ro KS (2012) Impact of pyrolysis temperature and manure source on physicochemical characteristics of biochar. Bioresource Technology 107:419–428. doi: 10.1016/j.biortech.2011.11.084

Cao X, Harris W (2010) Properties of dairy-manure-derived biochar pertinent to its potential use in remediation. Bioresource Technology 101:5222–5228. doi: 10.1016/j.biortech.2010.02.052

Chan KY, Zwieten LV, Meszaros I, Downie A, Joseph S (2008) Using poultry litter biochars as soil amendments. Soil Research 46:437. doi: 10.1071/sr08036

Chen D, Guo H, Li R, Li L, Pan G, Chang A, Joseph S (2016) Low uptake affinity cultivars with biochar to tackle Cd-tainted rice — A field study over four rice seasons

in Hunan, China. Science of The Total Environment 541:1489–1498. doi: 10.1016/j.scitotenv.2015.10.052

Chia CH, Gong B, Joseph SD, Marjo CE, Munroe P, Rich AM (2012) Imaging of mineral-enriched biochar by FTIR, Raman and SEM–EDX. Vibrational Spectroscopy 62:248–257. doi: 10.1016/j.vibspec.2012.06.006

Church C, Spargo J, Fishel S (2017) Strong Acid Extraction Methods for "Total Phosphorus" in Soils: EPA Method 3050B and EPA Method 3051. ael. doi: 10.2134/ael2016.09.0037

Farrell M, Rangott G, Krull E (2013) Difficulties in using soil-based methods to assess plant availability of potentially toxic elements in biochars and their feedstocks. Journal of Hazardous Materials 250-251:29–36. doi: 10.1016/j.jhazmat.2013.01.073

Feinstein K (2018) Representative Compounds. Guide to Spectroscopic Identification of Organic Compounds 53–73. doi: 10.1201/9780203719626-3

Fellet G, Marchiol L, Vedove GD, Peressotti A (2011) Application of biochar on mine tailings: Effects and perspectives for land reclamation. Chemosphere 83:1262–1267. doi: 10.1016/j.chemosphere.2011.03.053

Ghosh M, Singh S (2005) A comparative study of cadmium phytoextraction by accumulator and weed species. Environmental Pollution 133:365–371. doi: 10.1016/j.envpol.2004.05.015

Gondek K, Mierzwa-Hersztek M (2016) Effect of low-temperature biochar derived from pig manure and poultry litter on mobile and organic matter-bound forms of Cu, Cd, Pb and Zn in sandy soil. Soil Use and Management 32:357–367. doi: 10.1111/sum.12285

Gouzie D (2018) Potential Remediation Methods And Their Applicability To The Tri-State Mining District, Usa. doi: 10.1130/abs/2018am-319581

Houben D, Evrard L, Sonnet P (2013) Mobility, bioavailability and pH-dependent leaching of cadmium, zinc and lead in a contaminated soil amended with biochar. Chemosphere 92:1450–1457. doi: 10.1016/j.chemosphere.2013.03.055

Hu H, Shine J, Wright RO (2007) The Challenge Posed to Childrens Health by Mixtures of Toxic Waste: The Tar Creek Superfund Site as a Case-Study. Pediatric Clinics of North America 54:155–175. doi: 10.1016/j.pcl.2006.11.009

Huang L, Li WC, Tam NFY, Ye Z (2019) Effects of root morphology and anatomy on cadmium uptake and translocation in rice (Oryza sativa L.). Journal of Environmental Sciences 75:296–306. doi: 10.1016/j.jes.2018.04.005

Jarvis SC, Jones LHP, Hopper MJ (1976) Cadmium uptake from solution by plants and its transport from roots to shoots. Plant and Soil 44:179–191. doi: 10.1007/bf00016965

Jiang T-Y, Jiang J, Xu R-K, Li Z (2012) Adsorption of Pb(II) on variable charge soils amended with rice-straw derived biochar. Chemosphere 89:249–256. doi: 10.1016/j.chemosphere.2012.04.028

Kachurina O, Zhang H, Raun W, Krenzer E (2000) Simultaneous determination of soil aluminum, ammonium- and nitrate-nitrogen using 1 M potassium chloride extraction. Communications in Soil Science and Plant Analysis 31:893–903. doi: 10.1080/00103620009370485

Karami N, Clemente R, Moreno-Jiménez E, Lepp NW, Beesley L (2011) Efficiency of green waste compost and biochar soil amendments for reducing lead and copper

mobility and uptake to ryegrass. Journal of Hazardous Materials 191:41–48. doi: 10.1016/j.jhazmat.2011.04.025

Keiluweit M, Nico PS, Johnson MG, Kleber M (2010) Dynamic Molecular Structure of Plant Biomass-Derived Black Carbon (Biochar). Environmental Science & Technology 44:1247–1253. doi: 10.1021/es9031419

Lahori AH, Guo Z, Zhang Z, Li R, Mahar A, Awasthi MK, Shen F, Sial TA, Kumbhar F, Wang P, Jiang S (2017) Use of Biochar as an Amendment for Remediation of Heavy Metal-Contaminated Soils: Prospects and Challenges. Pedosphere 27:991–1014. doi: 10.1016/s1002-0160(17)60490-9

Laird D, Fleming P, Wang B, Horton R, Karlen D (2010) Biochar impact on nutrient leaching from a Midwestern agricultural soil. Geoderma 158:436–442. doi: 10.1016/j.geoderma.2010.05.012

Lehmann J (2015) Biochar for Environmental Management. doi: 10.4324/9780203762264

Li H, Ye X, Geng Z, Zhou H, Guo X, Zhang Y, Zhao H, Wang G (2016) The influence of biochar type on long-term stabilization for Cd and Cu in contaminated paddy soils. Journal of Hazardous Materials 304:40–48. doi: 10.1016/j.jhazmat.2015.10.048

Lu H, Li Z, Fu S, Méndez A, Gascó G, Paz-Ferreiro J (2015) Effect of Biochar in Cadmium Availability and Soil Biological Activity in an Anthrosol Following Acid Rain Deposition and Aging. Water, Air, & Soil Pollution. doi: 10.1007/s11270-015-2401-y

Lu K, Yang X, Shen J, Robinson B, Huang H, Liu D, Bolan N, Pei J, Wang H (2014) Effect of bamboo and rice straw biochars on the bioavailability of Cd, Cu, Pb and Zn

to Sedum plumbizincicola. Agriculture, Ecosystems & Environment 191:124–132. doi: 10.1016/j.agee.2014.04.010

Lu K, Yang X, Gielen G, Bolan N, Ok YS, Niazi NK, Xu S, Yuan G, Chen X, Zhang X, Liu D, Song Z, Liu X, Wang H (2017) Effect of bamboo and rice straw biochars on the mobility and redistribution of heavy metals (Cd, Cu, Pb and Zn) in contaminated soil. Journal of Environmental Management 186:285–292. doi: 10.1016/j.jenvman.2016.05.068

Mehlich A (1984) Mehlich 3 soil test extractant: A modification of Mehlich 2 extractant. Communications in Soil Science and Plant Analysis 15:1409–1416. doi: 10.1080/00103628409367568

Mohamed I, Zhang G-S, Li Z-G, Liu Y, Chen F, Dai K (2015) Ecological restoration of an acidic Cd contaminated soil using bamboo biochar application. Ecological Engineering 84:67–76. doi: 10.1016/j.ecoleng.2015.07.009

Montoroi J-P (2018) Soil Salinization and Management of Salty Soils. Soils as a Key Component of the Critical Zone 5 97–126. doi: 10.1002/9781119438298.ch5

Moreno-Castilla C, López-Ramón M, Carrasco-Marín F (2000) Changes in surface chemistry of activated carbons by wet oxidation. Carbon 38:1995–2001. doi: 10.1016/s0008-6223(00)00048-8

Neuberger JS, Hu SC, Drake KD, Jim R (2008) Potential health impacts of heavy-metal exposure at the Tar Creek Superfund site, Ottawa County, Oklahoma. Environmental Geochemistry and Health 31:47–59. doi: 10.1007/s10653-008-9154-0

Novak JM, Busscher WJ, Laird DL, Ahmedna M, Watts DW, Niandou MAS (2009) Impact of Biochar Amendment on Fertility of a Southeastern Coastal Plain Soil. Soil Science 174:105–112. doi: 10.1097/ss.0b013e3181981d9a

Park JH, Choppala GK, Bolan NS, Chung JW, Chuasavathi T (2011) Biochar reduces the bioavailability and phytotoxicity of heavy metals. Plant and Soil 348:439–451. doi: 10.1007/s11104-011-0948-y

Peng X, Ye L, Wang C, Zhou H, Sun B (2011) Temperature- and duration-dependent rice straw-derived biochar: Characteristics and its effects on soil properties of an Ultisol in southern China. Soil and Tillage Research 112:159–166. doi: 10.1016/j.still.2011.01.002

Puga A, Abreu C, Melo L, Beesley L (2015) Biochar application to a contaminated soil reduces the availability and plant uptake of zinc, lead and cadmium. Journal of Environmental Management 159:86–93. doi: 10.1016/j.jenvman.2015.05.036

Qian K, Kumar A, Patil K, Bellmer D, Wang D, Yuan W, Huhnke R (2013) Effects of Biomass Feedstocks and Gasification Conditions on the Physiochemical Properties of Char. Energies 6:3972–3986. doi: 10.3390/en6083972

Qiu M, Sun K, Jin J, Han L, Sun H, Zhao Y, Xia X, Wu F, Xing B (2015) Metal/metalloid elements and polycyclic aromatic hydrocarbon in various biochars: The effect of feedstock, temperature, minerals, and properties. Environmental Pollution 206:298–305. doi: 10.1016/j.envpol.2015.07.026

Rajkovich S, Enders A, Hanley K, Hyland C, Zimmerman AR, Lehmann J (2011) Corn growth and nitrogen nutrition after additions of biochars with varying properties to a

temperate soil. Biology and Fertility of Soils 48:271–284. doi: 10.1007/s00374-011-0624-7

Rees F, Sterckeman T, Morel JL (2016) Root development of non-accumulating and hyperaccumulating plants in metal-contaminated soils amended with biochar. Chemosphere 142:48–55. doi: 10.1016/j.chemosphere.2015.03.068

Richards JR, Schroder JL, Zhang H, Basta NT, Wang Y, Payton ME (2012) Trace elements in benchmark soils of Oklahoma. Soil Science Society of America Journal 76:2031-2040. doi: 10.2136/sssaj2012.0100

Sas Institute (2011) Sas/Graph 9.3: Graph Template Language User's Guide. SAS Institute.

Sidhu V, Sarkar D, Datta R (2016) Effects of biosolids and compost amendment on chemistry of soils contaminated with copper from mining activities. Environmental Monitoring and Assessment. doi: 10.1007/s10661-016-5185-7

Streubel JD, Collins HP, Garcia-Perez M, Tarara J, Granatstein D, Kruger C (2011) Influence of Contrasting Biochar Types on Five Soils at Increasing Rates of Application. Soil Science Society of America Journal 75:1402. doi: 10.2136/sssaj2010.0325

Uchimiya M, Klasson KT, Wartelle LH, Lima IM (2011) Influence of soil properties on heavy metal sequestration by biochar amendment: 1. Copper sorption isotherms and the release of cations. Chemosphere 82:1431–1437. doi: 10.1016/j.chemosphere.2010.11.050

Wang Y, Wang HS, Tang CS, Gu K, Shi B (2019) Remediation of Heavy Metal Contaminated Soils by Biochar: a Review. Environmental Geotechnics 7:1-4. doi: 10.1680/jenge.18.00091

Westerman R, Jones JB, Case VW (1990) Sampling, Handling, and Analyzing Plant Tissue Samples. SSSA Book Series Soil Testing and Plant Analysis. doi: 10.2136/sssabookser3.3ed.c15

Woldetsadik D, Drechsel P, Keraita B, Marschner B, Itanna F, Gebrekidan H (2016) Effects of biochar and alkaline amendments on cadmium immobilization, selected nutrient and cadmium concentrations of lettuce (Lactuca sativa) in two contrasting soils. SpringerPlus. doi: 10.1186/s40064-016-2019-6

Xu P, Sun C-X, Ye X-Z, Xiao W-D, Zhang Q, Wang Q (2016) The effect of biochar and crop straws on heavy metal bioavailability and plant accumulation in a Cd and Pb polluted soil. Ecotoxicology and Environmental Safety 132:94–100. doi: 10.1016/j.ecoenv.2016.05.031

Xu R-K, Zhao A-Z, Yuan J-H, Jiang J (2012) pH buffering capacity of acid soils from tropical and subtropical regions of China as influenced by incorporation of crop straw biochars. Journal of Soils and Sediments 12:494–502. doi: 10.1007/s11368-012-0483-3

Yuan J-H, Xu R-K, Zhang H (2011) The forms of alkalis in the biochar produced from crop residues at different temperatures. Bioresource Technology 102:3488–3497. doi: 10.1016/j.biortech.2010.11.018

Zhang G, Guo X, Zhao Z, He Q, Wang S, Zhu Y, Yan Y, Liu X, Sun K, Zhao Y, Qian T (2016) Effects of biochars on the availability of heavy metals to ryegrass in an

alkaline contaminated soil. Environmental Pollution 218:513–522. doi: 10.1016/j.envpol.2016.07.031

Zhang H, Dotson P (1994) The use of microwave muffle furnace for dry ashing plant tissue samples. Communications in Soil Science and Plant Analysis 25:1321–1327. doi: 10.1080/00103629409369118

Zhang R-H, Li Z-G, Liu X-D, Wang B-C, Zhou G-L, Huang X-X, Lin C-F, Wang A-H, Brooks M (2017) Immobilization and bioavailability of heavy metals in greenhouse soils amended with rice straw-derived biochar. Ecological Engineering 98:183–188. doi: 10.1016/j.ecoleng.2016.10.057

Zhao B, Xu R, Ma F, Li Y, Wang L (2016) Effects of biochars derived from chicken manure and rape straw on speciation and phytoavailability of Cd to maize in artificially contaminated loess soil. Journal of Environmental Management 184:569–574. doi: 10.1016/j.jenvman.2016.10.020

Zota AR, Schaider LA, Ettinger AS, Wright RO, Shine JP, Spengler JD (2011) Metal sources and exposures in the homes of young children living near a mining-impacted Superfund site. Journal of Exposure Science & Environmental Epidemiology 21:495–505. doi: 10.1038/jes.2011.21

Supplementary material

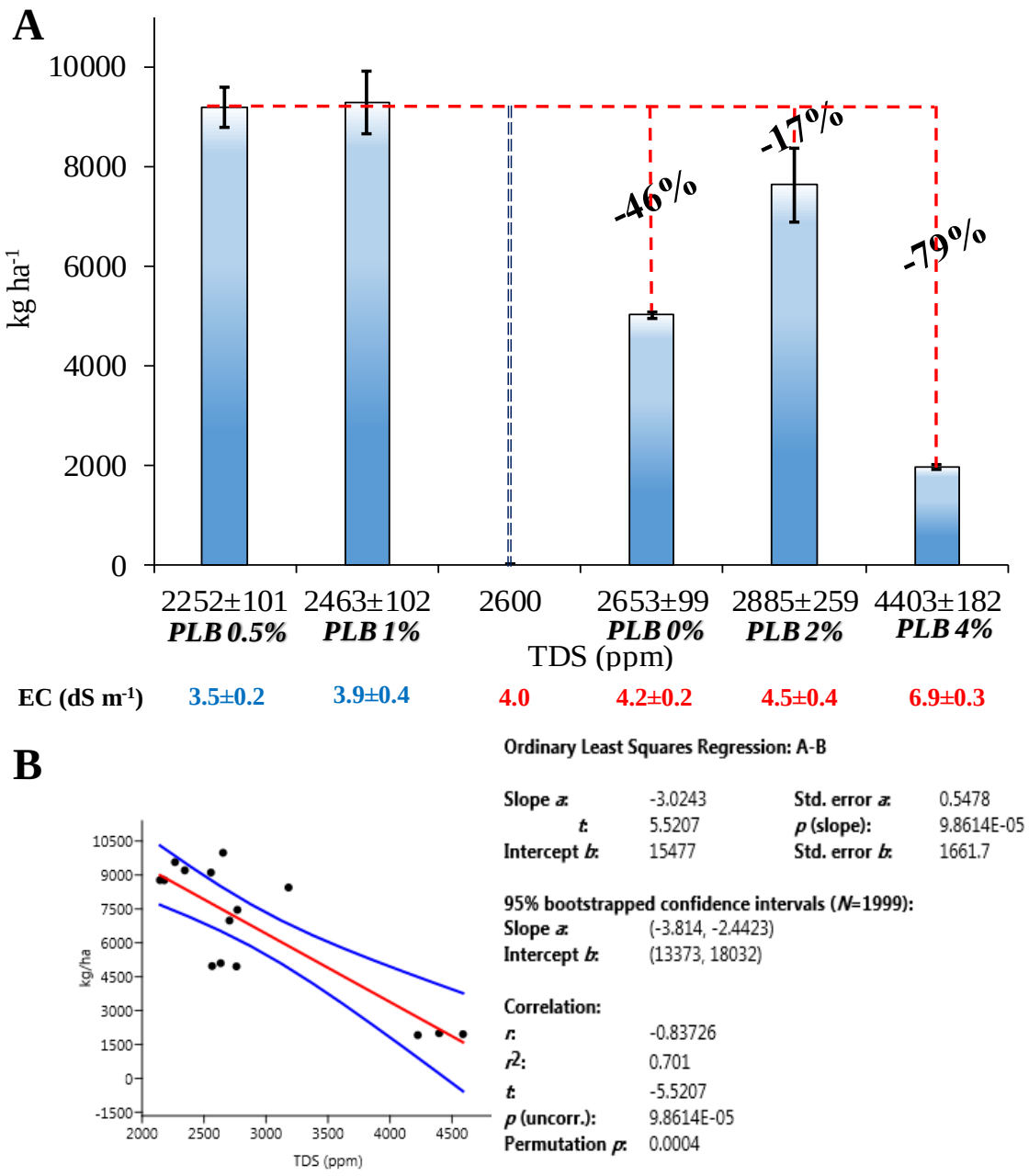

Fig. S1. (**A**) Ryegrass yield (kg ha^{-1}) as a function of total dissolved solids (TDS) from poultry litter biochar (PLB) application rates. (**B**) Linear regression between ryegrass yield (kg ha^{-1}) and TDS from poultry litter biochar application rates

Fig. S2. Perennial ryegrass cultivated in heavy metals contaminated soil treated with various rates of poultry litter derived biochars (PLB)

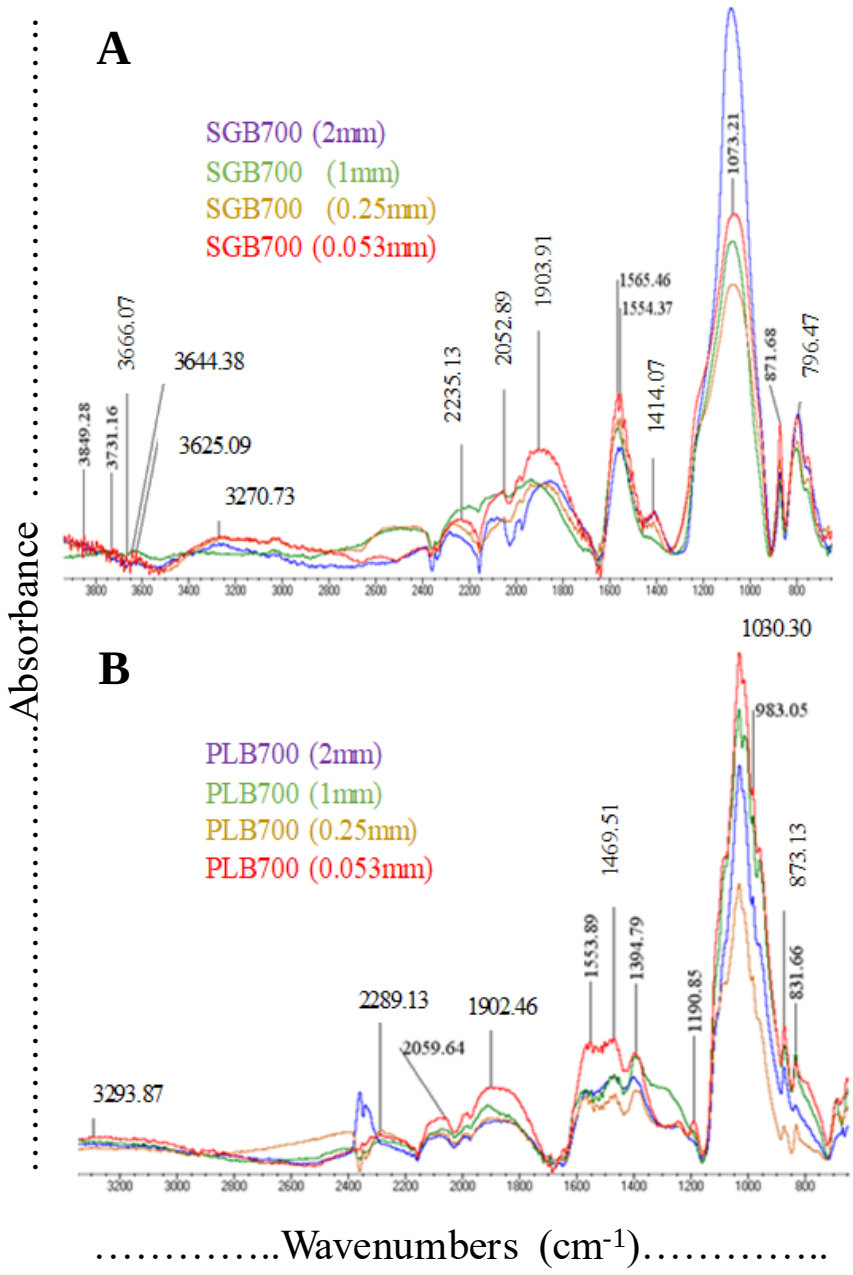

Fig. S3. FTIR spectra of switchgrass (**A**) and poultry litter-derived biochars (**B**) pyrolyzed at 700 ^{o}C and sieved by 2, 1, 0.25 and 0.053 mm

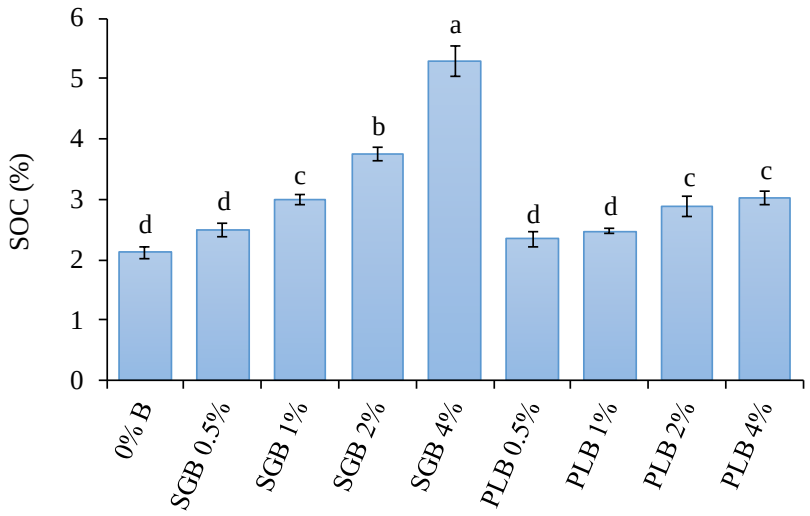

Fig. S4. Soil organic carbon (SOC) as affected by SGB and PLB application rates in the Tar Creek soil cultivated with ryegrass. Results are significant at $p<0.01$

Table S1. Ryegrass germination and biomass as a function of biochars application rates

Treatment	Germination		…….Dry mass (g pot^{-1}) …….					
	%		Shoots		Roots		Shoots+Roots	
Control	59.0	bc	9.8	c	4.3	c	14.0	c
SGB 0.5%	45.8	c	9.2	c	4.5	c	13.7	c
SGB 1.0%	56.2	bc	9.1	c	4.4	c	13.5	c
SGB 2.0%	64.6	abc	7.9	c	3.7	c	11.6	c
SGB 4.0%	70.8	ab	3.4	d	3.7	d	7.1	d
PLB 0.5%	70.1	ab	17.9	a	8.0	a	25.9	a
PLB 1.0%	81.9	a	18.1	a	8.7	a	26.8	a
PLB 2.0%	81.3	a	14.9	b	7.1	b	21.9	b
PLB 4.0%	71.5	ab	3.8	d	2.9	d	6.7	d
F value	8.8	**	170.4	**	26.9	**	164	**
Average	66.8		10.4		5.3		15.7	
Stdev	6.9		0.7		0.7		1.0	
CV (%)	19.6		6.9		13.4		6.5	

**p<0.01. Same letters in the column are not different from Tukey test at 1%
Stdev: Standard deviation; CV: Coefficient of variation

Table S2. Pearson correlations between phytoavailable heavy metals and their concentration in ryegrass shoots and roots

	Shoots	Roots	Shoots+Roots
	……..……..Zn……..……..		
SGB	0.99***	0.98***	0.99***
PLB	0.89***	0.99***	0.95***
SGB+PLB	0.84***	0.98***	0.95***
	……..……..Pb……..……..		
SGB	0.99***	0.96***	0.99***
PLB	0.99***	0.86**	0.85**
SGB+PLB	0.99***	0.81***	0.81***
	……..……..Cd……..……..		
SGB	0.99***	0.96***	0.92***
PLB	0.76**	0.88***	0.86***
SGB+PLB	0.81***	0.67**	0.66**

***: $p<0.001$; **: $p<0.01$.

Table S3. Pearson correlations between biomass and heavy metal concentrations in ryegrass shoots and roots

	Shoots	Roots	Shoots+Roots
	……..……..Zn……..……..		
SGB	0.54^{NS}	0.75**	0.78**
PLB	-0.17^{NS}	0.77**	0.58^{NS}
SGB+PLB	-0.01^{NS}	0.81***	0.70**
	……..……..Pb……..……..		
SGB	0.34	0.61*	0.36
PLB	-0.33^{NS}	0.28^{NS}	-0.07^{NS}
SGB+PLB	-0.08^{NS}	0.21^{NS}	0.03^{NS}
	……..……..Cd……..……..		
SGB	0.74**	0.70**	0.70**
PLB	0.34^{NS}	0.67**	0.64*
SGB+PLB	0.53**	0.26^{NS}	0.34^{NS}

***: $p<0.001$; **: $p<0.01$; *: $p<0.05$; NS: non-significant ($p>0.05$)

VITA

Joao Arthur Antonangelo

Candidate for the Degree of

Doctor of Philosophy

Thesis: NUTRIENT DYNAMICS IN A HIGHLY WEATHERED SOIL UNDER NO-TILL AND HEAVY METAL PHYTOAVAILABILITY AS AFFECTED BY BIOCHAR AMENDMENT

Major Field: Soil Science

Biographical:

Education:

Completed the requirements for the Doctor of Philosophy in Soil Science at Oklahoma State University, Stillwater, Oklahoma in July, 2019.

Completed the requirements for the Master of Science in Plant and Soil Sciences at University of Sao Paulo, Piracicaba, Sao Paulo, Brazil in 2015.

Completed the requirements for the Bachelor of Science in Agricultural Engineering at Sao Paulo State University, Botucatu, Sao Paulo, Brazil in 2012.

Experience:

Ph.D. Graduate Research Associate at University of Sao Paulo (USP), Piracicaba, Sao Paulo, Brazil. July 2015 – July 2016.

Visiting Scientist at Lakehead University (LU), Thunder Bay, Ontario, Canada. June 2014 – November 2014.

M.S. Graduate Research Assistant at University of Sao Paulo (USP), Piracicaba, Sao Paulo, Brazil. February 2013 – June 2015.

Professional Memberships:

American Society of Agronomy. 2017 - Current.
Crop Science Society of America. 2017 - Current.
Soil Science Society of America. 2017 - Current.